

OVERDUE FINES: 25¢ per day per item

RETURNING LIBRARY MATERIALS: Place in book return to remove charge from circulation records

T. THE DECOMPOSITION KINETICS OF NICKELACYCLOPENTANES

II. THE IN SITU DECOMPOSITION OF NICKELACYCLOBUTANES

III. STUDIES TOWARD THE HOMOGENEOUS CATALYTIC REDUCTION OF CARBON MONOXIDE

Ву

Richard Kingsley Stuart, Jr.

A DISSERTATION

Submitted to

Michigan State University

in partial fulfillment of the requirement

for the degree of

DOCTOR OF PHILOSOPHY

Department of Chemistry

ABSTRACT

- I. THE DECOMPOSITION KINETICS OF NICKELACYCLOPENTANES
 - II. THE IN SITU DECOMPOSITION OF
 NICKELACYCLOBUTANES
 - III. STUDIES TOWARD THE HOMOGENEOUS CATALYTIC
 REDUCTION OF CARBON MONOXIDE

Ву

Richard K. Stuart, Jr.

The thermal decomposition kinetics of a series of phosphine and pyridine stabilized nickelacyclopentanes were measured. The change in activation parameters (most notably the energy of activation) in the series was correlated with both the steric and electronic properties of the ligands. It was found that the monodentate and flexible chelate ligands impart lower activation energies to the complexes while rigid chelates thermally decompose with higher activation energies. The trans effecting ability of the ligands also parallel the change in activation energies. Ligands of high trans effect as in bistion energies. Ligands of high trans effect as in bistirphenylphosphine)tetramethylene nickel(II) significantly weaken the nickel-carbon bonds resulting in a low activation energy for thermal decomposition. Ligands of weak trans

effect as in (1,10-phenanthroline)tetramethylene nickel(II) decompose with higher activation energies.

A difference in stability between alicyclic nickel complexes and nickelacyclopentanes was also found. The increased stability of nickelacyclopentanes over their acyclic analogs is due to the steric constraints of the metal containing ring.

A series of phosphine and pyridine stabilized nickel-acyclobutanes were thermally decomposed in situ. The main decomposition pathway was found to be reductive elimination with $\alpha-\beta$ bond cleavage and β -hydride elimination pathways of lessor importance.

Studies were undertaken to develop a homogeneous catalytic analog to the methanation reaction of carbon monoxide. The proposed pathway involved the intermediacy of an oxygen stabilized "Fischer style" carbene complex. The experimental results indicate that the formation of the Fischer carbene under the reaction conditions was extremely slow. Attempts to increase the rate of formation of the metal carbene species by use of Lewis acid co-catalysts met with limited success.

ACKNOWLEDGMENTS

I would like to express my appreciation for the patience shown to me by my research preceptor, Professor Robert H. Grubbs.

I also want to thank my fellow graduate students for all the help, discussions and general good times which have made graduate school enjoyable. Chuck Hoppin, Rose Bartoszek and Bruce Osterby in particular have added immensely to my stay at MSU.

Finally, I thank my parents and family for the confidence, encouragement and support given to me throughout my academic career.

TABLE OF CONTENTS

Chapt	ter																						Page
LIST	OF	TABI	LES		•	•	•		•	•	•	•	•	•	•	•	•	•	•	•	•	•	iv
LIST	OF	FIGU	JRE	S	•	•	•		•	•	•	•	•			•	•	•	•	•	•	•	vi
I.		ECOMI YCLOI							T)	cs •	•)F	N]	CP •	ŒI	`A-	-	•	•	•	•	•	1
	I	ntro	luc	ti	on	•	•		•	•	•	•	•	•		•	•	•	•	•	•	•	1
	Re	esult	s	an	d	Di	sc	us	si	lon	. •	•	•	•	•	•	•	•	•	•	•	•	30
	E	xperi	Lme	nt	al	•	•	•	•	•	•	•	•	•	•	•	•	•	•	•	•	•	76
II.		HE IN											OI •		•	•	•	•	•	•	•	•	87
	Ir	ntrod	luc	ti	on	•	•			•			•	•	•	•	•	•	•	•	•	•	87
	Re	esult	s	an	đ	Di	sc	us	ssi	lon	•		•	•		•	•	•		•	•		94
	Ez	xperi	lme	nt	al	•	•	•	•	•	•	•	•	•	•	•	•	•	•	•	•	•	101
III.	CI	TUDIE YTALY CXONC	TI	C 1	RE	DU	CI	CIC			C				JS •	•	•	•	•	•	•	•	102
	Ir	ntrod	luc	ti	on	•			•		•	•		•						•		•	102
	Re	esult	s	an	đ	Di	.sc	us	si	on	•			•		•	•	•			•		110
	Ez	kperi	Lme	nt	al	•	•	•	•	•	•	•	•	•	•	•		•	•	•	•	•	116
REFEE	RENC	CES.			_	_			_		_												118

LIST OF TABLES

Table		Page
1	Rate data for $(\phi_3P)_2$ Ni	32
2	Activation parameters for	
	(φ ₃ P) ₂ Ni	33
3	Kinetics and activation data for	
	$(\phi_3P)_2Ni(CH_3)_2$	40
4	Rate data and activation parameters	
	for (dpe)Ni	41
5	Rate data and activation parameters	
	for (dpp)Ni	46
6	Rate data and activation parameters	
	for (dipy)Ni	49
7	Rate data and activation parameters	
	for (n-Bu ₃ P)Ni	58
8	Rate data and activation parameters	
	for $(\phi_3P)_3N_1$	64
9	Activation parameters for nickela-	
	cyclopentanes	73
10	Standard deviation of rate constants	
	and Arrhenius slopes	74
11	Decomposition products for nickela-	
	cyclobutanes	95
12	Decomposition products for methyl	
	substituted nickelacyclobutanes	96

Table		Page
13	Methanation mechanisms	106
14	Summary of carbon monoxide	
	reduction reactions	111
15	Summary of CO reductions with	
	co-catalysts	112
16	Solvent degradations	115

LIST OF FIGURES

Figure						Page
1	Cyclodimerization mechanism for					
	l,l-dimethylcyclopropane	•	•	•		6
2	Decomposition of di-n-butylbis-					
	(triphenylphosphine) platinum(II) .	•	•	•	•	9
3	β -Hydride elimination pathway	•	•	•	•	14
4	Steric requirements of the metalla-					
	cycle and alicyclic complex	•	•	•	•	18
5	Proposed decomposition pathway					
	for (Bu ₃ P) ₂ Pt	•	•	•	•	20
6	Characteristic reactions of					
	nickelacyclopentanes	•	•	•	•	22
7	Gas composition as a function of					
	added $(n-Bu)_3P$ for $(Cy_3P)Ni$	•	•	•	•	24
8	Gas composition versus phosphine/					
	nickel ratio	•	•	•	•	25
9	Cyclodimerization of ethylene by					
	$(\phi_3P)_3N_1$	•	•	•	•	28
10	Moles of decomposition gas as a					
	function of time	•	•	•	•	31
11	$Log [(\phi_3 P)_2 Ni)]$ as a function of					
	time in minutes at 40°C	•	•	•	•	34
12	$Log [(\phi_3 P)_2 Ni]$ as a function of					
	time in minutes at 30° (\triangle) and 19°C	(0	(כ	•	•	35

Figure		Page
13	Arrhenius plot for $(\phi_3P)_2N_1$	36
14	$Log [(\phi_3P)_2Ni(CH_3)_2]$ as a function of	
	time in minutes at 6° (\triangle) and 20°C (\square)	37
15	$Log [(\phi_3P)_2Ni(CH_3)_2]$ as a function	
	of time in minutes at 30°C	38
16	Arrhenius plot for $(\phi_3P)_2Ni(CH_3)_2$	39
17	Log [P Ni] as a function of ϕ_2	
	time in minutes at 80°C	42
18	Log $\begin{bmatrix} P \\ P \end{bmatrix}$ Ni as a function of ϕ_2	
	time in minutes at 90° (\square) and 100° (\triangle)	43
19	Arrhenius plot for $\begin{bmatrix} P \\ P \end{bmatrix}$ $\begin{bmatrix} Ni \\ \phi_2 \end{bmatrix}$ \vdots	44
20	Reorganization of the metallacycles	
	during thermal decomposition	45
21	Log [P Ni] as a function of time Φ_2	
	in minutes at 90° (o), 100° (□) and	
	110°C (Δ)	47

Figure	^ф 2	Page
22	Arrhenius plot for (P) Ni	48
23	Log [(dipy)Ni] as a function of	
	time in minutes at 80° (0) and 60°C	
	(Δ)	51
24	Log [(dipy)Ni] as a function of	
	time in minutes at 65° (\triangle) and 70°C	
	(a)	52
25	Arrhenius plot for (dipy)Ni	53
26	Log [(1,10-phen)Ni] as a function	
	of time in minutes at 75° (a), 70° (o)	
	and 80°C (△)	54
27	Arrhenius plot for (1,10-phen)Ni	55
28	Relative d orbital energy levels	
	for nickel(II)	56
29	Log [(nBu ₃ P) ₂ Ni] as a function of	
	time in minutes at 20°C	59
30	Log [(n-Bu3P)2Ni] as a function of	
	time in minutes at 30°C	60
31	Log [(n-Bu3P)2N1] as a function of	
	time in minutes at 40°C	61
32	Arrhenius plot for (n-Bu ₃ P)Ni	62
33	A possible decomposition mode for	
	$(R_3P)N_1$	64

Log [(\$\phi_3P)_3Ni] as a function of time in minutes at 20°C	Figure		Page
Log [(\$\phi_3P)_3Ni] as a function of time in minutes at 20°C	34	$Log [(\phi_3 P)_3 N_1)]$ as a function of	
time in minutes at 20°C		time in minutes at 0°C	66
Log [(φ ₃ P) ₃ Ni] as a function of time in minutes at 30°C	35	$Log [(\phi_3 P)_3 N_1)]$ as a function of	
time in minutes at 30°C		time in minutes at 20°C	67
Arrhenius plot for (φ ₃ P) ₃ Ni	36	$Log [(\phi_3 P)_3 Ni]$ as a function of	
Proposed decomposition pathway of (φ ₃ P) ₃ Ni Newman projection of the tetrahedral complex		time in minutes at 30°C	68
(φ ₃ P) ₃ Ni 70 39 Newman projection of the tetrahedral complex 71 40 Current mechanism for olefin metathesis 88 41 Proposed mechanism for Natta-Ziegler polymerization 89 42 Possible decomposition pathways for L ₂ X ₂ Pt 91 43 Products of (Cp) ₂ W by photochemical decomposition 92 44 Proposed pathway for coupling of α-w dihaloalkanes 93 45 Newman projection of nickela-cyclobutane 98	37	Arrhenius plot for $(\phi_3 P)_3 N_1$	69
Newman projection of the tetrahedral complex	38	Proposed decomposition pathway of	
complex		(φ ₃ P) ₃ N ₁	70
Current mechanism for olefin metathesis	39	Newman projection of the tetrahedral	
metathesis		complex	71
Proposed mechanism for Natta-Ziegler polymerization	40	Current mechanism for olefin	
polymerization		metathesis	88
Possible decomposition pathways for L_2X_2Pt	41	Proposed mechanism for Natta-Ziegler	
L ₂ X ₂ Pt		polymerization	89
Products of (Cp) ₂ W by photochemical decomposition	42	Possible decomposition pathways for	
decomposition		L_2X_2Pt	91
Proposed pathway for coupling of α-w dihaloalkanes	43	Products of (Cp) ₂ W by photochemical	
α-w dihaloalkanes		decomposition	92
Newman projection of nickela- cyclobutane	44	Proposed pathway for coupling of	
cyclobutane		αw dihaloalkanes	93
^	45	Newman projection of nickela-	
46 Decomposition modes for L_2Ni 99		cyclobutane	98
	46	Decomposition modes for L_2Ni	99

Figure		Page
47	Recent proposed Fischer-Tropsch	
	mechanism	107
48	Proposed homogeneous pathway for	
	CO reduction	109

CHAPTER I

THE DECOMPOSITION KINETICS OF NICKELCYCLOPENTANES

INTRODUCTION

Heterocyclic compounds are an important class of compounds and have played a major role in the development of organic chemistry. When the heteroatom is a transition metal the heterocycle is referred to as a metallacycle. It is becoming apparent that metallacycles play a major role in the development of organometallic chemistry. Many transition metal catalyzed reactions of olefins and acetylene are believed to utilize metallacycles as intermediates. Metallacyclopentanes have been demonstrated to be intermediates in many metal catalyzed cycloaddition and cycloreversions reactions of olefins. 1

In this introductory section, the reader will become familiar with the role and extent of metallacycles in transition metal chemistry. The preparation of metallacycles as well as their characteristic modes of reaction including their decompositions modes will be contrasted and compared to alicyclic transition metal complexes.

A discussion of the effect of additives on the decomposition of metallacycles will also be presented.

In 1961 F. G. A. Stone² reported the preparation of tetrakis(difluoromethylene)Iron(II) tetracarbonyl by the

reaction of iron pentacarbonyl and tetrafluoroethylene. This complex was characterized as a white, volatile, air stable solid with a melting point of 76-77°. This is the first reported preparation of a metallacyclopentane.

A decade later, Osborn³ isolated an iridacycle 2 from the 2+2 cycloaddition reaction of norbornadiene in acetone in the presence of [Ir(1,5 cyclooctadiene)Cl]₂. The identity of the iridacycle 2 was confirmed by an X-ray

$$Fe(CO)_5 + F_2C=CF_2$$
 Fe(CO)₄

determination. When 2 was treated with an excess of triphenyl phosphine the exo-trans-exo dimer 3 of norbornadiene

$$\frac{\operatorname{Ir}(\operatorname{COD})_2\operatorname{Cl}_2}{\operatorname{CH}_3\operatorname{COCH}_3} \xrightarrow{\operatorname{Excess}} \xrightarrow{\operatorname{Excess}} \underbrace{\mathbb{P}h_3\operatorname{P}}$$

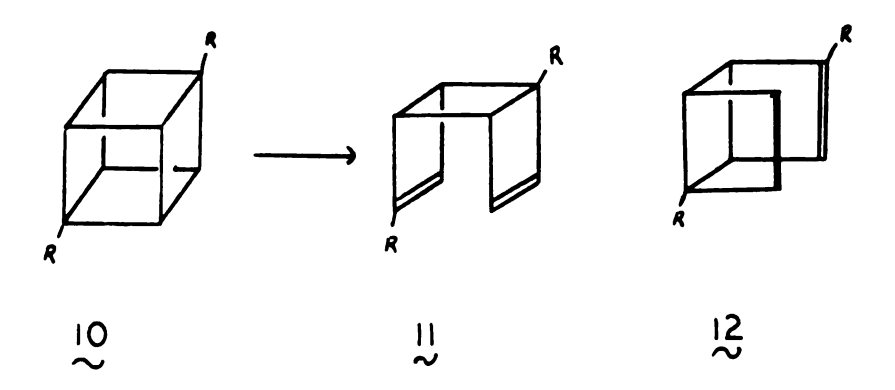
was formed in 35 percent yield. This was the first reported case where a metallacycle was isolated from a reaction mixture and then shown to be a true reaction intermediate by its further reaction to give the expected

products.

Katz⁴ and Cerefice treated exo-tricyclo[3.2.1.0^{2,4}]-octene $\frac{1}{2}$ at 90° for 2 hr with tris(triphenylphosphine)-rhodium(I)chloride and obtained a quantitative mixture of three isomers. Compound $\frac{1}{2}$ is formally related to $\frac{1}{2}$ by an electrocyclic rearrangement while compound $\frac{1}{2}$ is not.

Labeling studies showed that a specific deuterium shift was required to convert 4 to 5. To account for these intramolecular processes a pathway involving metallacycles 8 and 9 as intermediates was proposed.

The highly strained cubane molecule is remarkably stable thermally. This presumably reflects the constraints of the Woodward-Hoffman orbital symmetry conservation rules. The conversion of cubane to syn-tricyclooctadienes is thermally forbidden.



However, in the presence of catalytic amounts of $[Rh(CO)_2Cl]_2$ the conversion of 10 to 11 and 12 proceeds quantitatively. When a stoichiometric amount of catalyst was added, the rhodacycle 13 was isolated in 90 percent yield. In the presence of excess triphenyl phosphine the rhodacycle undergoes reductive elimination to form the corresponding

ketone and $Rh(CO)Cl(\phi_3P)_2$. The trapped rhodacycle prompted Halpern and Eaton to propose a non-concerted series of oxidative addition steps to account for the observed results. That is, they proposed a mechanism involving metallacycles for the conversion of 10 to 11 and 12.

Binger et al. ⁶ have isolated nickelacyclopentane derivatives from the $[2\pi+2\pi]$ cycloaddition reaction of strained ring olefins and nickel(o) catalysts. From the reaction of 3,3-dimethylcyclopropene and bis(1,5COD)Ni(o) in the presence of dipyridyl, Binger was able to isolate in addition to the cyclodimerization product a metallacycle $1\frac{14}{4}$. Treatment of the nickelacyclopentane $1\frac{14}{4}$ with

activated olefins (such as maleic anhydride) results in the formation of the cyclodimer 15. The metallacycle 14 is a dark green, diamagnetic, air sensitive, crystalline complex thermally stable to about 80°C. The proposed mechanism for the cyclodimerization of these reactive olefins is shown in Figure 1. The key step in the formation of metallacycles from strained olefins is the

Figure 1. Cyclodimerization mechanism for 1,1-dimethyl-cyclopropane.

isomerization of the bis olefin complex 16 to the metallacycle 17. Attempts to isolate the unsubstituted nickel-acyclopentane complex from the analogous reaction with ethylene failed. This may be in part due to the lack of strain in ethylene and hence its lower reactivity. However, Binger was successful in preparing the parent nickel-acyclopentane from (bipy)Ni(COD) and 1,4-dibromobutane. Incidentally this is one of the best methods of preparing amine stabilized nickelacyclopentanes.

Traditionally the metal-carbon sigma bond is thought

to be very weak. In the last fifteen years much effort has been devoted to preparing complexes which contain strong field ligands in addition to sigma bonded alkyl groups. Strong field ligands such as carbon monoxide, tertiary phosphines, and the π -cyclopentadienyl group

are believed to stabilize metal-alkyl σ bonds by their ability to π -bond. A widely accepted π -bonding theory $^{7-9}$ has been proposed to account for the stabilizing ability of these π accepting ligands. Homolytic cleavage of the metal alkyl bond occurs by excitation of an electron from a bonding orbital to a nonbonding or antibonding orbital. This weakens or breaks the bond to form radicals. This process should be hindered by strong field ligands which increase the ligand field splitting. This theory was initially accepted because homolytic fission of metalalkyl bonds was believed to be the main mechanism operating for the decompositions of metal alkyl bonds.

As more evidence became available the "supporting - ligand" theory became less attractive. Many organometallic complexes are now known which contain ligands with no π -bonding ability such as $[PhCH_2Cr(OH_2)_5]^{+2}$ 10 and a number with no supporting ligands such as $(PhCH_2)_4Ti^{11}$ and $(Ph_3C)_2Ni$. Spectroscopic and bond length data suggest that transition metal-carbon bonds are of the same strength as main group metal-carbon bonds which are not greatly affected by the presence of π accepting ligands. Finally the promotional mechanism as originally proposed is unlikely to be applicable under thermal conditions. 13

It was also proposed that π accepting ligands were necessary simply to block the coordination sites necessary for low energy pathways of bond cleavage such as B-hydride

elimination to occur. 14 A series of metal-alkyl complexes are known which are stable to β -hydride elimination and do not have additional ligands to block coordination sites. 15

Many transition metal organometallic complexes are thermally labile. This lability stems from the characteristic transition metal properties of variable co-ordination number and oxidation state. These two properties allow a number of low energy decomposition pathways to be available which are denied to main group elements. The most important of the low energy pathways will now be discussed.

The thermal decomposition chemistry of alicyclic complexes is dominated by β -hydride elimination. Whitesides 16 has found that the thermal decomposition of n-butyl(tri-n-butylphosphine)copper(1) proceeds by β -hydride elimination forming 1-butene and an intermediate copper hydride which reduces another copper carbon bond to form butane, tri-n-butylphosphine and copper metal.

In another study Whitesides 17 investigated the thermal chemistry of Di-n-butyl bis(triphenylphosphineplatinum(II).

The products on thermolysis were 1-butene, butane and a platinum(0) species. Figure 2 outlines the proposed mechanism for the decomposition of di(n)butyl bis(triphenylphosphine)platinum(II) by β -hydride elimination.

Figure 2. Decomposition of di-n-butylbis(triphenylphos-phine)platinum(II).

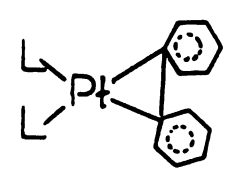
The first step is the loss of a phosphine which leaves a vacant coordination site which a hydride from a β carbon fills in the second step. β -Hydride elimination yields a molecule of 1-butene σ bonded to platinum. The next step is a reductive elimination of a hydride and butyl moiety to form butane. Trapping studies in this system failed to trap any products arising from the formation of butyl radical. Hence Whitesides concluded that free radicals were not involved in their decomposition.

It is also interesting to note that no (less than 1%) octane, the reductive elimination product, was formed.

Another possible thermal decomposition mode is reductive elimination. Semmelheck found that bis(1,5 cyclo-octadiene) nickel (0) would couple aryl halides or alkenyl halides. The following mechanism was proposed.

The key step in biaryl formation is the decomposition of the diarylnickeldihalide by reductive elimination. This is proposed to occur by a concerted cis elimination.

G. B. Young 19 investigated the kinetics and mechanism of the reductive elimination of diaryls from diaryl bis(phosphine)platinum(II) complexes. Reductive elimination is the preferred mode of thermal decomposition in these complexes which occurs by a concerted first order unimolecular reaction. Young envisioned the transition state for this reaction to be a species where the two aromatic rings start bond making at the same time the platinum



aryl bonds are breaking.

In addition to β -hydride elimination and reductive elimination metallacycles can decompose by β - γ carboncarbon bond cleavage. That is, a metallacyclopentane decomposes to a bis(olefin) complex which then loses one or both of the olefins.

$$L_{2}M^{1} \longrightarrow L_{2}M =$$

1,4 tetramethylene bis(cyclopentadienyl)titanium(IV) was thermally decomposed by Whitesides.²⁰ It produced 92 percent ethylene and 8 percent 1-butene.

No reductive elimination (formation of cyclobutane) was reported while β -hydride elimination (formation of l-butene) occurred to only eight percent.

The change of a metallacycle to a bis olefin complex appears to be a reversible process. That is, when bis(cyclopentadienyl) titanium dichloride is reduced to titanocene in the presence of ethylene, a titanacyclopentane

is formed. The titanacycle was trapped with carbon monoxide to give cyclopentanone in 20 percent yield.

Another possible decomposition pathway available to transition metal carbon σ -bonded complexes is α -hydride elimination. This involves migration of a substituent from the α -carbon to the metal with subsequent formation of a metal carbonoid species. The metal carbon double bond then isomerizes via a metal hydride to the primary

alkene and a reduce metal species. α -Hydride elimination is generally less well documented for transition metal carbon σ -bonds than β -hydride elimination is. Otsuka²¹ found from the decomposition of NiBr(ϕ_3 P)₂(CH₂CO₂CH₂CH₃)

prepared in situ from ethyl α -bromoacetate and tetrakis-(triphenylphosphine)nickel(0) that both diethyl fumarate and diethyl succinate were formed. The main product,

$$Ni (\phi_3 P)_4 \xrightarrow{BrCH_2CO_2CH_2CH_3} \phi_3 P \xrightarrow{\phi_3 P} Ni \xrightarrow{CH_2CO_2CH_2CH_3} CH_2CO_2CH_2CH_3$$

diethyl succinate, arises from homolytic cleavage which produces the alkyl coupling product and a reduced nickel species. More interestingly the diethyl fumarate arises from α -hydride elimination with subsequent coupling as in Figure 3.

For completeness one final thermal decomposition pathway is presented. Homolytic cleavage of the metal carbon σ -bond produces free radicals which may then undergo any reaction characteristic of free radicals (coupling, rearrangement, radical abstraction, etc.). Homolysis of transition metal carbon σ bonds is uncommon because it

$$\begin{array}{c} \phi_{3}^{P} \\ \downarrow \\ \phi_{3}^{P} \end{array} \stackrel{\text{CH}_{2}^{CO_{2}Et}}{\longrightarrow} \begin{array}{c} \phi_{3}^{P} \\ Br \end{array} \stackrel{\text{Ni}}{\longrightarrow} \begin{array}{c} CHCO_{2}Et \\ H \end{array} \stackrel{\text{Br-Ni-CHCO}_{2}Et} \\ \longrightarrow \begin{array}{c} CHCO_{2}Et \\ Br-Ni-CHCO_{2}Et \end{array} \stackrel{\text{CH}=CH}{\longrightarrow} \begin{array}{c} CO_{2}Et \\ CO_{2}Et \end{array}$$

Figure 3. α -Hydride elimination pathway.

usually is a more energetic process (higher activation energy) than alternate decomposition pathways. Mercury(II) complexes 22 decompose by this pathway. Divalent mercury complexes may decompose by this process in a concerted or stepwise manner.

Slow
$$HgR_2 \rightarrow RHg \cdot R \cdot$$

Fast
 $RHg \cdot + Hg^\circ + R \cdot$

or $HgR_2 \rightarrow Hg^\circ + 2R \cdot$

The thermal decomposition of Pt(IV) metallacyclopentanes was investigated by Puddephatt. ²³ The decomposition of bis(dimethylphenylphosphine)diiodotetramethylene platinum(IV) in the solid state gives exclusively 1-butene generated by β -hydride abstraction. The probable pathway involves the initial disassociation of a phosphine ligand

$$(CH_3)_2 \stackrel{\text{P}}{\downarrow} \stackrel{\text{I}}{\longrightarrow} \stackrel{\text{CH}}{\longrightarrow} \stackrel{\text{I}}{\downarrow} \stackrel{\text{I}}{\downarrow} \stackrel{\text{I}}{\longrightarrow} \stackrel{\text{I}}{\longrightarrow}$$

followed by β -hydride elimination with subsequent reductive elimination of the hydride and hydrocarbon moiety. The decomposition of α , α 'dipyridyl(iodo)methyltetramethylene platinum(IV) leads to the formation of butenes and methane.

After initial β-hydride elimination the intermediate ½% can reductively eliminate by cleavage of the Pt-H and Pt-CH₃ bonds or by cleavage of the Pt-H and Pt-CH₂ bonds. The cis reductive elimination of the hydride and methylene moiety predominates. l-butene is formed in forty percent and methane is formed in fourteen percent yield. 2-butene is formed in thirty percent yield by isomerizing l-butene.

The thermal decomposition of bis(methyldiphenylphosphine) methyl(iodo)tetramethylene platinum(IV) gives a variety of products with 1-pentene as the major product. In this case initial reductive elimination of the methyl and a methylene from the ring occurs to give the n-pentyl complex $\frac{18}{50}$ which $\frac{18}{50}$ -hydride eliminates to give 1-pentene. The two pathways

$$\begin{array}{c} \begin{array}{c} CH_3 \\ \\ PH \end{array} \end{array} \longrightarrow \begin{array}{c} CH_3 \\ \\ \\ \end{array} \longrightarrow \begin{array}{c} CH_3 \\ \\ \end{array}$$

operating in the preceding example also operate here.

It is interesting to note that no cyclobutane is formed in any of the platinum(IV) decompositions. Puddephatt believes the lack of cyclobutane production from a reductive

elimination process is due to the higher activation energy needed to close the strained ring cyclobutane.

Whitesides 24 prepared and decomposed a series of platinum(II) metallacyclopentanes and compared the rates of thermal decomposition to the appropriate alicyclic platinum(II) complexes. The decompositions were done in methylene chloride solution and were first order to approximately sixty percent decomposition. It was found that the rate of decomposition of bis(triphenylphosphine) tetramethylene platinum(II) was 10⁴ times slower than the rate of thermal decomposition of bis(triphenylphosphine)di-n-butyl platinum(II). Both complexes decompose by β -hydride elimination. Whitesides suggests the increased stability of the platinacyclopentane toward \(\beta - \text{hydride} \) elimination stems from the unfavorable dihedral angle between the metal and β -hydride atom. That is, the optimum dihedral angle for β-elimination is zero degrees which an alicyclic compound can obtain. However, the steric constraints of the metallacycle prevent the dihedral angle from obtaining this optimum value as Figure 4 illustrates. Again, it is interesting that cyclobutane which would come from reductive elimination was not produced.

In a more detailed study Whitesides ²⁵ found that bis-(triphenylphosphine) tetramethylene platinum(II) does not lose a ligand previous to decomposition as both the platinum(IV) and platinum(II) dialkyl complexes do. In



Figure 4. Steric requirements of the metallacycle and alicyclic complex.

fact it was found that added triphenyl phosphine increases the rate of decomposition of platinacyclopentanes while the rate of decomposition of acyclic platinum(II) complexes is decreased by added phosphine.

Bis(tri-n-butylphosphine)tetramethylene platinum(II) 19 decomposes at 120°C in methylene chloride to yield products very different from the triphenylphosphine platinum metallacycle. The reductive elimination product, cyclobutane, was the major product with lessor amounts of butenes and a trace of butadiene. The corresponding bis(tri-n-butylphosphine)diethyl platinum(II) thermally decomposed by β -hydride elimination to give ethylene and

$$Bu_3^P$$
 Pt \longrightarrow \bigcirc

ethane, hence the supporting ligand change is not responsible for the change in products. It was found that the decomposition of 19 in hydrocarbon or ether solvents gave 1-butene as the major product in an analogous manner with the other platinum(II) metallacycles. This reactivity pattern was explained 26 by oxidative addition of a solvent molecule to form a platinum(IV) species. Figure 5 shows the proposed pathway to explain the product distribution. Two generalities concerning the decomposition of platinacyclopentanes are obvious from this work. First, reductive elimination of two alkyl groups occurs readily from platinum(IV) but not from platinum(II). 27 The decomposition of platinum(II) metallacycles is dominated by β-hydride elimination in the absence of other oxidative addition processes. Second, the distribution of linear and cyclic decomposition products from an alkyl tetramethylene platinum (IV) complex is very sensitive to the structure of the starting complex. Several factors may be reflected including the strain involved in cyclobutane formation and the increased stability of platinum-carbon g bonds with electronegatively substituted carbon. 28 The production of cycloalkane is favored when R is electron withdrawing. production of linear products is favored when R is electron donating.

Grubbs et al. 29 prepared and isolated bis(tertiary-phosphine) nickelacyclopentanes. The appropriate

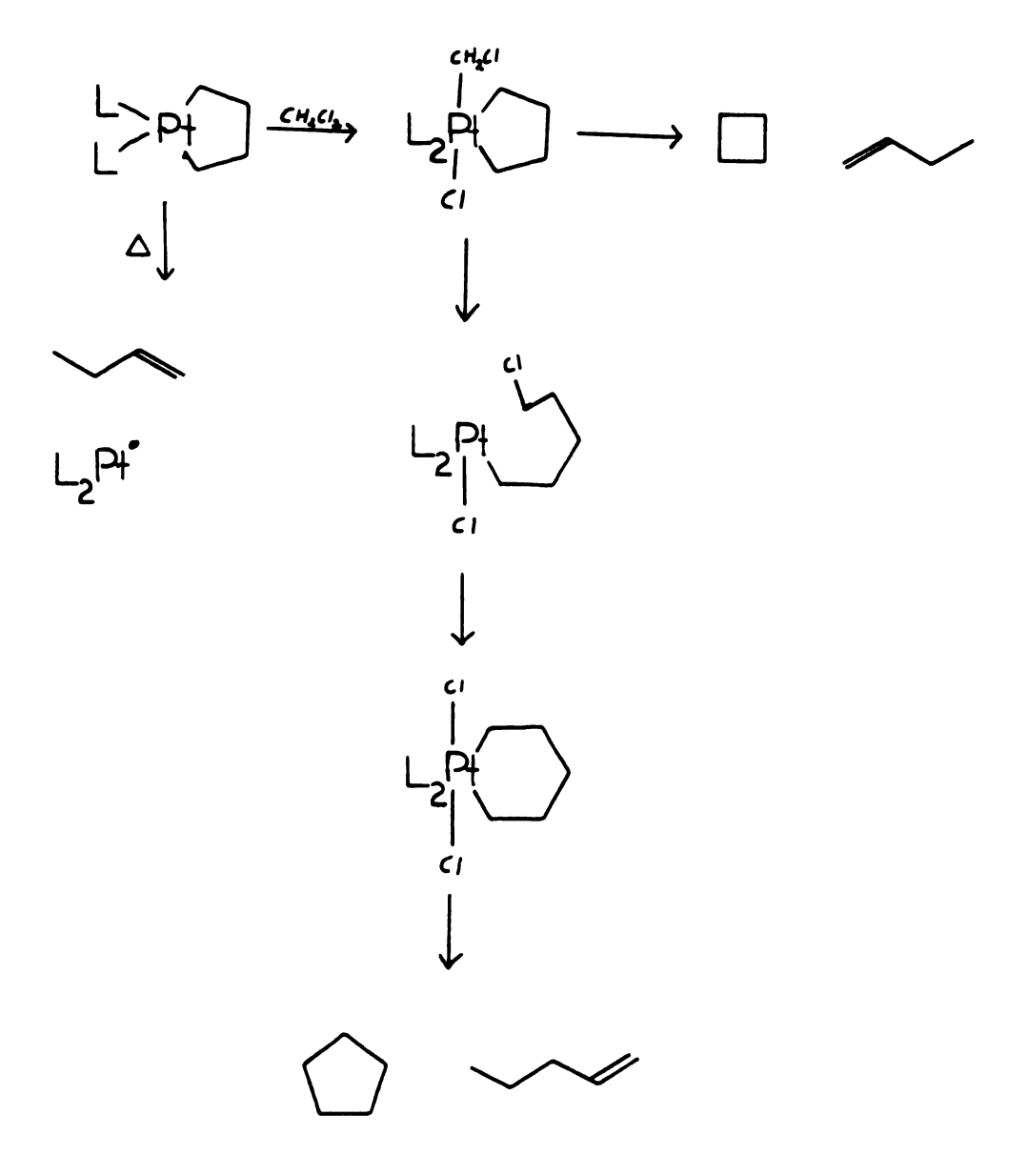


Figure 5. Proposed decomposition pathway for (Bu₃P)₂Pt

$$\begin{array}{c|c}
R = CF_{3} \\
\hline
R = CH_{3}
\end{array}$$

bis(phosphine) nickel dichloride and 1,4-dilithiobutane were mixed at -78°C in ether. As the solution was allowed to warm to -20°C yellow crystals of the metallacycle were formed. The nickelacyclopentanes were characterized as shown in Figure 6.

In an initial study on the decomposition of nickelacyclopentanes Miyashita and Grubbs 30 found that the coordination number of the nickel has a great effect on the decomposition pathway. Three coordinated nickelacycles decompose by β -hydride elimination to give 1-butene. Four coordinated nickelacycles decompose by reductive elimination to give cyclobutane while five coordinated nickelacyclopentanes decompose by β - γ bond cleavage to give

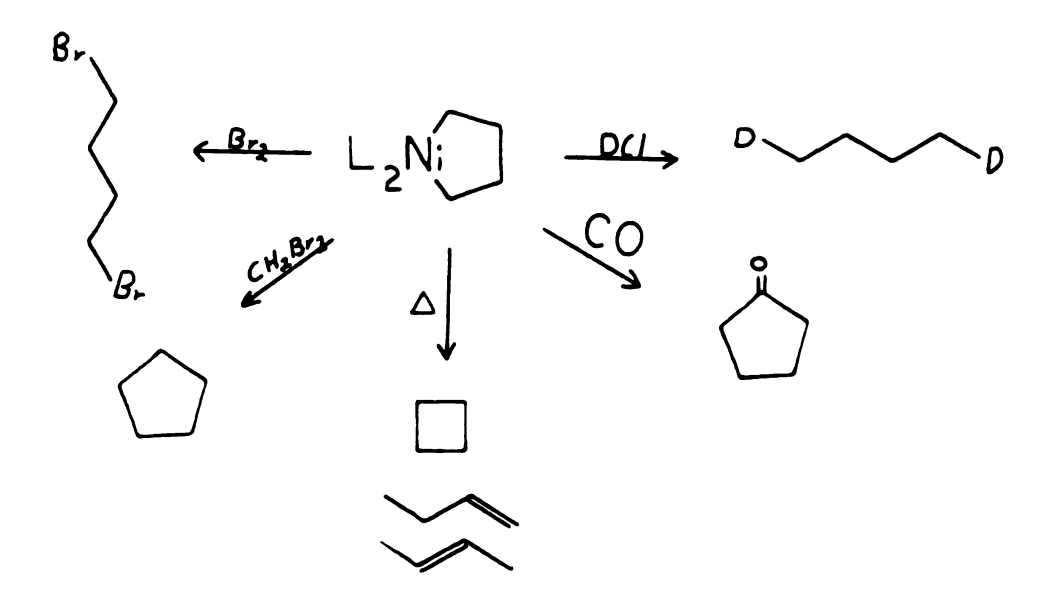
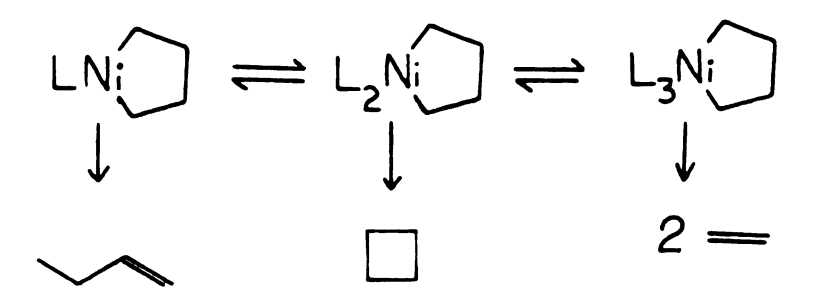
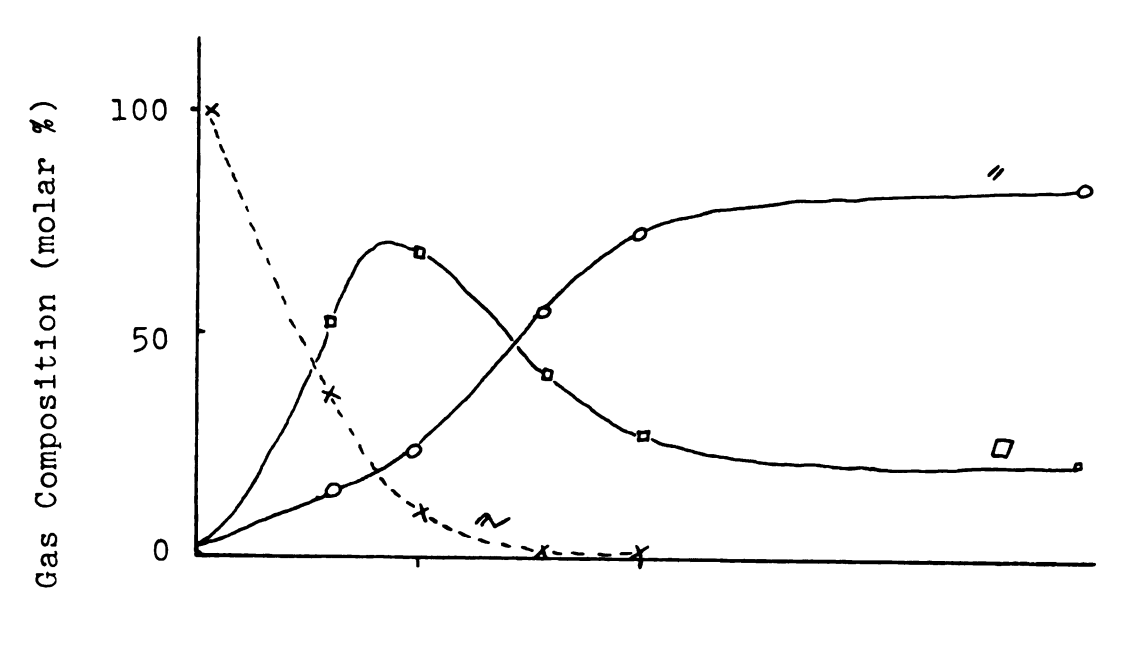


Figure 6. Characteristic reactions of nickelacyclopentanes.



two molecules of ethylene. Figure 9 summarizes the results of a study on the effect of added phosphine on the decomposition of tricyclohexylphosphine tetramethylene nickel(II). Figure 7 is a graph of decomposition gas composition as a function of the amount of added tri-n-butylphosphine. With no added tri-n-butylphosphine the decomposition gas is mostly 1-butene which arises from the three coordinated nickelacycle decomposition with traces of cyclobutane and ethylene. As the amount of added phosphine increases so does the amount of cyclobutane. At a phosphine to nickel ratio of five the cyclobutane in the decomposition gas is at a maximum which implies that the main species in solution is the four coordinated nickelacycle. At higher phosphine to nickel ratios the decomposition gas is mainly ethylene which originates from the decomposition of the five coordinated nickelacyclopentane. This type of behavior is characteristic of bis(monodentate tertiaryphosphine)tetramethylene nickel(II) complexes, but the behavior of chelated phosphine tetramethylene nickel(II) complexes is very



 $[(n-Bu)_3P]$ added

Figure 7. Gas composition as a function of added $(n-Bu)_3P$ for $(Cy_3P)Ni$

different. The corresponding graph of decomposition gas composition as a function of added phosphine shows a different trend as seen in Figure 8 for bis(diphenylphosphino)-ethane tetramethylene nickel(II). The four coordinated

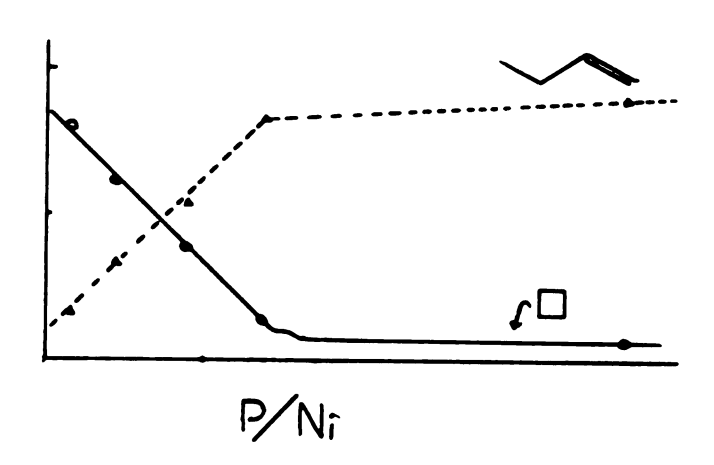


Figure 8. Gas composition versus phosphine/nickel ratio.

The addition of free phosphine causes the amount of cyclo-butane in the decomposition gas to decrease while the amount of butene and butane increases. In the case of the mono-dentate phosphine, ethylene production increased at higher phosphine to nickel ratios rather than butene production as in this case. This apparent incongruent phosphine

effect is explained by the inability of the chelated phosphine metallacycle to form a five coordinated complex. The added phosphine does not complex to the nickel in this case 30 but rather acts as a base to promote β -hydride elimination type products 25 (butenes).

$$\begin{array}{c} L \\ N \end{array} \longrightarrow \begin{array}{c} L_3 N \end{array} \longrightarrow \begin{array}{c} L \\ N \end{array} \longrightarrow \begin{array}{c} N \end{array}$$

In a complimentary ³¹P NMR study³⁰ on bis(triphenyl-phosphine)tetramethylene nickel(II) it was found that free phosphine exchanges with the five coordinated nickela-cyclopentane but it does not involve the square planar

four coordinated nickelacyclopentane. Hence, Grubbs proposed that the bis(phosphine) metallacycle in equilibrium with the tris(triphenylphosphine)metallacycle was the tetrahedral species and not the isolable square planar bis(phosphine) nickelacyclopentane.

$$L_{3}N_{i} \longrightarrow L_{2}N_{i} \longrightarrow L_{3}N_{i} \longrightarrow 0$$

$$\downarrow_{0} \longrightarrow L_{3}N_{i} \longrightarrow 0$$

$$\downarrow_{0} \longrightarrow L_{3}N_{i} \longrightarrow 0$$

In an elegant deuterium labeling study Miyashita and Grubbs³¹ presented evidence for an equilibrium between the tris(triphenylphosphine)tetramethylene nickel(II) and the corresponding bis(ethylene) complex. By labeling the 2 and 5 positions of the ring they were able to obtain tetradeuterated butanes (after quenching) where the labels were in the 2 and 3 positions rather than the 1 and 4 positions. Hence this is direct evidence that the tris(triphenylphosphine)tetramethylene nickel(II) is in equilibrium with the bis(ethylene)bis(triphenylphosphine)nickel(o) complex.

Miyashita and $Grubbs^{32}$ found that bis(triphenylphosphine)-

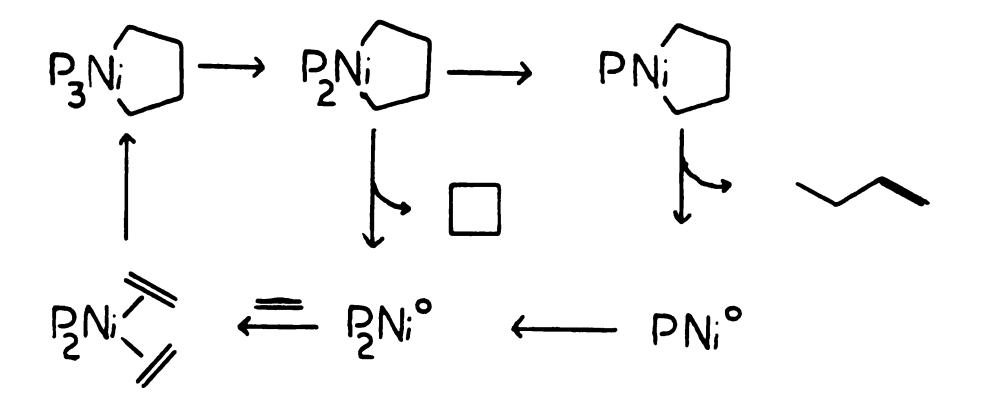


Figure 9. Cyclodimerization of ethylene by $(\phi_3 P)_3 N_1$

tetramethylene nickel(II) in the presence of triphenylphosphine will catalyticly cyclodimerize ethylene to
cyclobutane. Figure 9 summarizes the proposed reaction
sequence. This catalyst system is very different from
traditional nickel oligiomerization catalysts in that no
alkyl aluminum co-catalyst is required.

Bis(phosphine)tetramethylene nickel(II) complexes are a good system for the study of thermal decomposition modes other than β -hydride elimination. The decomposition of nickelacyclopentanes can be controlled to give predominately reductive elimination, β -hydride elimination or β - γ bond cleavage products by changing the coordination number of the nickel. The next section describes the quantification of these decomposition processes. The stability of nickelacyclopentanes makes manipulations possible without necessitating extreme temperatures for

decomposition. The comparisons and contrasts between the platinum and nickelacyclopentanes will be discussed along with experimental findings. The relative stability differences between nickelacyclopentane and nickel alkyls will also be presented.

RESULTS AND DISCUSSIONS

The decomposition kinetics of nickelacyclopentanes were determined by monitoring the appearance of products compared to an internal standard as a function of time. 33 A graph of moles of gas produced versus time yields a curve which increases to a certain value and then levels off. As Figure 10 shows the leveling off corresponds to complete decomposition of the metallacycle. By subtracting the moles of gas produced at a particular time from the total moles of gas produced after complete decomposition the amount of complex remaining at any particular time can be obtained. It is this value (Mr) which was used to obtain the rate constants. That is, the graph of the logarithm of the moles of complex remaining versus time gave a linear relationship which is expected for a first order unimolecular reaction. The relationship between moles of complex remaining and time was linear to at least fifty percent reaction with 80-90 percent reaction being typical.

The activation parameters were calculated from Eyring's transition state theory. The entropy of activation $\Delta S^{\not =}$ was calculated from

$$\Delta S^{\neq} = 4.576 \log (^{K}/T) + (^{E}/T) - 49.21$$

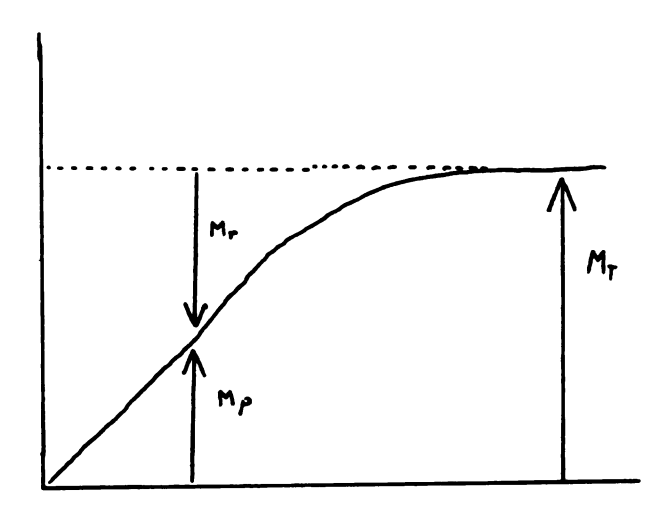


Figure 10. Moles of decomposition gas as a function of time.

where K is the rate constant at temperature T and E is the activation energy in calories/mole. The value of T used was a midpoint value of the temperature range studied. The enthalpy of activation ΔH^{\neq} was calculated from

$$\Delta H^{\neq} = E^{\neq} - RT$$

and the free energy of activation ΔG^{\neq} was calculated from

$$\Delta G^{\neq} = \Delta H^{\neq} - T\Delta S^{\neq}$$

The slopes of the rate constant plots (logarithm of the concentration of complex remaining versus time) were obtained from the best least square fitted line. The slope of the Arrhenius graphs (logarithm of the rate constants versus the inverse of the temperature) were also least squares fitted by the use of a Texas Instrument Ti-55 calculator.

The nickelacyclopentane decomposition kinetics described here are most conveniently divided into four classes: three coordinated, four coordinated, five coordinated, and chelated metallacycles.

Four Coordinated Nickelacyclopentanes

Four coordinated nickelacyclopentanes decompose by reductive elimination to give cyclobutane. Bis(triphenyl-phosphine)tetramethylene nickel(II) was decomposed at a temperature range of 19 to 40°C. Table 1 summarizes the

Table 1. Rate data for $(\phi_3 P)_2$ Ni

Temperature	Rate Constants	Half Life
19°C	$3.2 \times 10^{-5} \text{ sec}^{-1}$	361 mins
30°C	$1.2 \times 10^{-4} \text{ sec}^{-1}$	77 mins
40°C	$4.6 \times 10^{-4} \text{ sec}^{-1}$	22 mins

rate constants, half lives, and temperatures. Figures 11 and 12 show the first order rate plots of the logarithm of the concentration of undecomposed nickelacyclopentane as a function of time. Figure 13 is the Arrhenius plot. That is, a graph of the logarithm of the rate constants against the inverse temperature. The Arrhenius plot slope is 1.15×10^4 . Multiplication of this by the gas constant gives the activation energy. The activation energy was found to be 23 Kcals/mol. Table 2 summarizes the activation

Table 2. Activation parameters for $(\phi_3 P)_2 Ni$

	ΔE [≠]	ΔS [≠]	∆H [≠]	ΔG [≠]
(\$\phi_3P)_2Ni	23 Kcals/ mol	-2.3 eu	22 Kcals/ mol	23 Kcals/ mol

parameters for bis(triphenylphosphine)tetramethylene nickel(II).

It is interesting to compare these values with the corresponding data for bis(triphenylphosphine)dimethyl nickel(II). This complex also thermally decomposes by reductive elimination to give ethane. Table 3 summarizes the kinetics and activation parameters for bis(triphenylphosphine)dimethyl nickel(II). Figure 14 and 15 are the rate constant plots while Figure 16 is the Arrhenius plot. Two significant

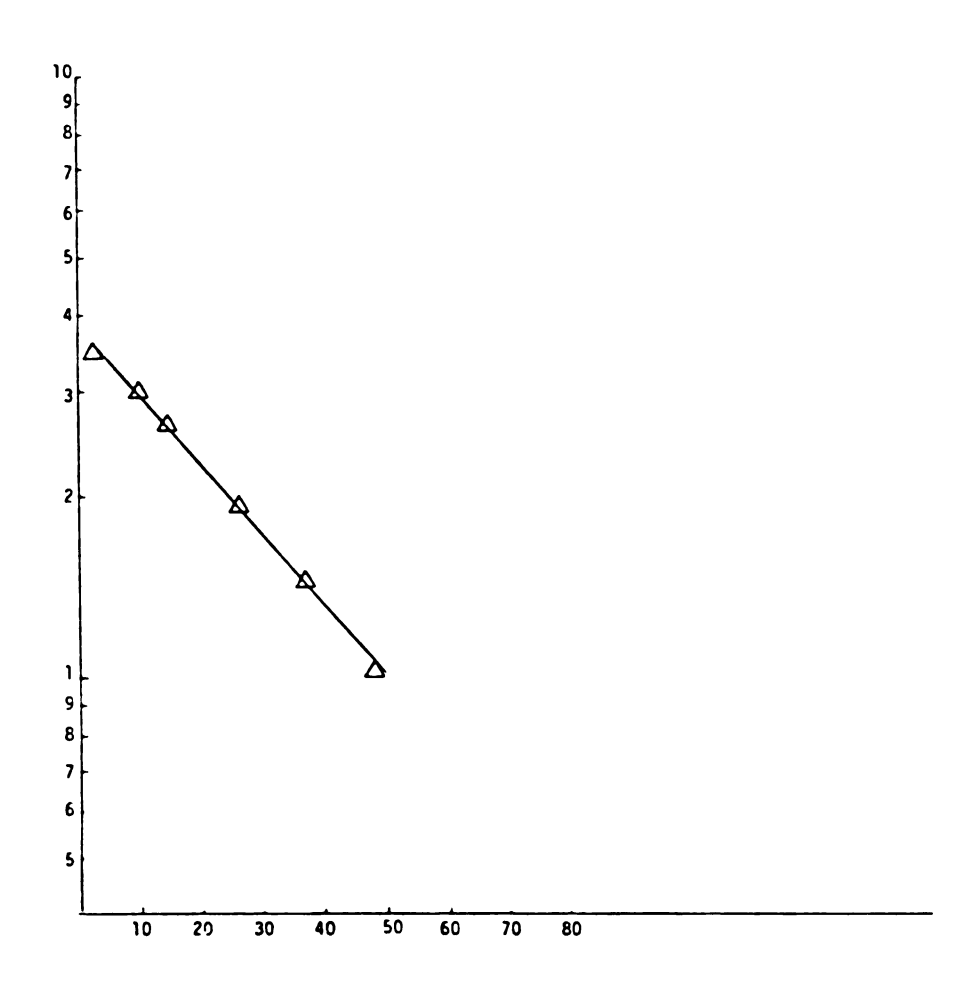


Figure 11. Log $[(\phi_3 P)_2 N i)$ as a function of time in minutes at $40 \, ^{\circ} C$.

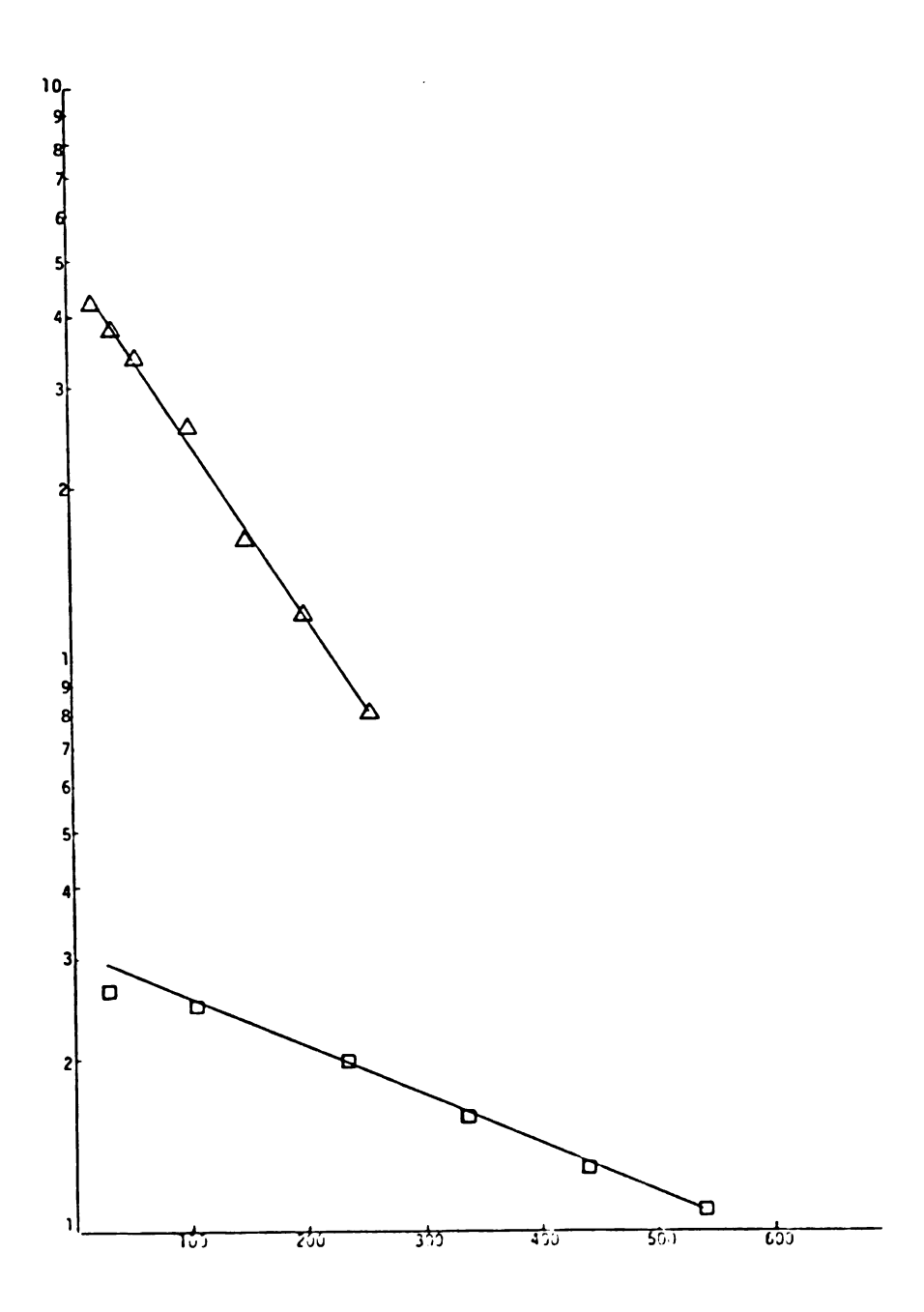


Figure 12. Log $[(\phi_3 P)_2 Ni)$] as a function of time in minutes at 30° (Δ) and 19°C (\square).

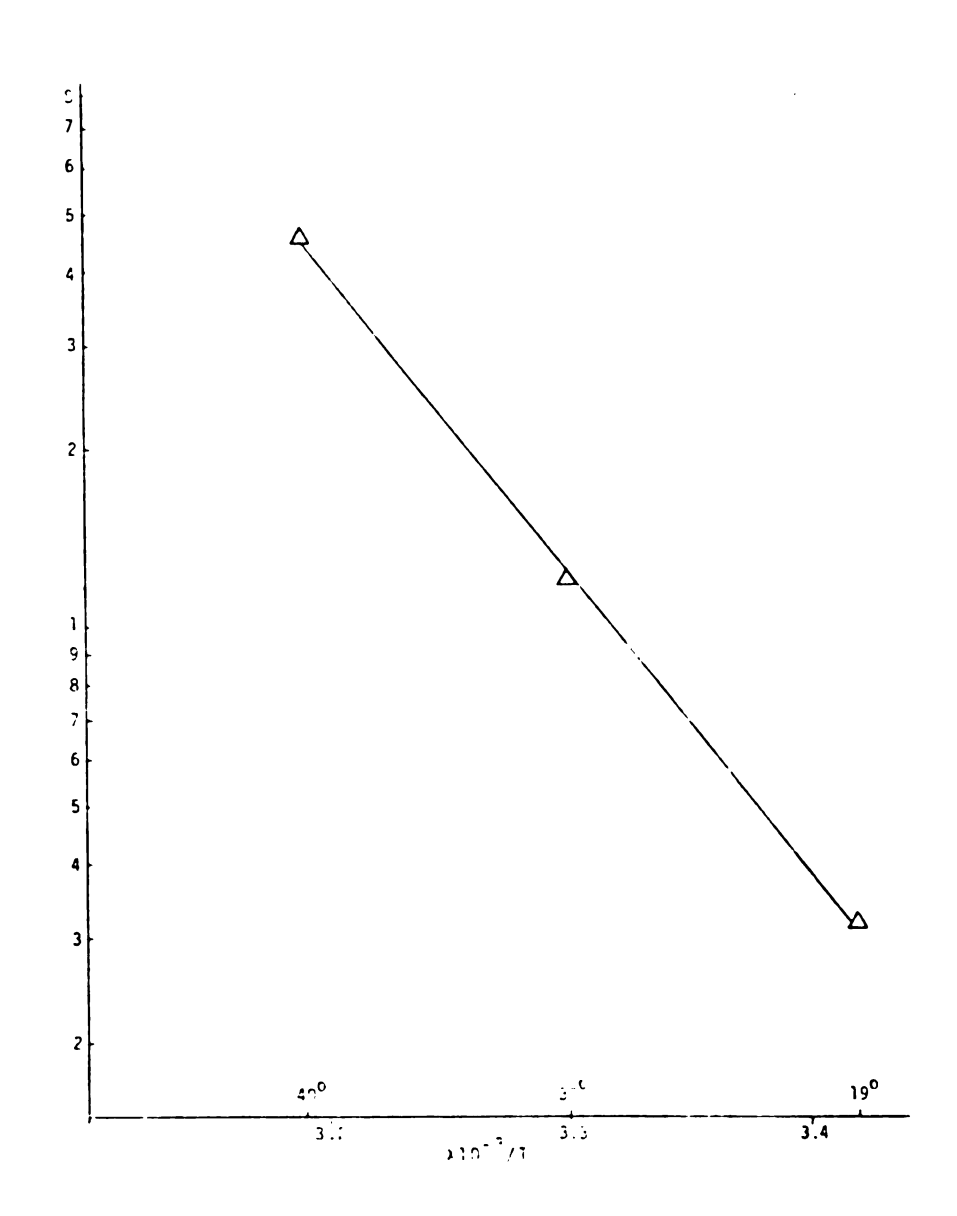


Figure 13. Arrhenius plot for $(\phi_3 P)_2$ Ni .

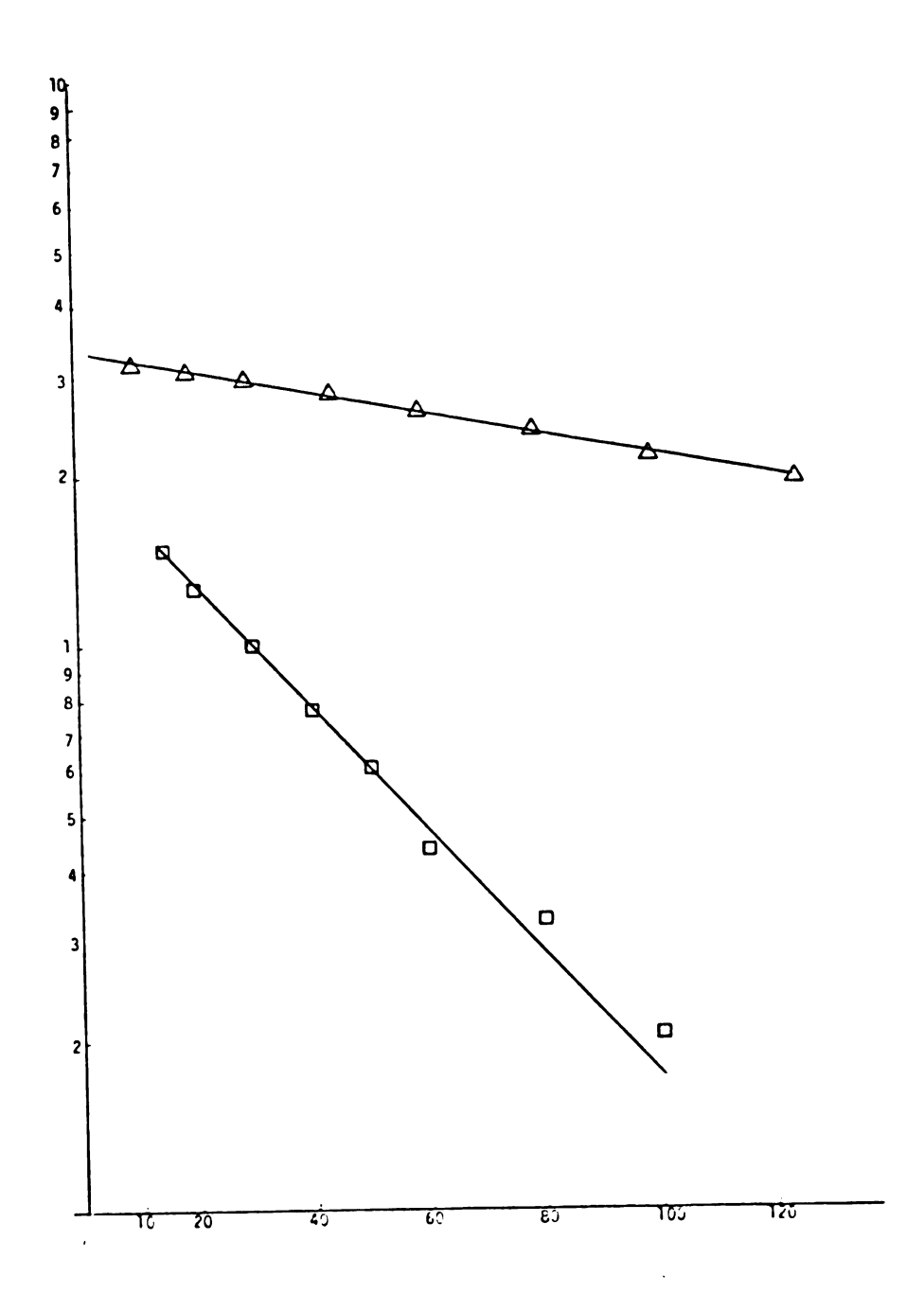


Figure 14. Log $[(\phi_3 P)_2 ^{Ni(CH_3)}_2]$ as a function of time in minutes at 6° (Δ) and 20°C (\square).

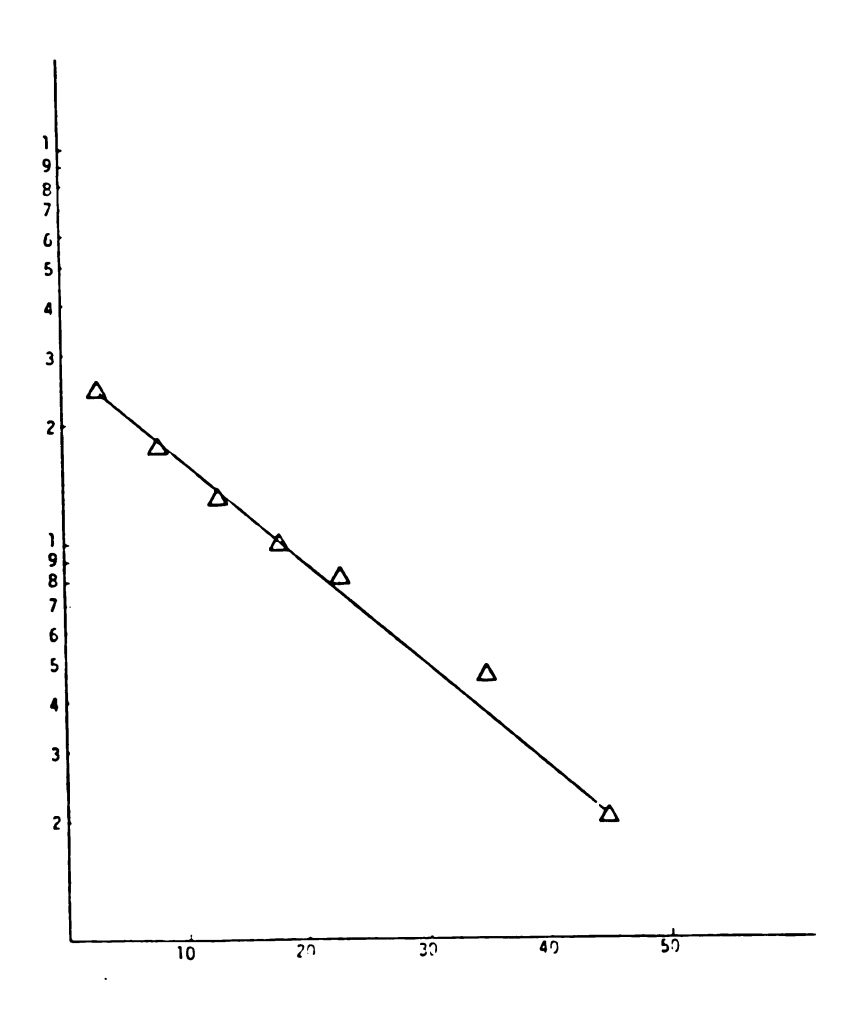


Figure 15. Log $[(\phi_3P)_2Ni(CH_3)_2]$ as a function of time in minutes at 30°C.

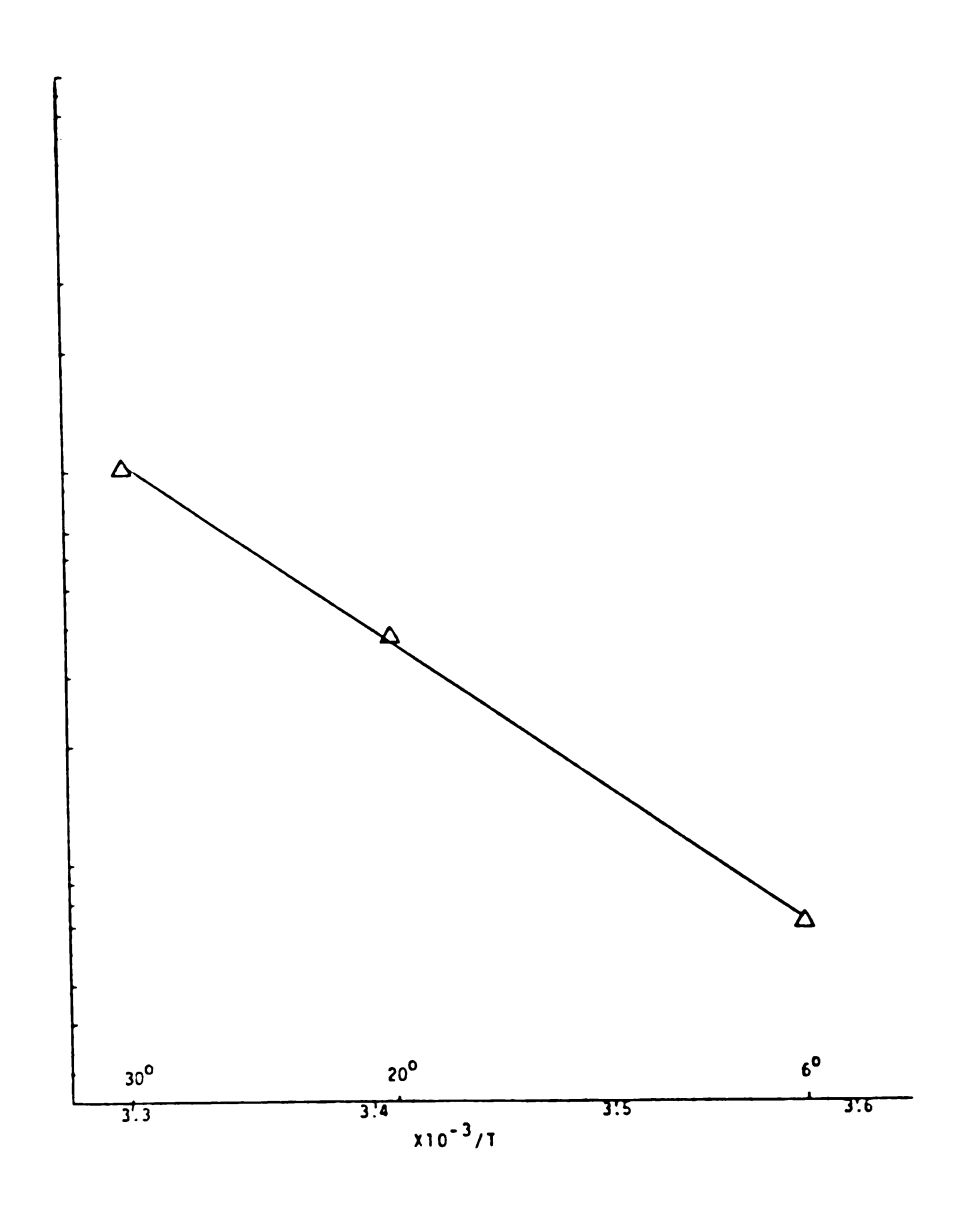


Figure 16. Arrhenius plot for $(\phi_3P)_2Ni(CH_3)_2$.

Table 3. Kinetics and activation data for $(\phi_3P)_2Ni(CH_3)_2$

Temp.	Rate Constant	Half Life	E≠	ΔS₹	∆H≠	ΔG [≠]
30°	1.0x10 ⁻³	11.5 min	19	-12.7 eu	18.	22.
20 °	3.7×10^{-4}	31 min				
6°	7.0×10^{-5}	165 min	Kcal/mol			

points need to be mentioned. First, the rate of thermal decomposition of bis(triphenylphosphine) dimethyl nickel(II) is twelve times faster than the rate for the metallacycle. This is similar to the trend Whitesides 26 found for β-hydride elimination for bis(triphenylphosphine(di-n-butyl) platinum(II) and the corresponding metallacycle. Second, the thermal decomposition activation energy for the dimethyl nickel complex is 4 Kcals/mol lower than for the metallacycle. Both of these differences can be accounted for by considering the nature of the organic moiety formed during the decomposition reaction. The formation of the highly strained cyclobutane molecule is a more energetic process than the formation of the stable ethane molecule.

Chelated Nickelacyclopentanes

Ethylene bis(diphenylphosphine)tetramethylene nickel(II) is a four coordinated complex which decomposes by reductive

elimination to form cyclobutane. The diphos metallacycle is considerably more stable both to heat and oxidation than the triphenylphosphine metallacycle. This light yellow metallacycle was decomposed at temperatures ranging from 80° to 100°C. The half lives, rate constants, and activation parameters are shown in Table 4. Figure 17 and 18 are the graphs of the logarithm of the remaining complex versus time while Figure 19 is the Arrhenius plot.

Table 4. Rate data and activation parameters for $\stackrel{\mathcal{C}}{\stackrel{\wedge}{\cap}} N_i$ $\stackrel{\wedge}{\stackrel{\vee}{\cap}} Q_2$

Temp.	Rate Constant	Half Life	E [≠]	ΔS≠	ΔH≠	ΔG≠
80	1.5x10 ⁻⁵ sec ⁻¹	770 min	37	21	36	28
90	7.0×10^{-5}	165	in Kcals/mol			
100	2.4x10 ⁻⁴	48				

The activation energy for thermal decomposition by reductive elimination for ethylene bis(diphenylphosphine)—tetramethylene nickel(II) is 37 Kcal/mol. This is significantly higher than 23 Kcal/mol found for bis(triphenylphosphine)tetramethylene nickel(II). The increase of 14 Kcal/mol can be accounted for by considering the reorganization of the nickel phosphine complex during the reduction.

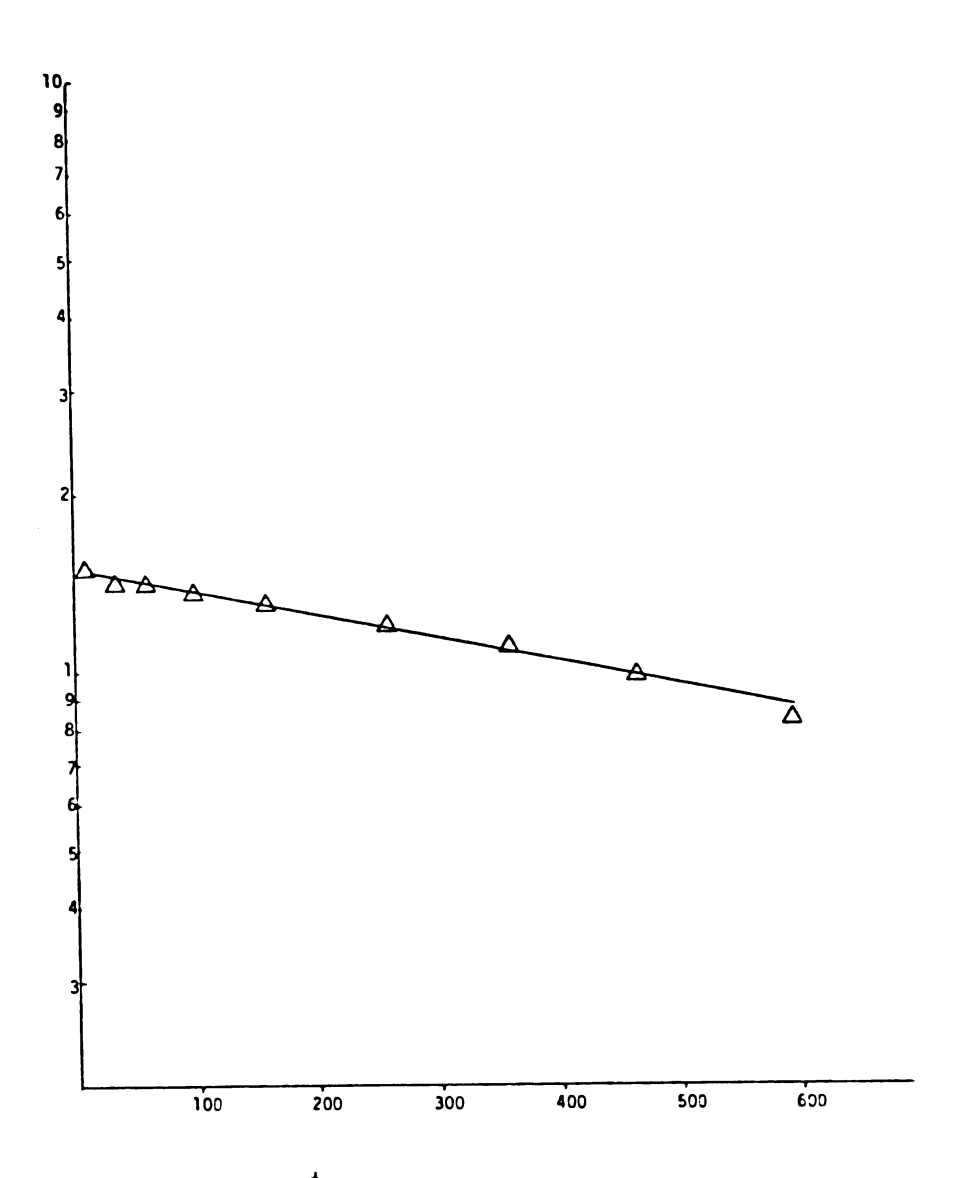


Figure 17. Log [$\stackrel{\phi_2}{P}$ Ni] as a function of time in minutes at 80°C.

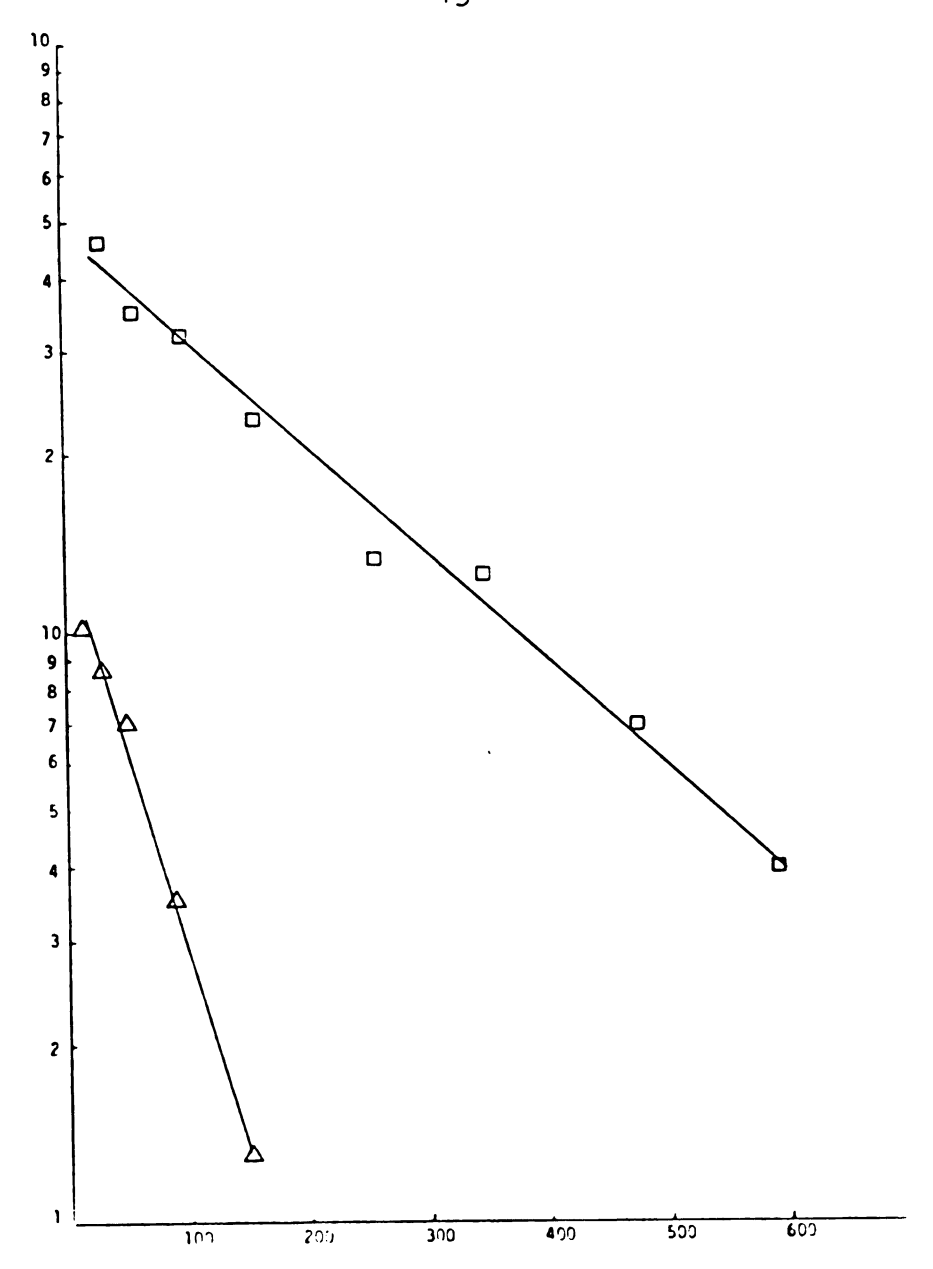


Figure 18. Log [$\stackrel{\varphi_2}{\stackrel{P}{\longrightarrow}}$ Ni $\stackrel{}{\bigcirc}$] as a function of time in $\stackrel{\varphi_2}{\stackrel{\varphi_2}{\longrightarrow}}$ minutes at 90° (\square) and 100° (\triangle).

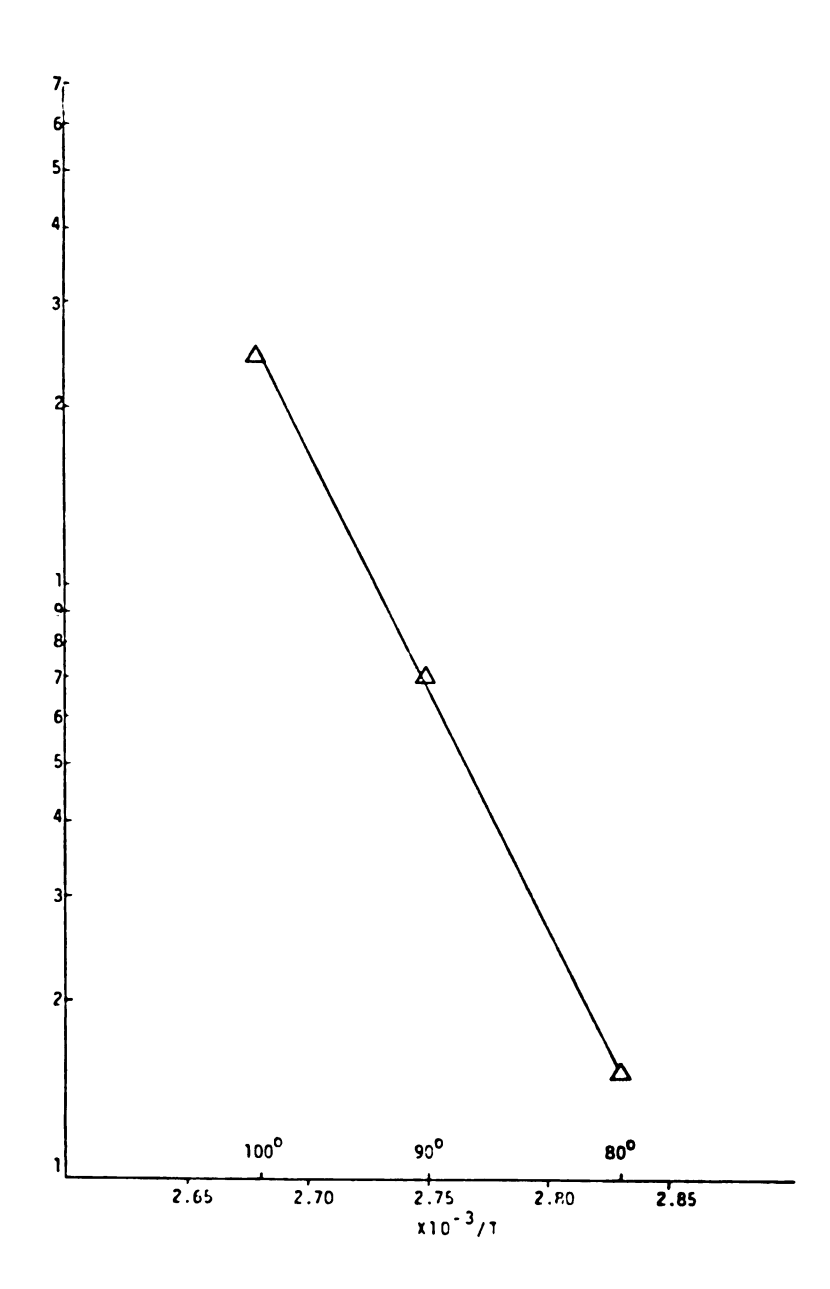


Figure 19. Arrhenius plot for $\begin{bmatrix} P \\ P \end{bmatrix}$ Ni

During the decomposition the nickel is reduced from four coordinated nickel(II) to a two coordinated nickel(o).

V.S.E.P.R. theory³⁵ predicts the two coordinated nickel(o) to be linear.³⁶ Hence as the reductive elimination occurs the phosphine ligands swing open from their square planar arrangement to a linear one. This opening up of the bond angle is quite easy for the triphenyl phosphine case but is considerably harder for the diphos metallacycle. Figure 20 illustrates the reorganization during the thermal decomposition for both cases.

$$\begin{array}{c}
P \\
P
\end{array}$$

$$\begin{bmatrix}
P \\
N
\end{bmatrix}
\rightarrow
\begin{bmatrix}
P \\
N
\end{bmatrix}$$

Figure 20. Reorganization of the metallacycles during thermal decomposition.

By changing the size of the hydrocarbon bridge between the two phosphines of the chelate a variation in activation energy with ring size is expected. Unfortunately, the bis(diphenylphosphine)methane metallacycle could not be prepared. The bis(diphenylphosphine)methane reacts with nickel dichloride as a monodentate ligand rather than as a bidentate ligand, ³⁶ hence only dimeric bis(diphenylphosphine) methane nickel dichloride species could be prepared. However, the larger chelate metallacycle, propylene bis(diphenylphosphine)tetramethylene nickel(II) was prepared. It also has a similar reactivity as the diphos nickelacyclopentane. It was decomposed at 90° to 110°C. Table 5 presents the kinetics and activation data.

Table 5. Rate data and activation parameters for

Φ_2	
	_
(PN:	ر
Φ_2	

Temp.	Rate Constant	Half Life	E≠	∆S≠	∆H≠	ΔG [≠]	
90	2.3x10 ⁻⁵	502	35	15	35	29	
100	8.2×10^{-5}	141	in Kcal/mol				
110	2.8x10 ⁻⁴	41					

Figure 21 is the rate constant plot for propylene bis(diphenylphosphine)tetramethylene nickel(II) and Figure 22 is

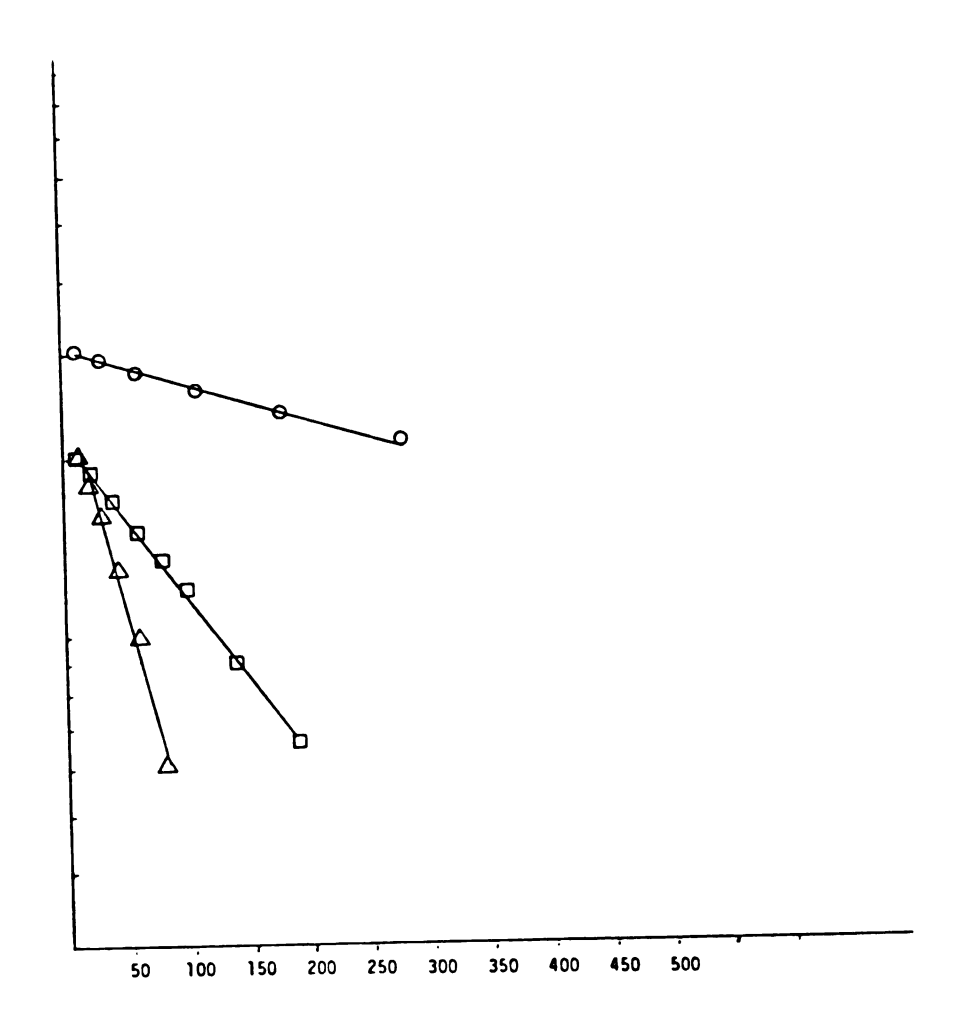


Figure 21. Log [$\stackrel{P}{\searrow}$ Ni] as a function of time in min- $\stackrel{\phi_2}{\searrow}$ utes at 90° (o), 100° (\square) and 110°C (\triangle).

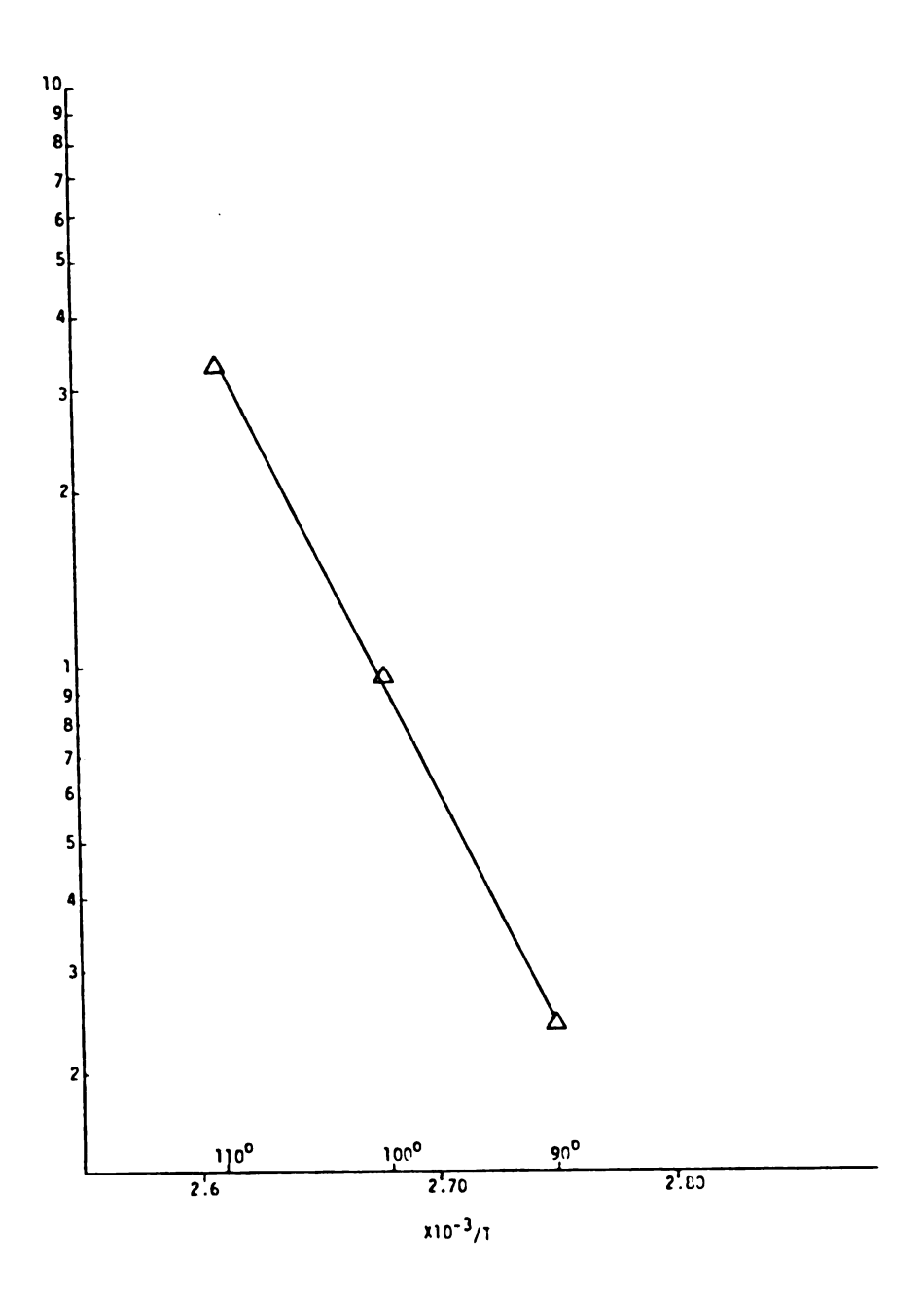


Figure 22. Arrhenius plot for P Ni ϕ_2

the Arrhenius plot for this system.

The activation energy for propylene bis(diphenylphos-phine)tetramethylene nickel(II) is lower than for ethylene bis(diphenylphosphine)tetramethylene nickel(II). They have activation energies of 35 and 37 Kcal/mol, respectively. The difference in ring flexibility between the five and six membered ring of the chelated ligand is significant. That is, the more flexible propylene bis(diphenylphosphine)tetramethylene nickel(II) has a lower activation energy than the smaller, more rigid chelate ring compound.

The α,α ' dipyridyl tetramethylene nickel(II) also thermally decomposes by reductive elimination to yield cyclobutane. This complex is a dark green extremely air sensitive crystalline solid. The decomposition temperature studied ranged from 60 to 80°C. As seen in Table 6

Table 6. Rate data and activation parameters for

Temp.	Rate Constants	Half Lives	E≠	ΔS [≠]	∆H≠	ΔG [≠]
60	6.9x10 ⁻⁷ sec ⁻¹	279	42	38	42	29
65	$1.6 \times 10^{-6} \text{sec}^{-1}$	120	in Kcals/mol			
70	4.5×10^{-6}	43				
80	2.6x10 ⁻⁵	7.5 hrs				

the temperature range was such that the rate constants are considerably smaller and the half lives are considerably larger than the previous cases. The rate constant graphs are Figure 23 and 24 and the Arrhenius plot is Figure 25. The activation energy for decomposition is 42 Kcal/mol.

The dipyridyl ligand is more rigid than the chelated phosphine ligands discussed earlier. The increase in activation energy for decomposition may reflect the increase rigidity of the supporting ligands.

If the stiffness of the supporting ligand is an important factor then a supporting ligand such as 1,10-phenanthroline should give the complex an even higher activation energy for decomposition. Initial studies over the limited temperature range of 70 to 80°C yielded an activation energy for reductive elimination of 45 Kcal/mole. Figure 26 gives the rate data and Figure 27 is the Arrhenius plot for the decomposition of 1,10-phenathroline tetramethylene nickel(II).

The relative activation energy ordering for the five nickelacyclopentanes discussed is supported by the trans³⁷ influencing ability of the ligands. The ligands with a weak trans directing effect (such as dipyridyl and 1,10-phenathroline) do not greatly weaken the trans nickel-carbon bonds and hence have a high thermal decomposition activation energy. The phosphine ligands, on the other hand, have a greater trans effect and weaken the trans

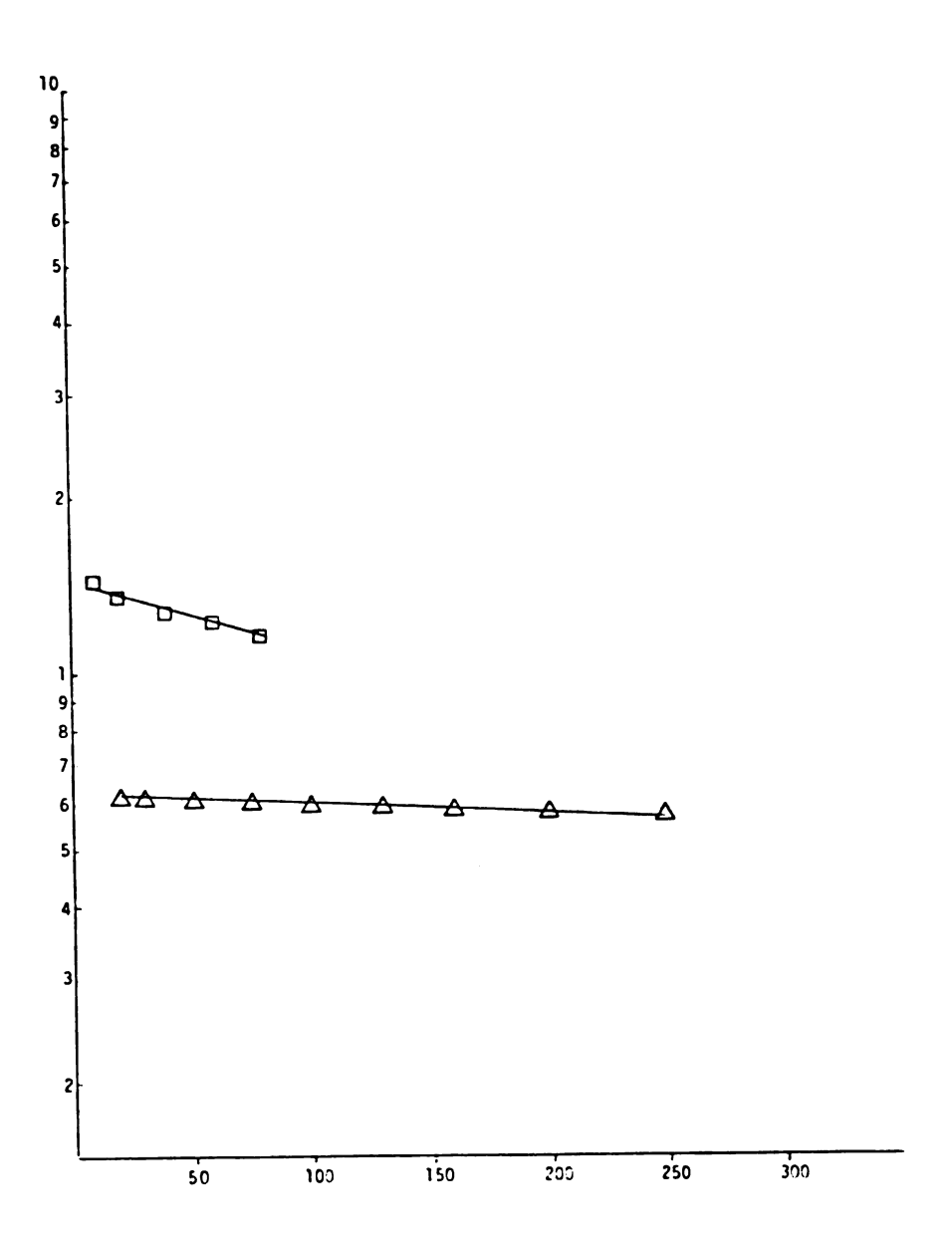


Figure 23. Log [(dipy)Ni] as a function of time in minutes at 80° (\Box) and 60°C (\triangle).

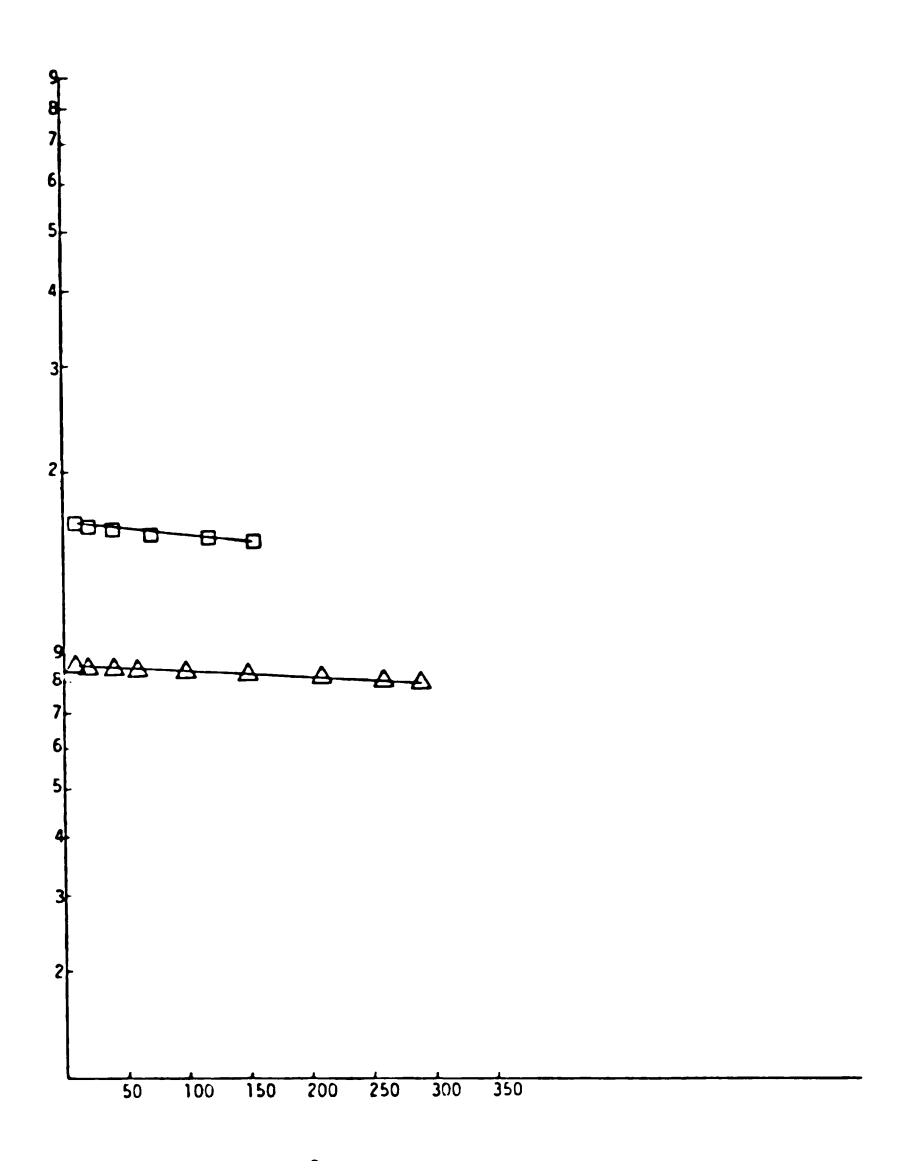


Figure 24. Log [(dipy)Ni] as a function of time in minutes at 65° (Δ) and 70°C (\Box).

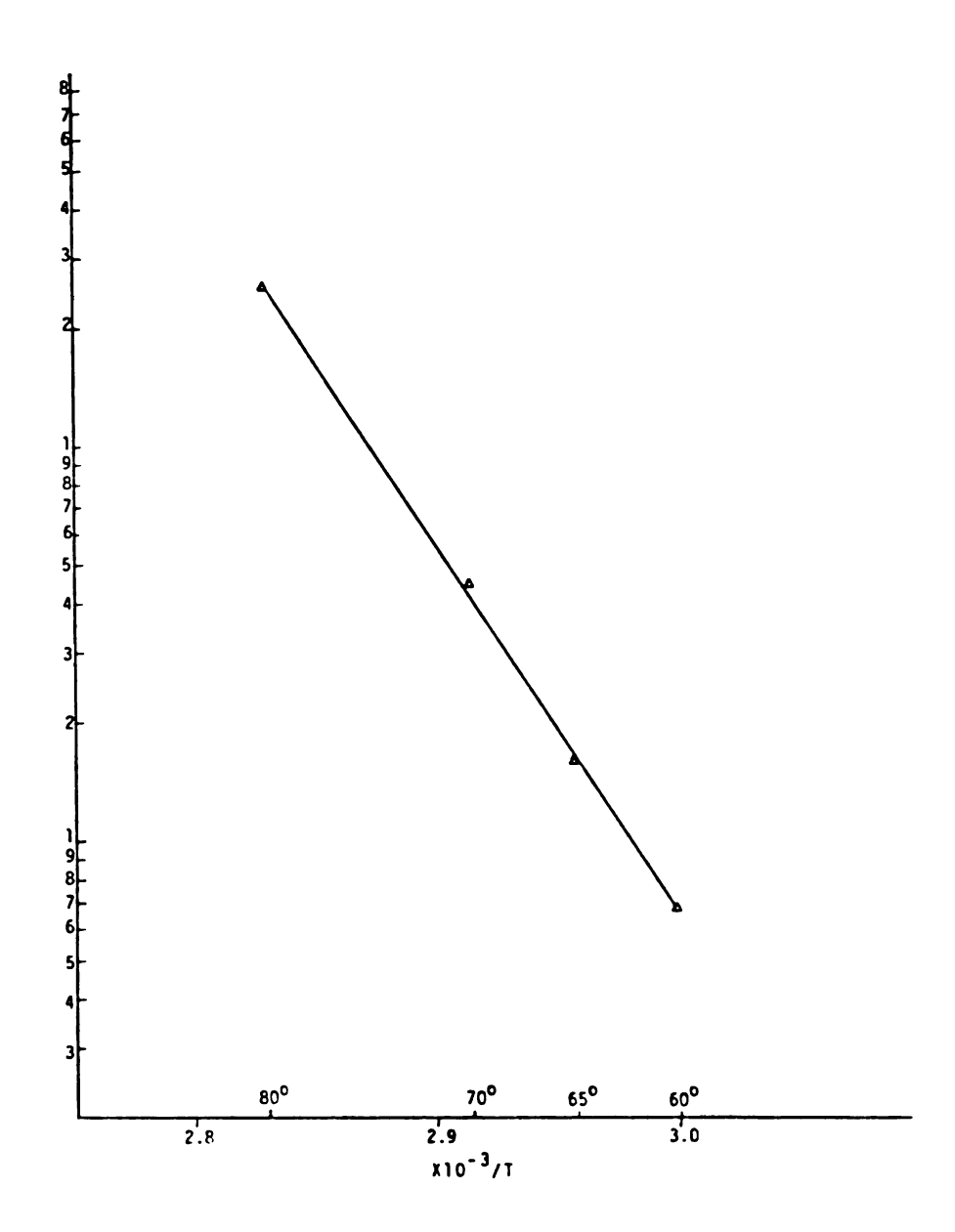


Figure 25. Arrhenius plot for (dipy)Ni .

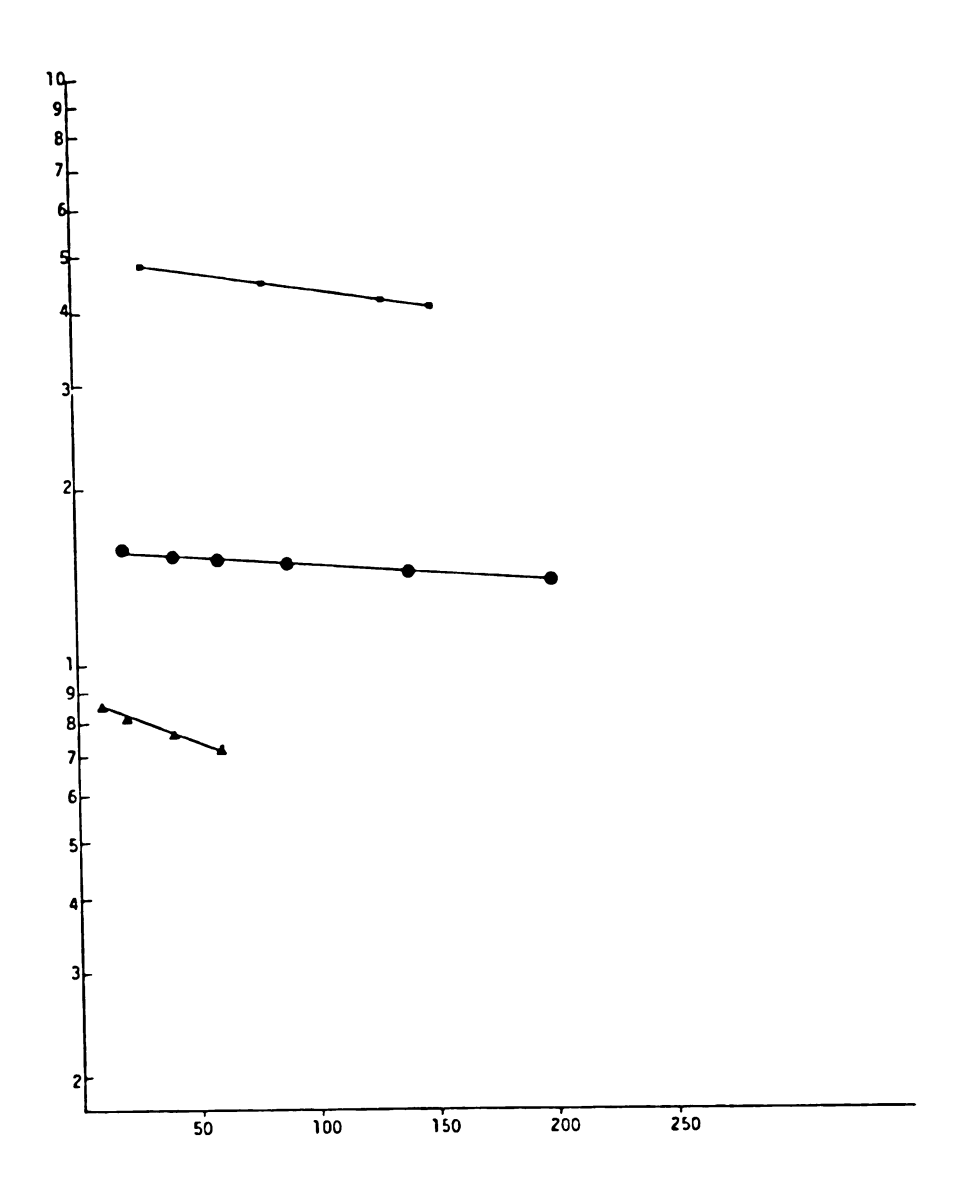


Figure 26. Log [(1,10-phen)Ni] as a function of time in minutes at 75° (\square), 70° (\bigcirc) and 80°C (\triangle).

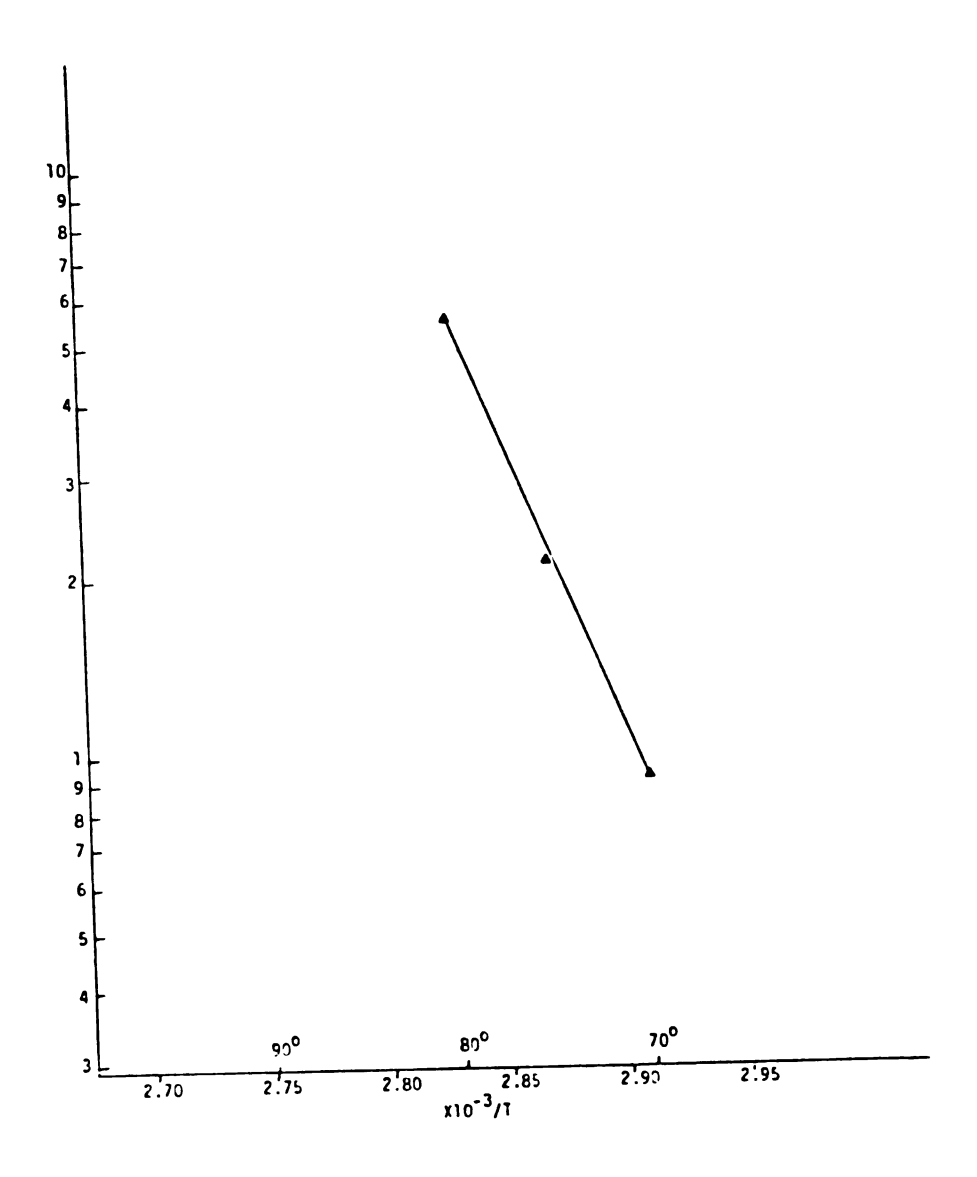


Figure 27. Arrhenius plot for (1,10-phen)Ni

nickel-carbon bonds. Because of the weakened carbonnickel bonds in the phosphine complexes a lower thermal decomposition activation energy is found.

Even though the crystal field stabilization energy interpretation of stability of organometallic complexes is not deemed as important as it once was, it, nevertheless, might be instructive to discuss the nickelacyclopentanes in terms of it. In particular, a comparison of ethylene bis(diphenylphosphine)tetramethylenenickel(II) and dipyridyl tetramethylene nickel(II) is interesting. In Figure 28 the d orbital energy spacing is shown for a

Figure 28. Relative d orbital energy levels for nickel(II).

square planar complex. Nickel(II) is a d^8 species so the energy difference between the dxy and the dx^2-y^2 orbitals is the energy gap of interest. That is, the dxy is the highest occupied orbital and dx^2-y^2 is the lowest unoccupied orbital.

Chatt³⁸ has measured the ultraviolet and visible spectra of a series of trans[L, piperidine $PtCl_2$] complexes. It was found that tri-n-propylphosphine is a stronger ligand than piperidine. The difference in energy between the dxy and dx^2-y^2 orbitals for the two complexes was found to be approximately 3 Kcal/mol. The crystal field effect of tri-n-propylphosphine and triphenylphosphine are very similar. Dipyridyl³⁹ is a stronger field ligand than piperidine. Hence the crystal field effects of dipyridyl and triphenylphosphine are very similar. That is, the energy difference between the dxy and dx^2-y^2 orbitals for the triphenylphosphine and dipyridyl nickelacycles should be very similar.

Yamamoto 40 has measured the activation energy for the thermal decomposition of dipyridyl di-n-propyl nickel(II). The complex was thermally decomposed in the solid state to give equal amounts of propane and propylene which are the β -hydride elimination products. The activation energy was found to be 16 Kcal/mol. A comparison with the corresponding dipyridyl metallacyclopentane shows the metallacycle to be more stable to thermal decomposition by 26 Kcal/mol. The increased stability most likely arises from the inhibition of β -hydride elimination in the metallacycle by the steric constraints of the alkyl ring.

Three Coordinated Nickelacyclopentanes

Molecular weight determination by the freezing point depression of benzene indicates that bis(tri-n-butylphos-phine)tetramethylene nickel(II) is three coordinated in solution. The yellow complex is extremely air sensitive and rather difficult to manipulate. Tri-n-butylphos-phine tetramethylene nickel(II) decomposes in toluene solutions by β -hydride elimination at a temperature range of 20 to 40°C. Table 7 shows the kinetics data as well as

Table 7. Rate data and activation parameters for (n- $Bu_3P)Ni$

Temp.	Rate Constant	Half Life	E≠	ΔS≠	∆H≠	ΔG≠
20	1.7x10 ⁻⁵ sec ⁻¹	680 min	35	36 eu	34	23
30	$1.3 \times 10^{-4} \text{ sec}^{-1}$	89 min	Kcal/ mol		Kcal/ mol	Kcal/ mol
40	$8.1 \times 10^{-4} \text{ sec}^{-1}$	14 min				

the activation parameters. Figure 29 to 31 are of the logarithm of the concentration of tri-n-butylphosphine-tetramethylene nickel(II) as a function of time and Figure 32 is the Arrhenius plot. The activation energy for this

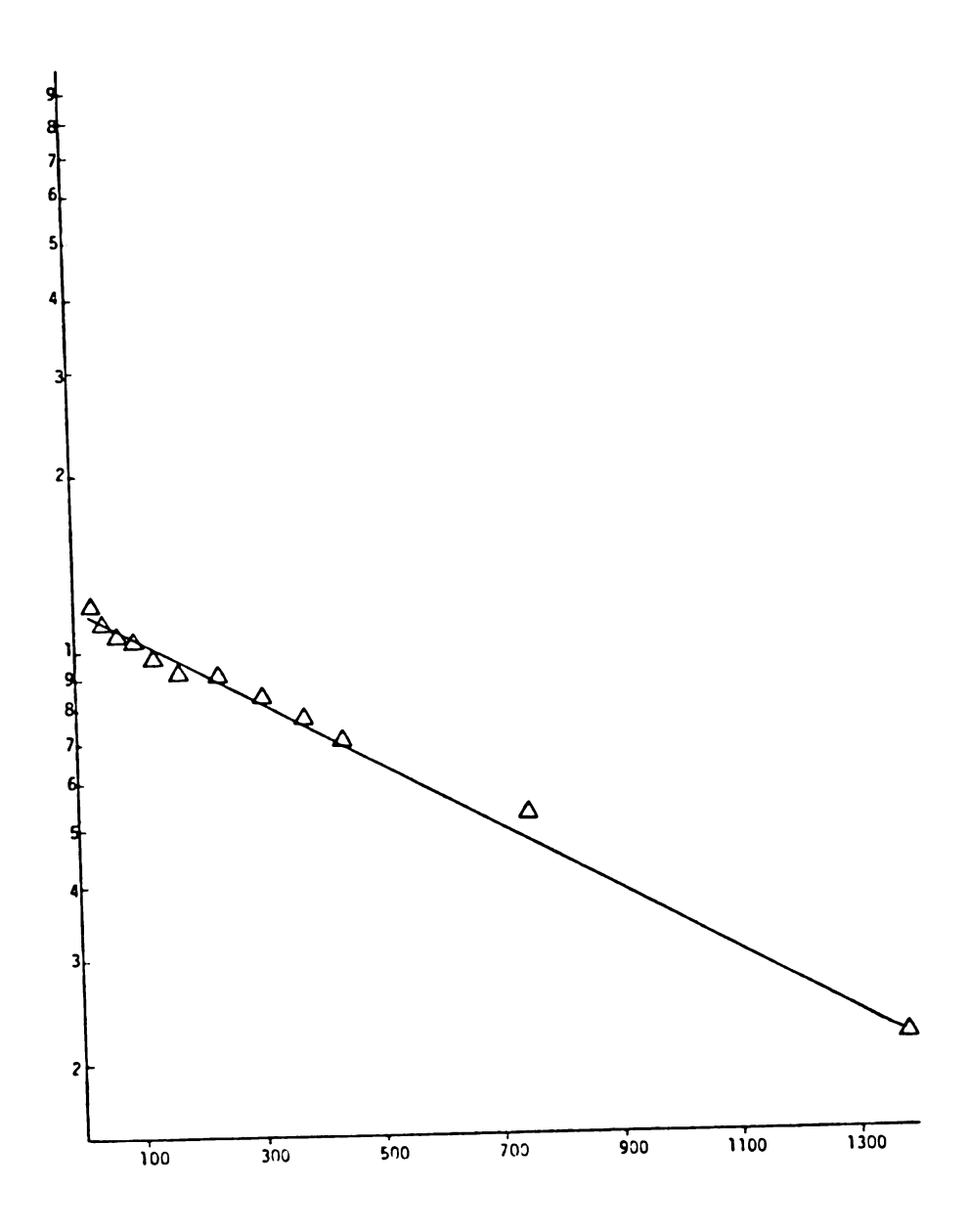


Figure 29. Log [(nBu₃P)₂Ni] as a function of time in minutes at 20°C.

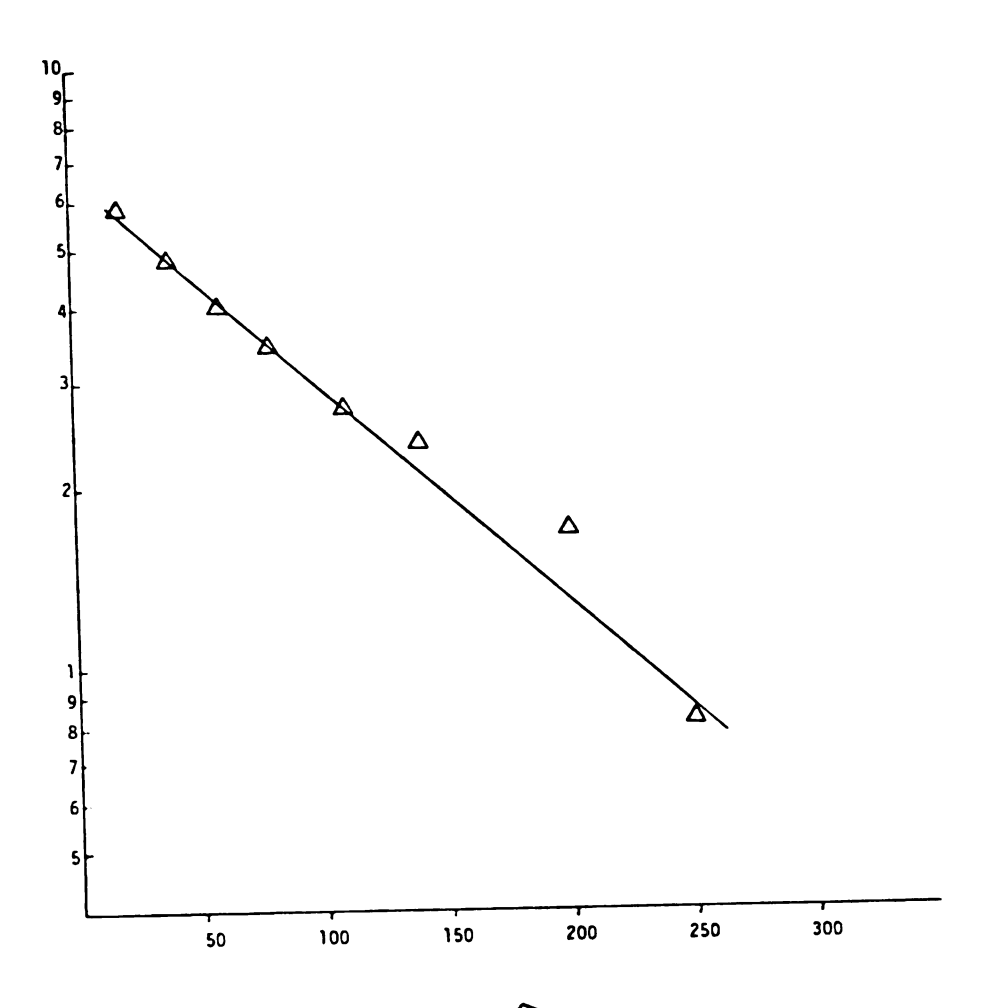


Figure 30. Log $[(n-Bu_3P)_2Ni \bigcirc]$ as a function of time in minutes at 30°C.

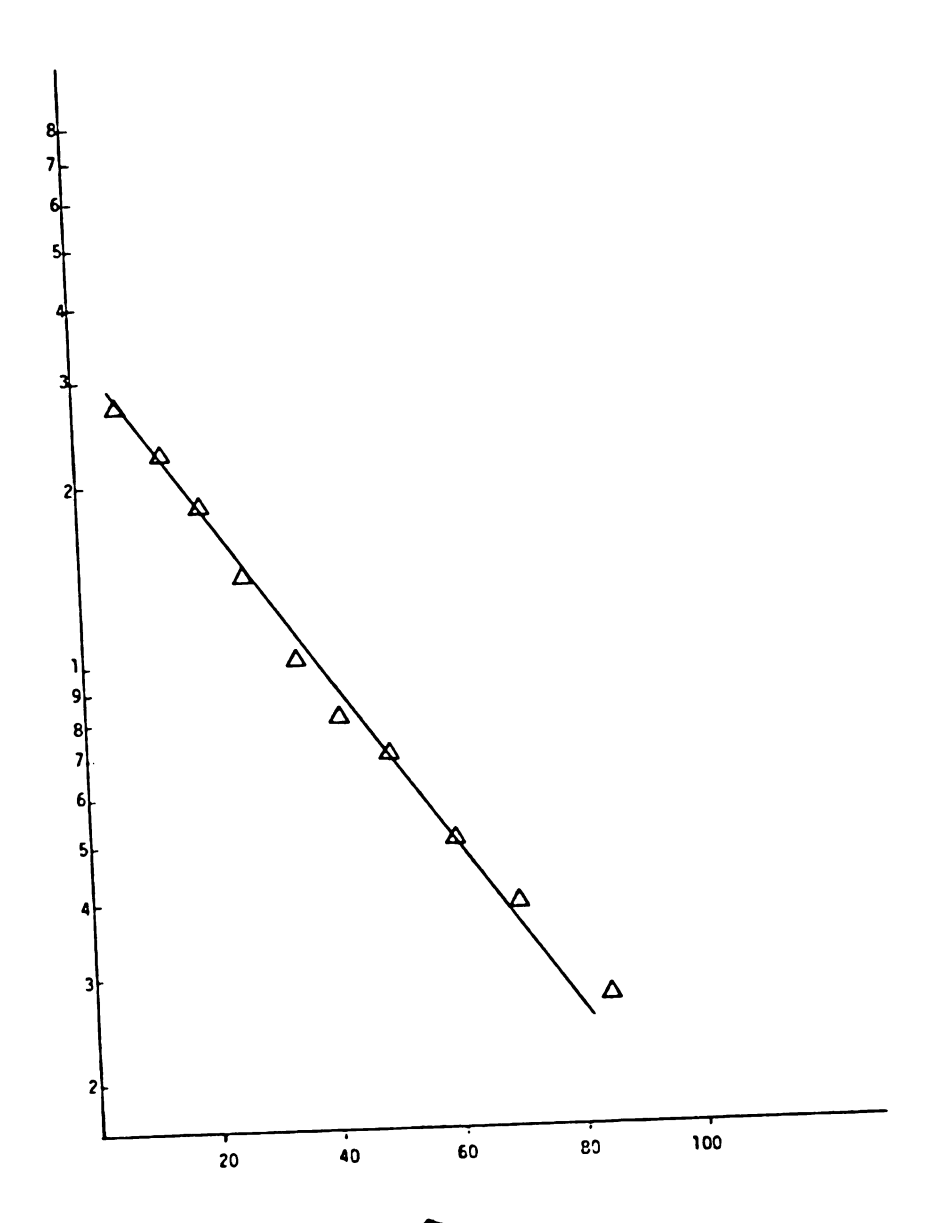


Figure 31. Log [(n-Bu₃P)₂Ni] as a function of time in minutes at 40°C.

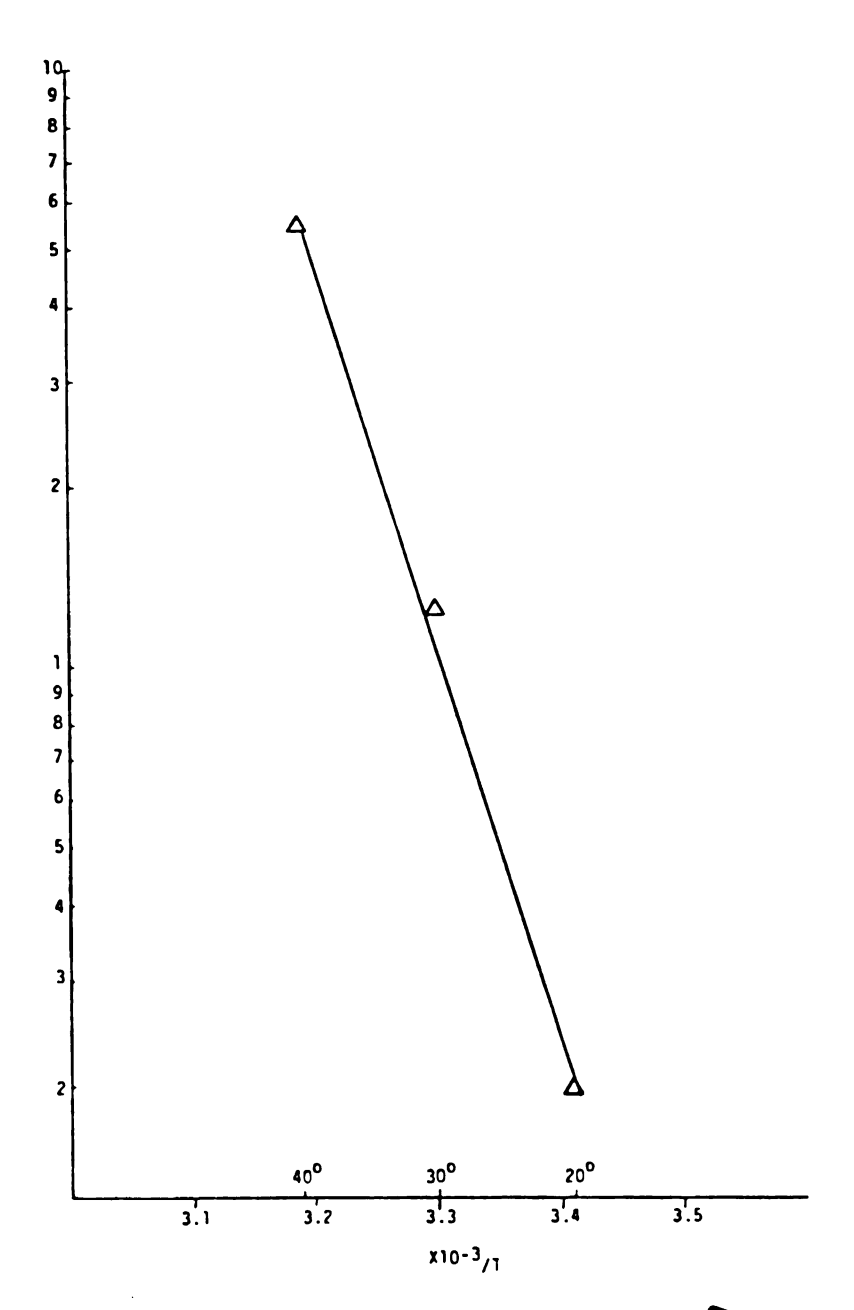


Figure 32. Arrhenius plot for (n-Bu₃P)Ni

process is 35 Kcal/mol. The driving force for β-hydride elimination from a metallacycle is not clear. The nickelβ-hydrogen dihedral angle is practically orthogonal to the optimum dihedral angle of 0°. A crystal structure 42 of bis(triphenylphosphine)tetramethylene platinum(II) shows that the metallacycle ring is puckered with an α -carbon .76 angstrom out of the plane and a β-carbon .4 angstrom out of the plane in the opposite direction. However, this distortion may not be adequate to allow the migration of a β -hydride to the nickel. Whitesides 43 also finds that bis(tri-n-butylphosphine)tetramethylene platinum(II) decomposes thermally in hydrocarbon solvents to give predominately 1-butene, the β -hydride elimination product. However, no explanation is offered for β -hydride elimination predominating over other reaction pathways in metallacycles.

One rationalization for β -hydride elimination from bis(phosphine)tetramethylene nickel(II) complexes which lose a ligand in solution is perhaps that the disassociated phosphine helps to promote β -hydride type products. For instance in Figure 33 the phosphine abstracts a proton to form 20 which then picks up the proton from the phosphine. However, the rate determining step cannot involve the free phosphine and still have first order kinetics.

The change in coordination number from four to three also changes the preferred ligand-nickel-ligand bond

$$\begin{array}{c} R_{3}P \\ R_{3}P \end{array} \longrightarrow \begin{array}{c} R_{3}P - N_{1} \\ \end{array} \longrightarrow \begin{array}{c} PR_{3} \\ \end{array} \longrightarrow \begin{array}{c} R_{3}P N_{1} \\ \end{array} \longrightarrow \begin{array}{c} 20 \\ H - PR_{3} \end{array} \longrightarrow \begin{array}{c} R_{3}P N_{1} \\ \end{array} \longrightarrow \begin{array}{c} R$$

Figure 33. A possible decomposition mode for $(R_3P)Ni$.

angle from 90° to 120°. The increase in the ligand-nickel-ligand bond angle introduces considerable strain in the hydrocarbon ring. The increase in ring strain may facilitate β -hydride elimination over other decomposition paths.

Five Coordinated Nickelacyclopentanes

In the presence of excess triphenylphosphine, bis(triphenylphosphine)tetramethylene nickel(II) will form
tris(triphenylphosphine)tetramethylene nickel(II). This
is a light brown or gold, air sensitive crystalline
solid. The complex decomposes at a temperature range of
0° to 30°C. Table 8 summarizes the kinetics and activation

Table 8. Rate data and activation parameters for $(\phi_3^P)_3^N$ i

Temp.	Rate Constant	Half	Life	E≠	ΔS≠	∆H≠	ΔG≠
0	3.6x10 ⁻⁶	53	hrs	19	-14 eu	19	23
20	4.4×10^{-5}	262	min		in Kcals/mol		
30	1.2x10 ⁻⁴	96	min				

parameters while Figures 34 to 36 summarize the rate data and Figure 37 is the Arrhenius plot. In order to prevent the dissociation of a phosphine ligand from the tris(triphenylphosphine)tetramethylene nickel(II) it was necessary to carry out the decomposition at low temperatures. temperatures shift the equilibrium between the square planar bisphosphine complex and trisphosphine complex toward the bis complex. The tris(triphenylphosphine)tetramethylene nickel(II) decomposes thermally by $\beta-\gamma$ bond cleavage to give two molecules of ethylene. The isomerization of a nickelacyclopentane to a bis olefin complex does not change the coordination number but reduces the oxidation state from two to zero. The trisphosphine nickelacycle is coordinately saturated so the isomerization to the bis olefin complex requires the prior loss of a phosphine. The ³¹P NMR studies of this complex reveal that the resultant four coordinated complex is probably the tetrahedral complex. The tetrahedral complex rapidly isomerizes to the bis olefin complex which in the rate determining step loses a molecule of ethylene. The products of the reaction are ethylene and bis(triphenylphosphine)ethylene nickel(0). The scheme is presented in Figure 38. The activation energy for this process was found to be 19 Kcal/mol.

A Newman projection of the tetrahedral complex shown in Figure 39 illustrates the geometric relation of the

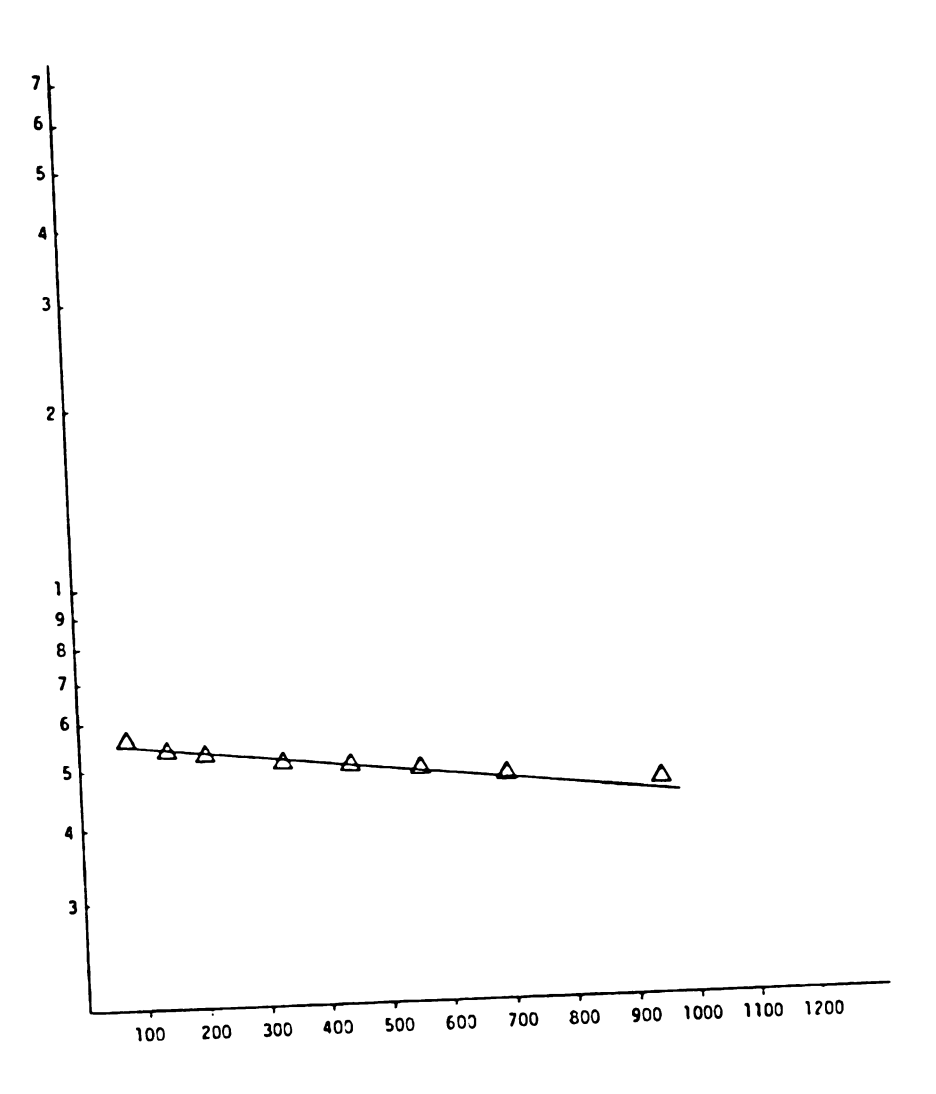


Figure 34. Log $[(\phi_3 P)_3 Ni)$] as a function of time in minutes at 0°C.

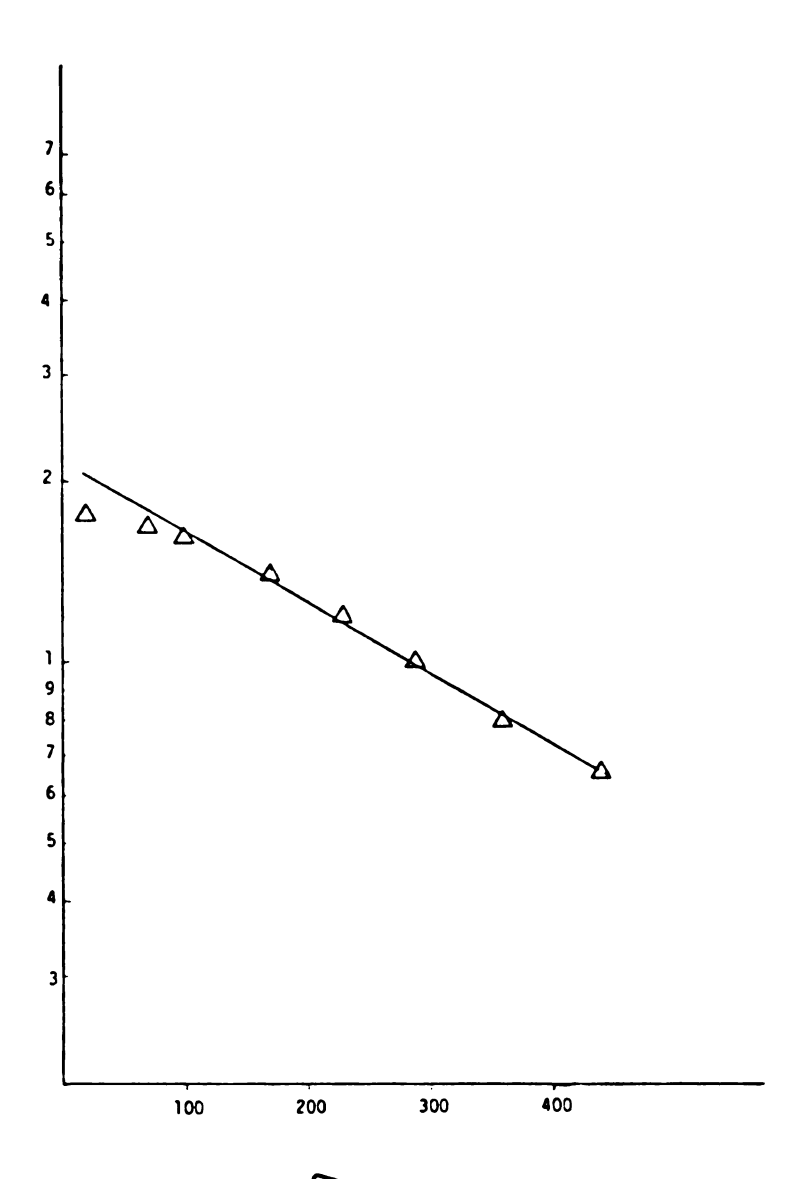


Figure 35. Log $[(\phi_3 P)_3 Ni)$] as a function of time in minutes at 20°C.

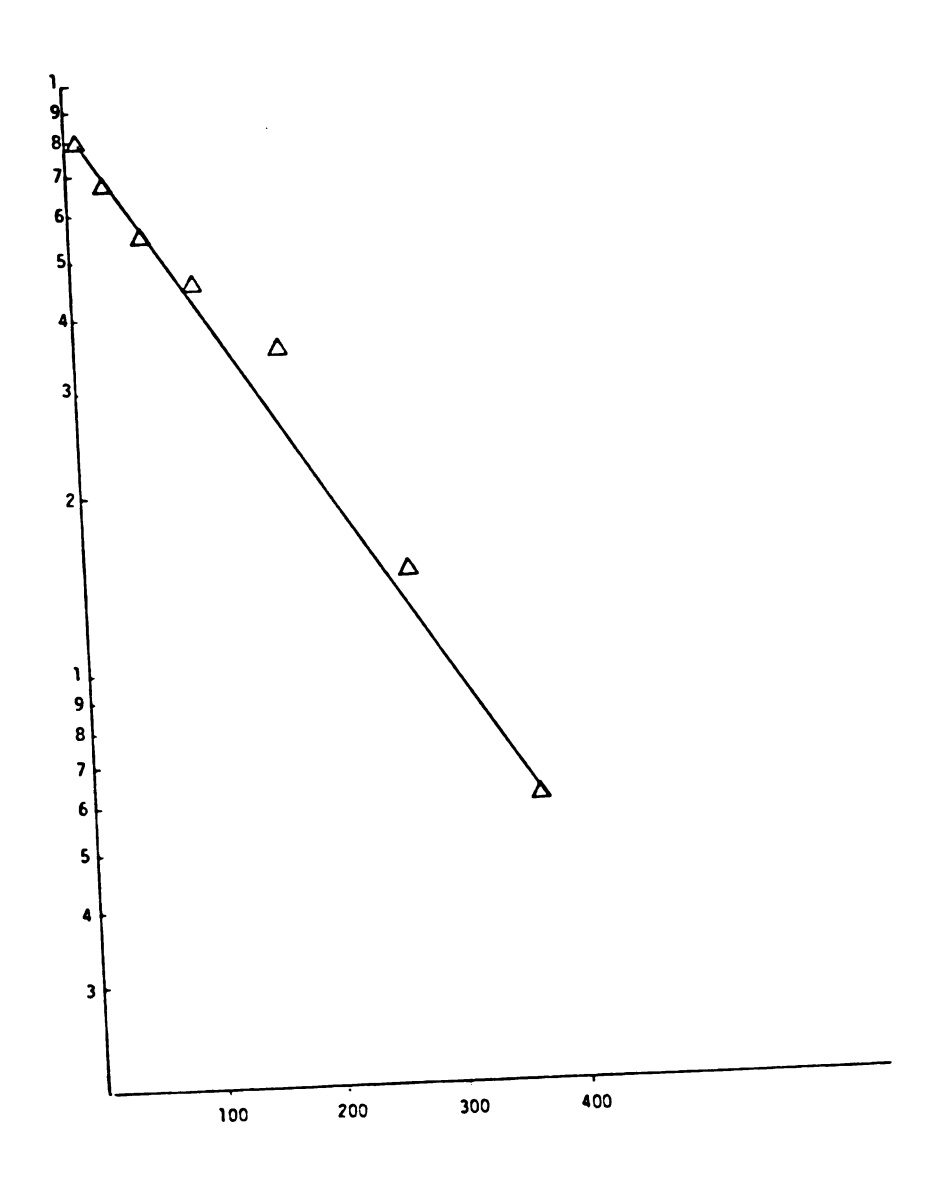


Figure 36. Log $[(\phi_3 P)_3 Ni)$] as a function of time in minutes at 30°C.

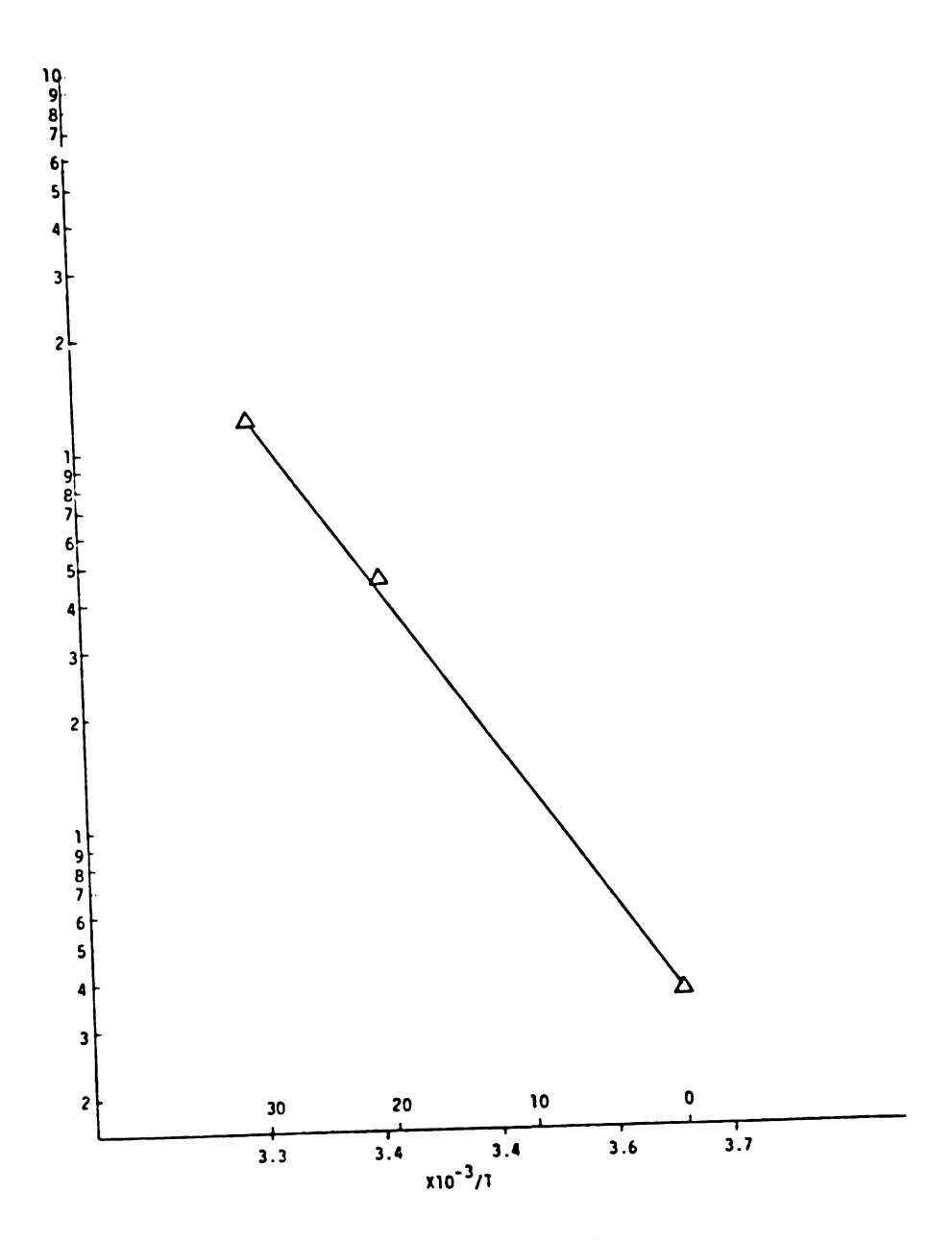


Figure 37. Arrhenius plot for $(\phi_3 P)_3 Ni$.

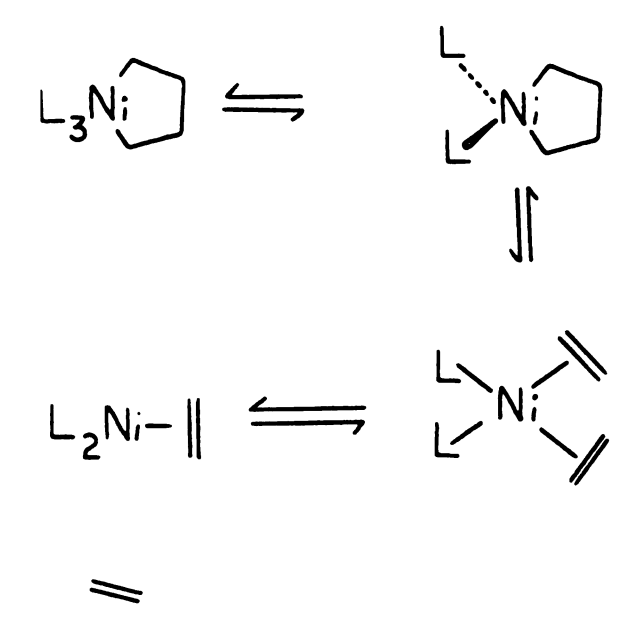


Figure 38. Proposed decomposition pathway of $(\phi_3 P)_3 Ni$.

ring. The $\beta-\gamma$ carbon-carbon bond is cis co-planar with the α -carbon nickel bond. This is the optimum geometry for elimination of nickel with an ethyl fragment from the two carbon unit which becomes ethylene.

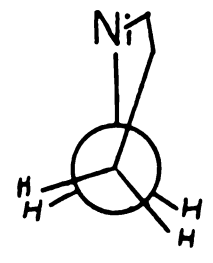


Figure 39. Newman projection of the tetrahedral complex.

Hoffman and Kochi 44 have experimentally investigated the reductive elimination of alkyl groups from trialkyl gold complexes, RqLAu, as well as theoretically calculating the energetics of the process. Triphenylphosphine-(trimethyl)gold(III) was calculated to isomerize with an activation energy of .4 eV and to reductively eliminate ethane with an activation energy of .8 eV. These values were obtained by using extended Huckel methods. Normally extended Huckel methods would not be used due to its inability to account for bond stretching deformations of molecules. However, in this case the calculated bond lengths corresponded extremely well with the actual lengths. The computed value of .8 eV for reductive elimination in the gold system corresponds to approximately 18.4 Kcal/mol. The value measured for bis(triphenylphosphine) dimethyl nickel(II) was 19 Kcal/mol. While perhaps running the risk of comparing apples and oranges the

agreement between the two values for reductive elimination is very good.

Initially, it was hoped that a series of metallacycles in which the substituents on the tertiary phosphines were varied in an orderly manner could be prepared and the thermal decompositions studied. The study of a series of phosphines such as $\phi_3 P$, $\phi_2 CH_3 P$, $\phi(CH_3)_2 P$ and $(CH_3)_3 P$ on nickelacyclopentane decomposition would give some insight into the electronic influence of the ligands. However, the preparation of bis(diphenylmethylphosphine)tetramethylene nickel(II) met with insurmountable technical problems as did the preparation of bis(dimethylphenylphosphine)tetramethylene nickel(II).

Table 9 summarizes the activation parameters for all the metallacycles of this study. The entropy of activation reflects the relative ordering of the transition state compared to the initial complex. No clear trend is apparent. The triphenylphosphine cases give negative entropies of activation while the others are positive.

The rate constants reported are presented in Table 10 along with the standard deviations. The standard deviations reflect the closeness of the best least squares fitted line to the actual data points. The agreement between the best line and the experimentally determined data points is moderate.

Experimental results verifying a number of low energy

Table 9. Activation parameters for nickelacyclopentanes.

Complex	Eact	Sact	Hact	Gact	Product
(\$\phi_3P)_2Ni	23	-2.3 eu	22	23	
(\$\phi_3^P)_2Ni<^{CH_3}_{CH_3}	19	- 13	18	22	сн ₃ сн ₃
(dpe)Ni	35	15	34	29	
(dpe)Ni	37	21	36	28	
(bipy)Ni	42	38	41	29	
(1,10-phen)Ni	45				
(n-Bu ₃ P) ₂ Ni	35	36	34	23	
(\$\phi_3\pi)_3\ni	19	-14	19	23	

Table 10. Standard deviation of rate constants and Arrhenius slopes.

Compound	Temp.	Rate Constant (Slope)	Standard Deviation
. ^	19	3.2x10 ⁻⁵	•33
(\$\phi_3^P)_2^Ni	30	$1.2x10^{-4}$.63
-	40	4.6×10^{-4}	.47
	Arrhenius	1.15E ⁴	1.3
(\$\phi_3\text{P})2\text{Ni<\frac{CH3}{CH3}}	6	6.3x10 ⁻⁵	.18
¹³ ² ^{30H} 3	20	3.7×10^{-4}	•54
	30	1.0x10 ⁻³	.83
	Arrhenius	9.5x10 ³	1.3
dipy)Nį	60	6.9x10 ⁻⁷	.002
	65	1.6x10 ⁻⁶	.012
	70	4.5x10 ⁻⁶	.016
	80	2.6x10 ⁻⁵	.008
	Arrhenius	2.14x10 ⁴	1.5
dpe)Ni	80	1.5x10 ⁻⁵	.19
	90	7.0x10 ⁻⁵	.91
	100	2.4×10^{-4}	.84
	Arrhenius	1.85x10 ⁴	1.3
dpp)Ni(90	2.3x10 ⁻⁵	. 44
	100	8.2x10 ⁻⁵	.31
	110	2.8x10 ⁻⁴	.14
	Arrhenius	1.78x10 ⁴	1.25
(Bu ₃ P)Ni	20	1.7x10 ⁻⁵	.22
3 /	30	1.3x10 ⁻⁴	.63
	40	8.1x10 ⁻⁴	.58
	Arrhenius	1.7x10 ⁴	1.9

decomposition pathways for nickelacyclopentanes have been presented. Nickelacycles were found to be more stable than their corresponding alicyclic analogues. Reductive elimination has been found to be the main decomposition pathway for four coordinated nickelacycles which is a dramatic change in reactivity from nickel alicyclic complexes. activation energies for this process were found to reflect the relative rigidity of the supporting ligand. The more rigid the ligand the higher the activation energy was found to be. Reductive elimination in nickelacycles was compared to reductive elimination of a non-ring analogue which also decomposed by reductive elimination. chapter describes the initial study of the decomposition of nickelacyclobutanes which are even less stable than nickelacyclopentanes.

EXPERIMENTAL

General

All reactions and manipulations were done under argon which had been purified by use of a BASF catalyst and molecular sieves. All solvents were freshly distilled from sodium (with added benzophenone) under nitrogen. Triphenylphosphine, bis(diphenylphosphine)ethane, bis-(diphenylphosphine)propane, tri-n-butylphosphine, and α, α' dipyridyl, and α' dipyridyl, and α'

Analytical glc was performed on a Varian series 1400 FID chromatograph with a 20' x 1/8" Durapak column or a 13 ft paraffin wax/5% silver nitrate on alumina column.

NMR analyses were obtained using a Varian T-60 spectrometer and δ values were recorded relative to TMS. Infrared spectra were obtained on a Perkin-Elmer 237B and were calibrated with polystyrene. Mass Spectra were run on a Hitachi-Perkin Elmer RMU-6 spectrometer.

Synthesis of bis(triphenylphosphine)nickel(II)dichloride

A modification of Venanzi's 46 procedure was used. A solution of 23.8 g (.1 mol) of nickel(II) dichloride hexahydrate in 250 mls of glacial acetic acid and 20 mls of water was added with stirring to a hot solution of 52.6 g

(.2 mol) of triphenylphosphine in 500 mls of glacial acetic acid. The drab green precipitate which formed was cooled overnight. Vacuum filtration yielded dark blue-black crystals which were washed with ether and vacuum dried. The yield was 52 grams (76%).

Synthesis and Standardization of 1,4 dilithiobutane

In a 500 ml three neck round bottom flask equipped with an addition funnel, argon line and magnetic stirrer were placed 9 g of flattened lithium wire cut into fine pieces and 250 mls of distilled ether. A solution of 20 mls of 1,4-dibromobutane in 150 ml of ether was slowly added with stirring over the course of three or four hours. After 2 or 3 mls were added the flask was cooled to 0°C with an ice bath for the remainder of the addition. When the addition was complete the mixture was stirred for an additional half hour and stored at 0°C until the suspension had settled. The solution was filtered under argon and standardized.

The concentration of the 1,4-dilithiobutane solution was determined by mixing a 10 ml portion of the 1,4-dilithiobutane solution with 3 mls of trimethylchlorosilane under argon. The bis(1,4-trimethylsilyl)butane formed was compared to a known amount (2 mmol) of 1,2,4,5-tetramethylbenzene (durene) by glc on an 8 ft DC550 column at 100°C.

Synthesis of bis(triphenylphosphine)tetramethylene nickel(II)

A 100 ml side arm round bottom flask was charged with 1 g (1.5 mmol) of bis(triphenylphosphine) nickel(II) dichloride, positive argon pressure and 3 mls of dry decygenated ether. The flask was cooled to dry ice/ethanol bath temperature and 30 mls (2.4 mmol) of 1,4-dilithio-butane/ether solution was added via syringe slowly. The solution was stirred for 10 minutes and then the cooling bath was allowed to warm up slowly. At temperatures between -35 and -15°C a bright yellow precipitate was seen. The mixture was then filtered under argon. The resulting yellow solid was washed with ether and vacuum dried.

The yellow solid was dissolved in dry oxygen free toluene at -20°C. The yellow solution was transferred via syringe to another vessel at -20°C leaving behind undissolved lithium salts. The clear yellow solution was condensed to half its original volume and stored at -78°C overnight. The yellow crystals which precipitated were filtered under argon and vacuum dried to give 22 percent of the product.

Analysis of bis(triphenylphosphine)tetramethylene nickel(II)

A weighed portion of the complex was transferred to a small schlenk tube fitted with a serum cap. Concentrated sulfuric or hydrochloric acid was added via syringe through

the cap. The resulting gas formed was analyzed by glc on a 20 ft Duropak column at 65°C. The complex was considered pure if more than 95% of the calculated gas volume as compared to an internal standard (propane) was found.

Analysis of nickel (glyxime test) 47

150 mls of water was added to the acid decomposed complex. The white precipitate (ϕ_3 P or ϕ_3 PO) which formed was warmed slightly on a hot plate, cooled, and filtered to give a clear solution. This solution was heated to 60°C and 20 mls of a freshly prepared one percent solution of dimethyl glyoxime in absolute ethanol was added. Concentrated ammonium hydroxide was added dropwise until the characteristic red precipitate no longer formed. The mixture was kept at 60°C for one additional hour and then cooled. The red solid was aspirator filtered into a tared fritted glass crucible. The solid was dried to constant weight at 130°C and the percent nickel present was calculated by the following relation.

%Ni = (wt. of ppt. x 20.313)/wt. of sample

Synthesis of ethylene bis(diphenylphospine) nickel(II)-dichloride

3.35 g of bis(diphenylphospine)ethane was dissolved in 250 mls of warm ethanol. An ethanol solution of nickel(II)-

dichloride hexahydrate (2 g in 77 mls) was added to the warm diphos solution with stirring. A dark solution resulted which suddenly turned orange with the production of a metallic orange precipitate. The solution was cooled and filtered. The product was vacuum dried to yield 3.8 g (86 percent) of product.

Synthesis of ethylene bis(diphenylphosphine)tetramethylene nickel(II)

In a 100 ml side arm round bottom flask connected to an argon line were placed 2 g (3.9 mmol) of ethylene bis-(diphenylphosphine) nickel(II) dichloride and 3 mls of dry oxygen free ether. The flask was cooled to dry ice-ethanol bath temperatures and 56 mls of a .11 M solution of 1,4-dilithiobutane in ether was added via syringe. The brownish solution was stirred for 10 minutes and slowly warmed by letting the dry ice bath warm up. At -10 to 0°C a yellow precipitate fell out which was filtered under argon. The solid was washed with ether, ethanol, and water. The solid was vacuum dried to yield .74 g (38%) of product.

Preparation of propylene bis(diphenylphosphine) nickel(II) dichloride

A one liter Erlenmeyer flask was charged with 8.2 g (20 mmol) of bis(diphenylphosphine) propane and 600 mls

of ethanol. The solution was heated to 60°C with stirring. A solution of 4.7 g (20 mmol) of nickel dichloride hexahydrate in 200 mls of ethanol was added to the phosphine solution and removed from the heat. A red solid precipitated which was cooled, filtered, and dried. The product was formed in 84 percent yield.

Synthesis of propylene bis(diphenylphosphine)tetramethylene nickel(II)

In a 100 ml round bottom side arm flask under argon were placed 1 g (1.8 mmol) of propylene bis(diphenyl-phosphine) nickel dichloride and 5 mls of ether. The flask was cooled to -78°C. As the suspension was stirred 20 mls (2.9 mmol) of 1,4-dilithiobutane/ether solution was added slowly. The cold bath was allowed to warm to -10°C. A yellow precipitate slowly formed as the solution warmed up. When all the red starting material was gone and the reaction was complete the solution was filtered under argon. The yellow solid was washed with deoxygenated ether, ethanol, and then water. The product was vacuum dried to yield .61 g of product which is 63 percent of the theoretical yield.

Synthesis of bis(triphenylphosphine)dimethyl nickel(II)48

In a 100 ml side arm flask purged with argon was placed 1 g (1.5 mmol) of bis(triphenylphosphine) nickel

dichloride, 5 mls of ether and 15 mls of tetrahydrofuran. The flask was cooled to -78°C. An addition funnel was charged with 20 mls of ether and 1.5 mls (3. mmol) of methyl lithium. The methyl lithium solution was slowly added at -78°C over the course of two hours. After an additional half hour of stirring the solution was a light yellowish brown. Filtration under argon at -78°C yielded a yellow solid which was washed with ether and then with water. After vacuum drying .54 g (58 percent) of the product was obtained.

Synthesis of bis(tri-n-butylphosphine) nickel(II) dichloride

9.5 g (40 mmol) of nickel(II) dichloride hexahydrate was dissolved in 25 mls of degassed ethanol. 22 mls (88 mmol) of tri-n-butylphosphine was added to the solution and the mixture was stirred for 40 minutes at room temperature. The solution was cooled and filtered. The purple crystals were recrystallized from hexane and vacuum dried to yield 7.2 g (75 percent) of product.

Synthesis of bis(tri-n-butylphosphine)tetramethylene nickel(II)

In a 200 ml side arm round bottom flask purged with argon were placed 3 g (5.6 mmol) of bis(tri-n-butylphos-phine) nickel(II) dichloride and 10 mls of ether. The

flask was cooled to -78°C with a dry ice/ethanol bath.

52 mls of a .18 M solution of 1,4-dilithiobutane (9.4 mmol) was added slowly via syringe. The suspension was stirred for two or three hours at temperatures below -35°C. During this time the solution slowly turned yellow and a precipitate formed. The solvent was removed in vacuo below -35°C. Pentane was then added to the dried gum and the resulting yellow solution was removed by syringe to another vessel also at -35°C. This was repeated until only a white residue was left in the flask. The pentane solution was condensed to half its original volume at -35°C and stored at -78°C for four days. The yellow crystals were collected and dried under vacuum. The yield was 10 percent.

Synthesis of tris(triphenylphosphine)tetramethylene nickel(II)

Method A. 20 mls (2.4 mmol) of an ether solution of 1,4-dilithiobutane was slowly added to 1 g (1.5 mmol) of bis(triphenylphosphine) nickel dichloride in 5 mls of ether at -78°C. The mixture was slowly allowed to warm to 0°C. The solution was stirred at this temperature for 45 minutes while the solution turned from dark brown to yellow. An excess of triphenylphosphine (1.5 g, 5.7 mmol) was slowly added to the solution. The color turned to brown with a golden precipitate. The solution was filtered. The golden solid was washed with ether and

recrystallized at -50°C from toluene which had been saturated with triphenylphosphine at -60°C. The golden crystals were obtained in 48 percent yield.

Method B. To a toluene solution of 1 gram (1.5 mmol) of bis(triphenylphosphine)tetramethylene nickel(II) at -20°C was added an excess of triphenylphosphine (.82 g 3.1 mmol). The solution was stirred for two hours at -10°C. The solution was then cooled to -78°C overnight and the golden solid was collected by filtration. The solid was washed with ether and recrystallized.

Preparation of anhydrous bis(2,4-pentanedionato) nickel(II) 49

A solution of 59.4 g (.25 mmol) of nickel(II) dichloride hexahydrate in 250 mls of water was added to a
solution of 50 g (.5 mmol) of 2,4-pentanedione in 100
mls of methanol. A solution of 68 g (.5 mol) of sodium
acetate in 150 mls of water was added. The solution was
heated briefly and cooled to 0°C in an ice bath. The
cooled light blue product was filtered and azeotrope dried
with toluene overnight. The dark green toluene solution
was filtered while warm to remove the sodium chloride.
The toluene was removed on a rotary evaporator until a
dark green oil remained. The oil was vacuum dried to
leave a green solid. The yield was 42 g (65%).

Preparation of bis(1,5-cyclooctadiene) nickel(0)⁵⁰

In a 3 neck 500 ml round bottom flask fitted with a dewar condensor, argon line, thermometer, and gas flow adapter were placed 25.7 g (.1 mol) of anhydrous bis(2,4pentanedionato) nickel(II), 10 mls of toluene and 54 g (.5 mol) of 1,5-cyclooctadiene which had previously been passed through neutral alumina. The flask was cooled to -20°C and a butadiene tank was connected to the gas flow adapter. The butadiene was passed over type 3A molecular sieves and then into the flask. About 5 g of gas was The gas flow adapter was removed and an addition funnel was attached. 100 mls of a 25% solution of triethyl aluminum in toluene was syringed into the addition funnel. The triethyl aluminum solution was added over the course of two hours while the flask temperature was maintained at -10 to 0°C. The green solution slowly turned brownish-yellow. After the addition of triethylaluminum was complete the mixture was stirred an additional half hour at 0° and then warmed to room temperature for three hours. It was recooled and filtered under argon to yield 23 grams (83%) of the bright yellow product. It would turn black upon exposure to moist air.

Synthesis of (a,a'-dipyridyl)tetramethylene nickel(II)⁵¹

.33 g (1.2 mmol) of bis(1,5-cyclooctadiene) nickel(0) was placed in an argon filled Schlenk tube and cooled in

an ice bath. A solution of .56 g (3.6 mmol) of α,α' dipyridyl in 6 mls of tetrahydrofuran was added via syringe. The resulting solution was a deep purple. The solution was stirred for 30 minutes and .14 mls (1.2 mmol) of 1,4-dibromobutane was added via syringe. The solution slowly turned green and a precipitate was formed. The stirring was stopped and the solid was allowed to settle. The green solution was transferred via syringe to another Schlenk tube and concentrated. Pentane was added and the green solid was filtered under argon to yield 20 percent of product. The complex is extremely air sensitive.

Measurement of a rate constant

A 30 ml Schlenk was purged with argon and charged with .04 to .1 g of the nickelacyclopentane. The tube was cooled and 10 to 20 mls of xylene was added via syringe. The tube was sealed with a serum cap and .2 mls of propane was added as an internal standard. The tube was stirred for 30 minutes then placed in a constant temperature bath. Gas samples were periodically removed with a 50 microliter syringe and analyzed by glc on a 20 ft Duropak column at 60°C. Product gases were identified by matching retention times with authentic samples and confirmed by co-injection techniques.

CHAPTER II

THE IN SITU DECOMPOSITION OF NICKELACYCLOBUTANES

INTRODUCTION

Metallacyclobutanes have been cited as intermediates in a number of important organometallic reactions. Both olefin metathesis ⁵² and Ziegler-Natta polymerization ⁵³ are believed to utilize metallacyclobutanes as reactive intermediates.

The current mechanism for olefin metathesis ⁵² proposes the alternation of a metal alkylidene species with a metal-lacyclobutane as shown in Figure 40. The key step, as far as product distribution is concerned, is the decomposition of the metallacyclobutane into an olefin and alkylidene moiety. Hughes ⁵⁴ reported metathesis to be first order in both olefin and catalyst. It was also found that the energy of activation for this reaction is less than 10 Kcal/mol.

A proposed mechanism⁵³ for polymerization involves a metallacyclobutane. Figure 41 is very similar to the mechanism for olefin metathesis except that the alkylidene complex has a hydride on the metal which assists in the decomposition of the metallacyclobutane. In polymerization the metallacyclobutane decomposes by reductive

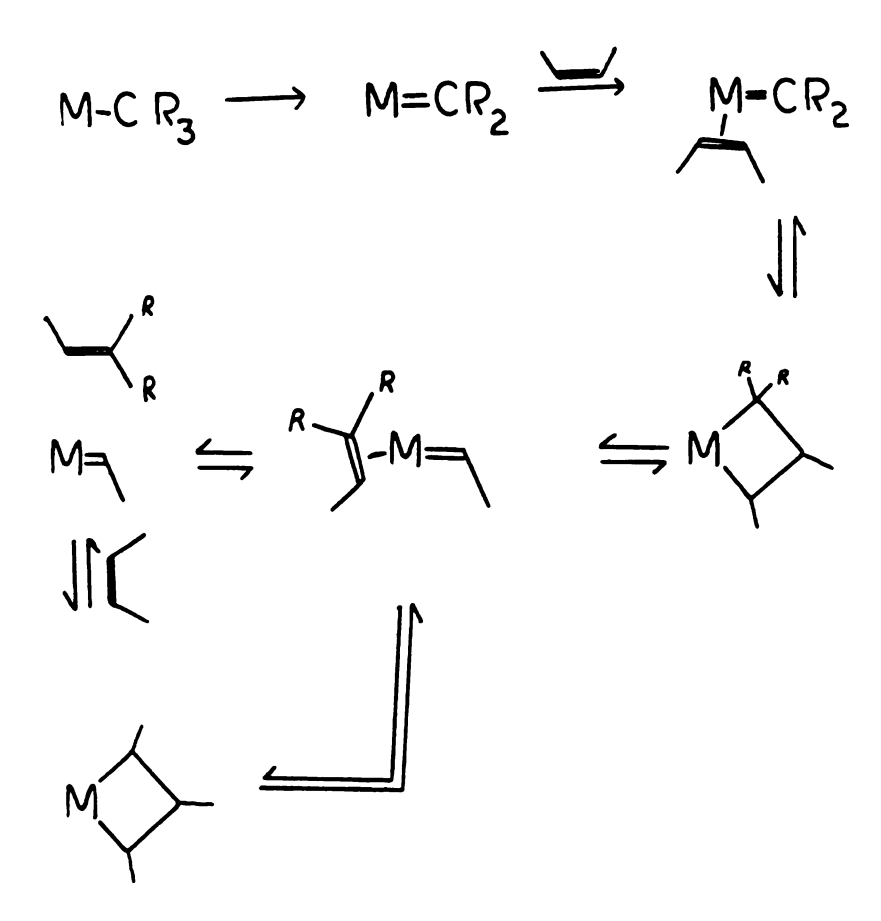


Figure 40. Current mechanism for olefin metathesis.

Figure 41. Proposed mechanism for Natta-Ziegler polymerization.

elimination of the hydride and one side of the ring whereas in metathesis the metallacyclobutane decomposes by $\beta\!-\!\gamma$ bond cleavage.

Platinum, 55 tungsten, 56 and molybdenum 57 metallacyclobutanes have been isolated and their chemistry investigated. Brown 58 has prepared dichloro(3-methyltrimethylene)platinum(IV) by the reaction of methylcyclopropane with Zeise's dimer ([PtCl₂(C₂H₄)]₂). This is reported to be the easiest and most convenient preparation

of platinacyclobutanes.

Tipper⁵⁹ has investigated the thermal properties of trimethylene platinum(IV) complexes by differential scanning calorimetry. He found that platinacyclobutanes of the general formula $PtX_2(CH_2CH_2CH_2)$ and $PtX_2L_2(CH_2CH_2CH_2)$ where L is a nitrogen donor ligand decompose by reductive elimination to give cyclopropane or via a π allyl hydridocomplex as shown in Figure 42 to give propylene. The mode of decomposition depends on the trans influence of the ligand. Ligands of high trans influence (such as ethylenediamine, dipyridyl, tertiary phosphines) follow path A to give cyclopropane. Ligands of low trans influence

Figure 42. Possible decomposition pathways for L_2X_2Pt .

(such as ethylenediamine, dipyridyl, tertiary phosphines) follow path A to give cyclopropane. Ligands of low trans influence (such as pyridine, methylpyridine, halogens) follow path B to give propylene. The bond strengths calculated for the platinum carbon bonds is 27-30 Kcal/mol which is considerably lower than other platinum carbon bond strengths. A typical value of 39 Kcal/mol was found for the platinum methyl bond in $(C_5H_5)Pt(CH_3)_3$. The weaker bonds in platinacyclobutanes reflect the ring strain in the platinacyclobutane.

Green⁶¹ has studied the thermal decomposition of bis(cyclopentadienyl)trimethylene tungsten and molybdenum. The decomposition at 80°C yields a mixture of predominately

cyclopropane with some propylene. However, the corresponding methyl derivatives $(C_5H_5)W(CH_2CH(CH_3)CH_2)$ and $(C_2H_5)_2W-(CH_2CH_2CH(CH_3))$ evolve isobutane and 1-butene as major products upon thermal decomposition. The methyl substituent changes the major decomposition pathway from reductive elimination to β -hydride elimination. He has also found that photochemical decomposition yields the olefin of one less carbon numbers as shown in Figure 43.

Figure 43. Products of $(Cp)_2W$ by photochemical decomposition.

Hagihara 62 has used nickel(0) dipyridyl complexes to couple α ,w-dihaloalkanes to cyclic hydrocarbons. He proposed that the coupling proceeds through a metallacycle as depicted in Figure 44.

It was felt that this coupling reaction warranted closer investigation. That is, when 1,3-dibromopropane was used did the resulting metallacyclobutane decompose exclusively by reductive elimination or were other products formed? The presence of ring substituents affected the

decomposition of platinacyclobutanes but was a similar decomposition mode change operative in the nickel system?

The next section describes the results on further investigations of this reaction.

Figure 44. Proposed pathway for coupling of α -w dihaloalkanes.

RESULTS AND DISCUSSION

A series of tertiary phosphine and nitrogen donor stabilized nickelacyclobutanes were prepared by the method of Hagihara and thermally decomposed without isolation. The product distribution and yields are listed in Table 11 for nickelacyclobutanes with no ring substitutents. The main product, cyclopropane, arises from a reductive elimination process. This is the same trend Green 61 found for tungsten and molybdacyclobutanes. A significant amount of ethylene was also formed. The ethylene could arise from $\beta-\gamma$ bond cleavage to give a metal alkylidene species and ethylene. The ultimate fate of the alkylidene unit is not clear. Dimerization of the carbenoid species would give ethylene. This has been proposed as one possible termination step in olefin metathesis. 63 Attempts to trap the metal alkylidene unit in these systems failed in part due to its low concentration. The decomposition of the nickelacyclobutane without any supporting ligand (entry 5) gave a very different product distribution from the previous examples which had supporting ligands. main decomposition product was ethylene with a lessor amount of cyclopropane.

The same series of ligands were used to prepare the 2-methyl nickelacyclobutanes shown in Table 12 along with the decomposition product distributions and yields. The

Table 11. Decomposition products for nickelacyclobutanes.

Entry Number	Complex Prepared in Situ	Decomposition	Product	Yields ^a CH ₂ CH ₂
1	dipyNi	92		2
2	(\$\phi_2^ \qu	82	10	7
3	(1,10phen)Ni	90	2	7
4	(diphos)Ni	88	3	9
5	(COD)Ni b	15		85

^aglc yields. Total yields were approximately 50 percent.

^bTotal yield was only 20 percent.

Table 12. Decomposition products for methyl substituted nickelacyclobutanes.

Entry Number	Complex Prepared in Situ	Decompos	ition	Prod	luct	Yields ^a
1	(dipy)Ni	trace	80		4	8
2	(\$\phi_3\P)_2\Ni	trace	17	10	52	20
3	(diphos)Ni	-	44	2		40
4	(1,10phen)Ni	-	70	3		7
5	(COD)Ni b	trace	9	9	5	77

^aglc yields. Total yields were approximately 50 percent.

^bTotal yield was 22 percent.

main thermal decomposition product again is the reductive elimination product, methylcyclopropane. Only in the case of triphenylphosphine nickela(2-methyl)cyclobutane was a significant amount of linear butenes formed. Again the nickelacycle without supporting ligands decomposed to form mostly ethylene.

At least three decomposition pathways are available to nickelacyclobutanes. Reductive elimination seems to be the major decomposition mode. This is not surprising in light of the decomposition pathway of nickelacyclopentanes. The production of propylene by β -hydride elimination is a minor pathway. The four membered metallacycle is even less puckered than metallacyclopentanes. Thus the nickel β-hydride dihedral angle is closer to the tetrahedral angle than the nickelacyclopentane case, so it should be an unfavored decomposition pathway. $\alpha-\beta$ carbon-carbon bond cleavage to form a metal carbene species and ethylene occurs to a small extent in these systems. This decomposition pathway is reasonable on steric grounds. The nickel and $\beta-\gamma$ carbon bond are cis co-planar (eclipsed along the α - β bond), the necessary geometry for concerted elimination. Figure 45 gives a Newman projection of a nickelacyclobutane looking down the $\beta-\alpha$ carbon bond of the ring.

It might be expected that the methyl substituent on the α -carbon of the ring would increase β -hydride elimination. Only for the triphenylphosphine case is there a

Figure 45. Newman projection of nickelacyclobutane.

significant production of linear butenes. Whitesides 25 found that an α -methyl substituent on the ring did not greatly increase β -hydride elimination in platinacyclopentanes. In the present study, triphenylphosphine is the only monodentate ligand investigated and perhaps the increased freedom over chelated ligands facilitate β -hydride elimination.

The methyl substituent also seems to increase the production of ethylene. The metallacyclobutane may decompose by $\alpha-\beta$ bond cleavage in two possible ways. As Figure 46 shows the initial $\alpha-\beta$ bond cleavage can occur to give either a molecule of ethylene or propylene with the corresponding alkylidene unit. Since only a trace of propylene is found in these reactions, path B is not a significant pathway. The metal ethylidene species from path A may rearrange by β -hydride migration to form a

Figure 46. Decomposition modes for
$$L_2Ni$$

 σ -bonded ethylene complex. This complex then reductively eliminates the hydride and σ -bonded ethylene to give ethylene as the product. This mechanism for the formation of ethylene from the alkylidene complex is similar to the proposed mechanism for α -hydride elimination. ⁶⁴

Attempts were made to trap the alkylidene unit formed in the decompositions. Since 1,5-cyclooctadiene was present in the reaction mixture it was thought that it might be reacting with the metal carbene to form bicyclo[6.1.0]-nona-3-ene. No trace of this compound could be found by

either NMR or glc. Running the reaction in cyclohexene also failed to trap the intermediate. In a parallel study 32 on nickelacyclohexanes it was possible to trap the nickel carbene species. However, even when the concentration of carbene complex is fairly high the yields of the trapped compound is low. Hence, in the present case where the nickel carbene species is present in low concentration it is reasonable that no carbene trapping product was detected.

In this preliminary study a series of nickelacyclo-butanes and α -methyl nickelocyclobutanes were thermally decomposed in situ. The main decomposition pathway is reductive elimination with α - β bond cleavage and β -hydride elimination pathways of lessor importance.

EXPERIMENTAL

Preparation and decomposition of dipyridyl trimethylene nickel(II)

In a 200 ml side arm Schlenk tube under argon were placed a .51 g (1.86 mmol) of bis(1,5-cyclooctadiene) nickel(0). The tube was cooled to 0°C and 10 mls of tetrahydrofuran was added. A solution of .87 g (5.6 mmol) of dipyridyl in 10 mls of degassed tetrahydrofuran was added via syringe. The mixture was stirred for 30 minutes and .11 mls (1.86 mmol) of 1,3-dibromopropane was added via syringe. The blue solution slowly turned green as it was allowed to warm to room temperature overnight. Gas samples were withdrawn from the head space after 24 hrs and analyzed by glc.

CHAPTER III

STUDIES TOWARD THE HOMOGENEOUS CATALYTIC REDUCTION OF CARBON MONOXIDE

INTRODUCTION

The synthesis of hydrocarbon products from carbon monoxide and hydrogen has been studied for the last fifty years. The synthesis of hydrocarbons, usually on heterogeneous catalysts, by the reductive polymerization of carbon monoxide is commonly referred to as the Fischer-Tropsch⁶⁷⁻⁶⁹ synthesis reaction. The catalytic reduction of carbon monoxide to methane is called the methanation reactions.⁷⁰ During World War II a tremendous research effort headed by Franz Fischer⁷¹ enabled Germany to produce large quantities of gasoline and diesel fuels from carbon monoxide derived from coal.

The current petroleum situation has renewed interest in Fischer-Tropsch processes. There is only one commercial Fischer-Tropsch plant in operation now. It is the SASOL plant in South Africa run by the South African Synthetic Oil Corporation, Ltd.

In the last two years efforts to find and develop homogeneous analogs of both the Fischer-Tropsch and methanation reaction have only been moderately successful.

Muetterties 72 has found that metal cluster complexes have catalytic activity for reduction of carbon monoxide. Bercaw 73 has found that mononuclear zirconium complexes will reduce carbon monoxide and Feder 74 has a mononuclear cobalt catalyst for the reduction.

Muetterties 75 reports that $Os_3(CO)_{12}$ and $Ir_4(CO)_{12}$ catalyze the production of methane from carbon monoxide. The catalyst displays excellent selectivity, no additional products were formed. The conditions employed in the reduction (140°C 2 atm pressure) were so mild that the reaction rate was very low, only one percent conversion after five days. However, by adding a molar equivalent of trimethylphosphine the rate increased three fold and the selectivity remained high. Addition of other phosphines, such as triphenylphosphine also increase the reaction rate but lowers the selectivity. That is, ethane and propane were also formed.

Muetterties 76 also found that the major product of carbon monoxide reduction could be shifted to ethane by changing the solvent from traditional organic solvents to molten NaCl·2AlCl₃. The use of Lewis acid solvents may result in substantial oxygen aluminum interactions facilitating the carbon oxygen bond cleavage. The use of ${\rm Ir}_4({\rm CO})_{12}$ in NaCl·2AlCl₃ at 180°C and 1.5 atm pressure $({\rm CO/H_2=1:3})$ for twelve to twenty-four hours resulted in the production of substantial amounts of methane and

ethane with minor amounts of propane and isobutane. Bercaw⁷³ has stoichiometrically reduced carbon monoxide to methanol with $(h^5-C_5Me_5)_2Zr(CO)_2$ at 25°C and 1.5 atm hydrogen pressure. A formyl complex⁷⁷ is proposed as an

$$C_{P_{2}}Z_{r,CO} \xrightarrow{H_{2}} C_{P_{2}}Z_{r,-CO} \xrightarrow{H_{2}} C_{P_{2}}Z_{r,H}$$

$$\downarrow_{H_{2}}$$

$$C_{H_{3}OH} \xrightarrow{HCI} C_{P_{2}}Z_{r,H}$$

intermediate in the reaction. This zirconium complex is the first reported mononuclear complex capable of reducing carbon monoxide. However, attempts to make the reaction catalytic have failed.

Feder and Rathke⁷⁴ found that $HCo(CO)_{4}$ catalyticly reduces carbon monoxide to primarily methanol and methyl formate with lessor amounts of ethanol, ethyl formate and 1-propanol. The reaction was run in benzene at 200°C and 300 atm of an equimolar mixture of hydrogen and carbon monoxide. It was found that in p-dioxane at 182°C carbon monoxide hydrogenation proceeded even more rapidly and

selectively. Feder believes that the ethanol and 1-propanol formed are products of secondary reactions.

A number of mechanisms have been proposed for the heterogeneous catalyzed methanation reaction. Two mechanisms are presented in Table 13. Fontaine's mechanism⁷⁸ proposes a metal formyl species which picks up a proton to form an oxygen stabilized alkylidene species or a bridging species. The other mechanism proposed by Vlasenko⁷⁹ also has an oxygen stabilized carbenoid species as an intermediate. A more recent mechanism⁸⁰ based on known homogeneous steps is shown in Figure 47 for the Fischer-Tropsch reaction. In step 7 of the mechanism a metal carbene is formed.

Heteroatom stabilized metal carbene complexes have been isolated 81 and their chemistry studied. The first preparation of moderately stable carbene complexes proceeded by the action of alkyl lithium on tungsten hexacarbonyl. Since the carbon of the coordinated carbonyl is the most positive center, alkylation occurs there. The resulting lithium salt is acidified and treated with diazomethane or alternately directly alkylated with trialkyloxonium tetrafluoroborate. 81

$$W(CO)_{6} \xrightarrow{\text{LiR}} (CO)_{5}W = C \xrightarrow{\text{NLi}} (CO)_{5}W = C \xrightarrow{\text{NLiR}} (CO)_{5}W = C \xrightarrow{\text{NLIR}}$$

Table 13. Methanation Mechanisms

Fontaine's Mechanism	Vlasenko's Mechanism
W ← W + OO OO	$M + e^- + H_2 + [M^{H2}]^-$
H = H + 2M + 2M	-9 + W + CO + W + CO + W
$\begin{array}{cccccccccccccccccccccccccccccccccccc$	$M + M^{H_2} - M^{HCOH} + e^- + M$
$M + M' + M' \rightarrow M'$	$M^{C=OH} + M^{H_2} + M^{CH_2} + H_2O + M$
H H CH2OH CH2OH W + M	$M^{CH_2} + M^{H_2} - + CH_{\downarrow \downarrow} + e^- + 2M$
сн ₂ он н ₂ сн ₄ + н ₂ о	
M = Metal coordination site	site

$$H-M \xrightarrow{CO} MC-M \xrightarrow{H_2} M-C-M \xrightarrow{3} H-C M-H$$

$$M-H + CH_3OH \xrightarrow{6} CH_2-M \xrightarrow{5} CH_2-M$$

$$H_2C = M$$

$$H_2C = M$$

$$CH_3-M \xrightarrow{OO} CH_3-C-M \xrightarrow{H_2} CH_3-C-M \xrightarrow{11} CH_3-CH-M OH H$$

$$-H_2O$$

Figure 47. Recent Proposed Fischer-Tropsch mechanism.

It was felt that one possible approach to developing a homogeneous analog of the methanation reaction might be to combine the preceding chemistries. That is, the treatment of a metal carbonyl with a nucleophile under hydrogen and carbon monoxide pressure might generate "Fischer style" carbenes which may react further to give hydrocarbons or alcohols. The proposed scheme is in Figure 48. The scheme shows two possible pathways, one giving hydrocarbons of increased carbon number, the other giving alcohols of increased carbon number. There are parallels which can be drawn between the proposed reaction sequence and the heterogeneous reaction mechanisms. carbene species are proposed as intermediates in both cases. Metal hydrides are present in both sequences. Bimolecular reaction pathway are possible in the proposed homogeneous reaction but will not be considered here.

The next section presents a discussion of the attempts to make the proposed scheme into a viable reaction path-way.

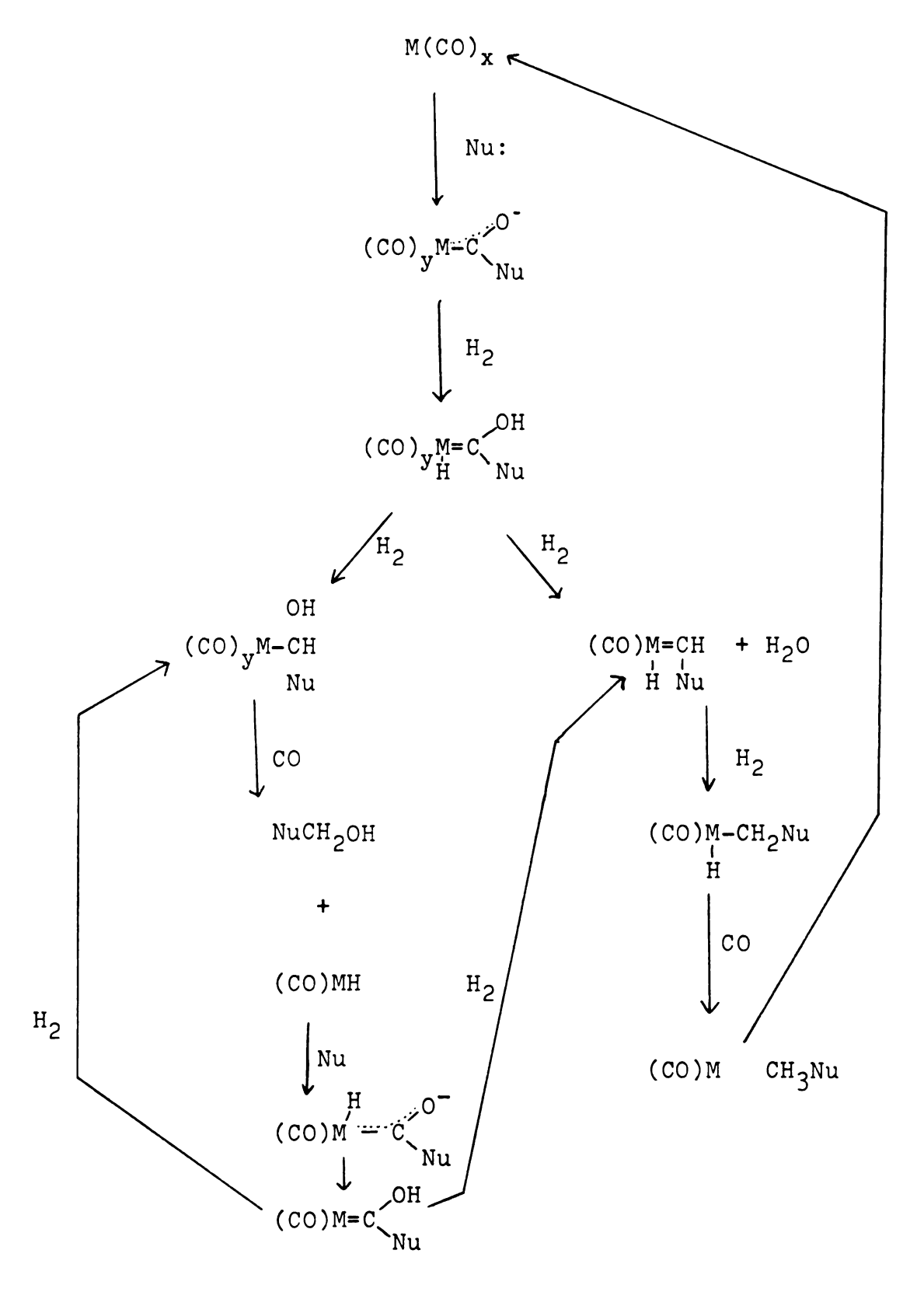


Figure 48. Proposed homogeneous pathway for CO reduction.

RESULTS AND DISCUSSION

Transition metal carbonyl complexes were treated in solution with various nucleophilic bases. These reactions were carried out under hydrogen and carbon monoxide pressures ranging from 45 to 70 psi. The ratio of hydrogen to carbon monoxide was varied from 1 to 4. Table 14 gives the reactants, conditions, and products for representative reactions. The reactions listed are the results of optimization of the reaction conditions. Entry five gave the highest yield of methane for a run without a cocatalyst. Longer reaction times did not increase the yields.

In an attempt to increase the yields of products, Lewis acid co-catalysts were added to the mixture. Aluminum isopropoxide had virtually no effect on the reaction as did vitride. 82 However, diisobutyl aluminum hydride did increase the yields of methane. As shown in Table 15 yields as high as 60 percent were obtained by using tungsten hexacarbonyl, sodium propoxide and diisobutylaluminum hydride in hexane at 105°C under 50 psi pressure. This modest yield of methane based on tungsten hexacarbonyl represents the highest yield for this study. Isobutyl aluminum hydride did not reduce carbon monoxide by itself under the conditions of the study.

The reduction of carbon monoxide was less than

Summary of carbon monoxide reduction reactions. Table 14.

Sequence									
Number	Catalyst	Base	B^a/M	Solvent	Н2	00	Temp.	Time	Products ^D
1	W(co) ₆	+0K _C	Н	THF	30	30	125	36	!!!
2	M(CO) ₆	+0K	9.5	THF	55	15	95	48	
က	M(CO) ₆	EtoK	7	THF	22	10	145	48	trace $\mathtt{CH}_{f \mu}$
7	M(CO) ₆	+0K	27	нс+	54	10	125	36	trace $\mathtt{CH}_{f \mu}$
7	M(CO) ⁶	КОН	43	decalin	20	20	110	54	10% CH_{4}
9	Mn ₂ (co) ₁₀	+0K	6	THF	52	10	25	54	!!!
7	$Mn_2(WO)_{10}$	+0K	6	THF	70	20	90	54	\$ 1 1
ω	Fe(CO) ₅	EtoK	143	decalin	35	10	130	48	trace $\mathtt{CH}_{f \mu}$
6	$Fe(CO)_5$ $CH_3(CH_2)_7O$) ₇ 0Na	72	decalin	35	11	130	48	!!!!!!!!!!!!!!!!!!!!!!!!!!!!!!!!!!!!!!!
10	RhC1($_3$ P) $_2$ CO	EtoK	158	dioxane	27	10	120	48	trace $\mathtt{CH}_{oldsymbol{\mu}}$
11	$\mathtt{Rh}_2\mathtt{Cl}_2\mathtt{(CO)}_{\mathfrak{h}}$	EtoK	95	THF	30	12	100	36	trace $\mathtt{CH}_{oldsymbol{\mu}}$

 $^{\mathbf{a}}$ Base to metal ratio. $^{\mathbf{b}}$ Yields are reported relative to metals.

 $c_+ = t_-butyl$

Table 15. Summary of CO reductions with co-catalysts.

Sequence Number	Catalyst	Cocatalyst	CC/M	Base	B/M	B/ _M Solvent	Н2 СО	00	Temp. Time	Time	Products
٦	Fe(CO) ₅	(bu) ₂ A1H	4.5	NaOPr	2	dioxane	33	12	110	8 7	-
2	M(CO)6	A1(OCH(CH ₃) ₂	8 (2(Etok	9	THF	17	10	145	8 7	!
٣	M(CO)6	(1Bu) ₂ AlH	35	NaOPr	2	hexane	35	15	105	8 7	60% СНц
7	M(co)6	(1Bu) ₂ AlH	33	NaOPr	7	dioxane	35	12	110	8 7	24% CH4
5	$M(co)_{\theta}$	(1Bu) ₂ AlH	t I	NaOPr	9	THF	0 7	20	90	54	1 1
9		(1Bu) ₂ AlH	!	1 1 1 1	I	hexane	35	10	90	12	trace $\mathtt{CH}_{m{\mu}}$
7	M(co) ₆	Vitride ^a	31	NaOPr	7	dioxane	35	25	100	54	trace $\mathtt{CH}_{oldsymbol{\mu}}$
80	! ! !	Vitride	ļ		ı	dioxane	35	25	100	8 7	trace $\mathtt{CH}_{m{\mu}}$
6	M(CO) ⁶	A1(OCH- (CH ₃) ₂)	35	ONa	09	A1(OCH- (CH ₃) ₂)	24	10	150	36	

 a Vitride is NaAlH₂(OCH₂CH₂OCH₃)₂.

stoichiometric so a study to determine which of the proposed steps was not operative or which was the difficult step was undertaken. The oxygen stabilized tungsten carbene complex 22 was prepared. The complex was added to the reaction in place of tungsten hexacarbonyl and

$$(CO)_5W = C_{CH_3}^{OLi}$$

stirred for 48 hours at 130°C under 30 psi of hydrogen. Ethanol was formed in 85 percent yield. Hence under the conditions used, if the carbene complex was formed, it should proceed smoothly to products. In order to see if the carbene complex was formed under the reaction conditions a 13C NMR study was performed. Tungsten hexacarbonyl and potassium T-butoxide were stirred in tetrahydrofuran for three hours and the spectra was obtained. A peak was seen at 332.5 ppm relative to TMS. The chemical shift of the peak is in the range characteristic of oxygen stabilized tungsten carbene complexes. 83 Hence it is possible that the carbene complex could be formed. An aliquot of a reaction mixture was removed and analyzed by ¹³C NMR. No peak in the range of 310-340 ppm was seen. That is, the carbene complex was not formed in appreciable concentrations under the reaction conditions. Attempts to

increase the concentration of tungsten hexacarbonyl in the reactions were limited by the low solubility of the complex.

It was hoped that by using stronger nucleophiles the concentration of the carbene species might be increased. A series of sodium and potassium alkoxides were used, but the nucleophilicity is roughly the same for all of them. The sodium salts of long chain thiols, such as laurylthiol, are more nucleophilic than the alkoxides. However they did not seem to have much affect on the product yields.

The sodium salt of diethylene glycol monomethyl ether was used as both a nucleophile and solvent. The results from this system, shown in Table 16 yielded considerable methane. However, the methane was a degradation product of the diethylene glycol monomethyl ether rather than a reduction product of carbon monoxide. That is, entry 6 shows that the methane was produced without the presence of carbon monoxide.

The homogeneous reduction of carbon monoxide by metal carbonyls and bases was unsuccessful because of low concentrations of "Fischer style" carbene complexes being formed in solution. That is, in order for the scheme to be usable a method of generating the oxygen stabilized carbene complex in greater yield is needed.

Table 16. Solvent degradations.

Sequence Number	Catalyst	Base (Solvent)	B/M H ₂ CO	Н2	CO	Temp Time	Time	Products ^b
ı	M(co) ⁶	CH ₃ (OCH ₂ CH ₂) ₅ ONa	!	30	5	135	36	$_{ m CH}_{ m h}$
2	9(00)M	CH ₃ (OCH ₂ CH ₂) ₅ ONa	09	32	∞	140	36	107% CH $_{ m h}$
8	M(CO)8	CH ₃ (OCH ₂ CH ₂) ₅ ONa	59	35	10	145	72	49% CH4
7	9(00)M	сн ₃ сн ₂ (осн ₂ сн ₂) ₂ ома 130	130	30	10	140	8 †	22% 2% CH ₄ , CH ₃ CH ₃
72	1	$cH_3(ocH_2cH_2)_5oNa$	-	30	10	140	48	25% CH4
9	M(CO)8	$cH_3(OCH_2CH_2)_5ONa$	1	30	30 psi ^a	140	77	10% CH_{L}

 $^{\rm a}$ 30 psf Argon in place of H₂,CO.

byields are based on tungsten.

EXPERIMENTAL

Synthesis of (CO) W=C(CH3)OLi 84

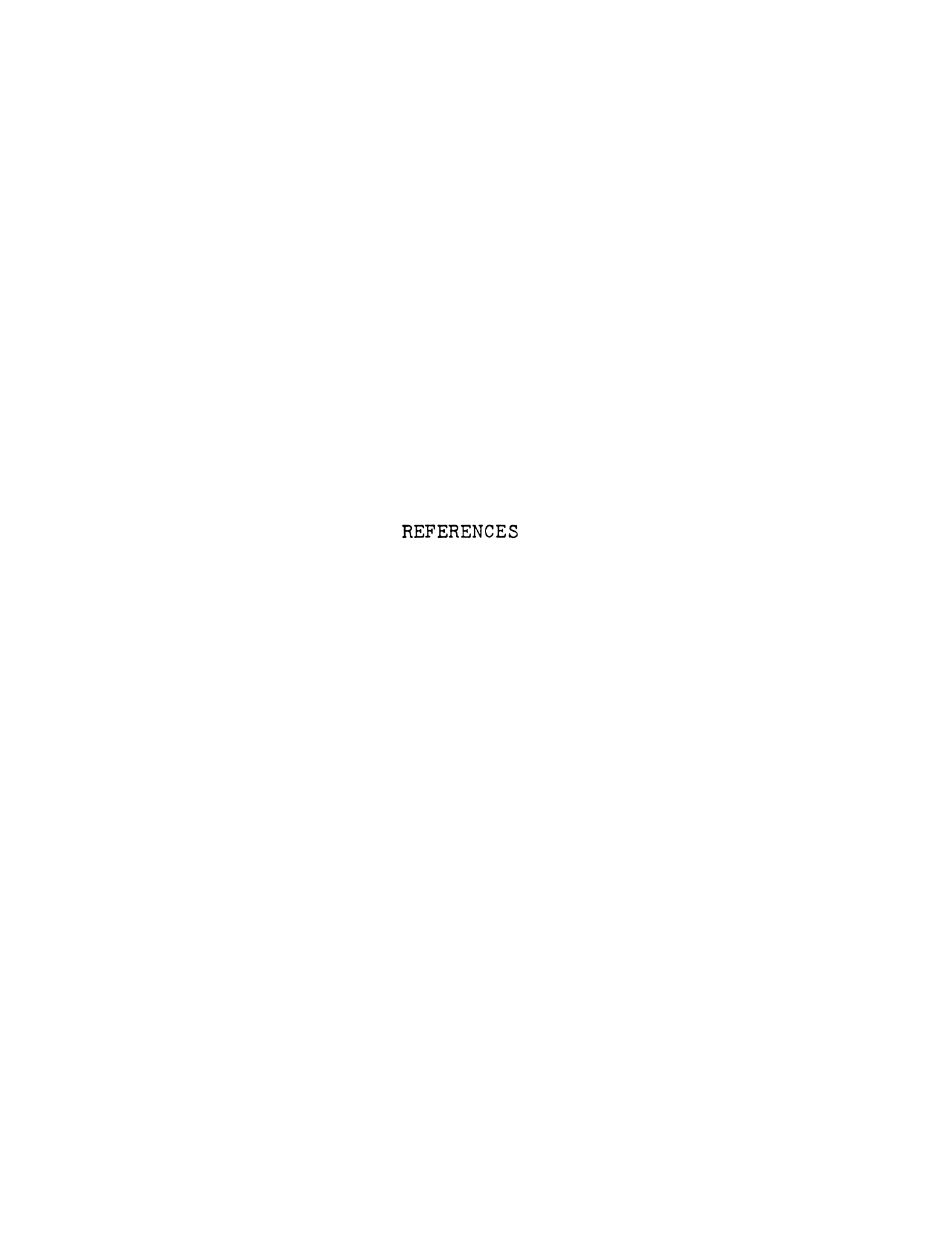
A three neck one liter round bottom flask was purged with argon and charged with 10.5 g (30 mmol) of tungsten hexacarbonyl and 500 mls of ether. 30 mmols of methyl lithium in 100 mls of ether was added via an addition funnel with rapid stirring. The yellow suspension slowly changed to a cloudy solution over the course of two hours. The solution was then filtered under argon to remove unreacted tungsten hexacarbonyl and concentrated to 70 mls of a dark oil. The oil was taken up in pentane and cooled to -78°C. Yellow crystals slowly formed which were collected and dried.

Hydrogenation of (CO)₅W=CCH₃OLi

1.8 grams (4.8 mmols) of the title compound was placed in a glass pressure bottle along with 25 mls of tetra-hydrofuran. The pressure bottle was charged with 30 psi of hydrogen and was heated to 130°C for 48 hrs. The bottle was opened and no volatile products were detected by glc. The liquid phase contained ethanol in 85% based on starting complex. The ethanol was analyzed by glc and confirmed by a mass spectrum.

Typical Carbon Monoxide Reduction Run

25 mls of a .05 M solution of tungsten hexacarbonyl (1.25 mmol) in tetrahydrofuran was placed in a pressure bottle along with .4 grams (4.75 mmol) of potassium ethoxide. The pressure vessel was then pressurized with 10 psi of carbon monoxide and 35 psi of hydrogen. The pressure bottle was then heated at 140° by means of an oil bath for 24 hrs. The pressure bottle was cooled and the gas phase was analyzed on a 10 ft molecular sieve column and the liquid phase was analyzed on a 16 ft DC 550 column at 60°C on a purapak Q column at 85°.



REFERENCES

- 1. R. Noyori, et al., J. Am. Chem. Soc. 96, 634 (1974).
- 2. F. G. A. Stone, T. A. Manuel, S. L. Stafford, <u>J. Am. Chem. Soc.</u>, §3, 249 (1961).
- 3. J. Osborn, et al., J. Am. Chem. Soc. 95, 597 (1973).
- 4. T. J. Katz and S. Cerefice, <u>J. Am. Chem. Soc.</u> 91, 2405 (1969).
- 5. J. Halpern and P. E. Eaton, <u>J. Am. Chem. Soc</u>. 92, 3515 (1970).
- 6. P. Binger, et al., J. C. S. Chem. Comm. 376 (1976).
- 7. G. E. Coates, M. L. H. Green, K. Wade, Organometallic Compounds, Vol. 2, Methuen, London, 3rd Ed. (1968).
- 8. J. Chatt and B. Shaw, J. Chem. Soc. (1959) 705.
- 9. J. Chatt and B. Shaw, J. Chem. Soc. (1960) 1718.
- 10. F. Anet and E. Leblanc, <u>J. Am. Chem. Soc.</u> 72, 2649 (1957).
- 11. U. Giannini and U. Zucchini, Chem. Comm. 940 (1968).
- 12. G. Wilke and H. Schott, Angew, Chem. Internat. Ed. 5, 583 (1966).
- 13. P. S. Braterman and R. J. Cross, <u>J. Chem. Soc.</u>
 Dalton, 657 (1972).
- 14. K. Thomas, et al., J. Chem. Soc. (A), 1968, 1801.
- 15. B. K. Bower and H. G. Tennent, <u>J. Am. Chem. Soc.</u>, 24, 2512 (1972).
- 16. G. M. Whitesides, et al., J. Am. Chem. Soc. 22, 1476 (1970).
- 17. G. M. Whitesides, et al., J. Am. Chem. Soc. 94, 5258 (1972).
- 18. M. F. Semmelheck, et al., J. Am. Chem. Soc. 93, 5910 (1971).
- 19. G. B. Young, et al., J. Chem. Soc. Dalton (1977) 1892.

- 20. G. M. Whitesides, et al., J. Am. Chem. Soc. 28, 6529 (1976).
- 21. S. Otsuka, et al., J. Am. Chem. Soc. 25, 3180 (1973).
- 22. S. J. W. Price in "Comprehensive Chemical Kinetics", Vol. 4, C. H. Bamford and C. H. H. Tipper, Ed., Elsevier, Amsterdam, 1972, p. 197.
- 23. R. J. Puddephatt, et al., J. Chem. Soc., Dalton (1976) 786.
- 24. G. M. Whitesides, et al., J. Am. Chem. Soc. 95, 4451 (1973).
- 25. G. M. Whitesides, J. Am. Chem. Soc. 28, 6521 (1976).
- 26. G. M. Whitesides, J. Am. Chem. Soc. 100, 5808 (1978).
- 27. Divinyl platinum(II) and diarylplatinum(II) complexes thermally decompose to yield butadienes or biaryls. These are exceptions to the generality.
- 28. P. S. Braterman, et al., J. Chem. Soc. Dalton, 1306 (1976).
- 29. R. H. Grubbs, et al., "Organotransition-Metal Chemistry", Y. Ishii and M. Tsatsui, Eds., Plenum Press, New York, 1975, p. 135.
- 30. A. Miyashita and R. H. Grubbs, J. Am. Chem. Soc. 22, 3863 (1977).
- 31. A. Miyashita and R. H. Grubbs, J. Am. Chem. Soc. 100, 1300 (1978).
- 32. A. Miyashita and R. H. Grubbs, <u>J. Am. Chem. Soc.</u> 100, 7416 (1978).
- 33. A. Yamamoto, et al., Bull. Chem. Soc. Jap, 50, 1109 (1977).
- 34. A. J. Gordon and R. A. Ford, The Chemist's Companion, John Wiley and Sons, New York, 1972, p. 135.
- 35. (a) R. J. Gillespie, <u>J. Chem. Educ.</u> 40, 295 (1963).
 - (b) S. Otsuka, et al., J. Am. Chem. Soc. 28, 5850 (1976).
- 36. G. Booth and J. Chatt, J. Chem. Soc. (1965) 3238.

- 37. F. A. Cotton and G. Wilkinson, <u>Advanced Inorganic Chem.</u>
 3rd Ed., Interscience, New York, p. 667 and references therein.
- 38. J. Chatt, et al., J. Chem. Soc. (1959) 1047.
- 39. C, K. Jorgensen, Modern Aspects of Ligand Field Theory, American Elsevier, New York, 1971, Chapter 26, p. 343.
- 40. A. Yamamoto, et al., J. Am. Chem. Soc. 93, 3350 (1971).
- 41. M. L. Lui and R. H. Grubbs, unpublished results.
- 42. H. A. Eick, et al., Inorg. Chem. 12, 2166 (1973).
- 43. G. M. Whitesides and B. Young, <u>J. Am. Chem. Soc.</u> 100, 5808 (1978).
- 44. R. Hoffmann, et al., J. Am. Chem. Soc. 98, 7255 (1976).
- 45. A. J. Gordon and R. A. Ford, The Chemist's Companion, Wiley Interscience, New York, 19, p. 439.
- 46. L. Venanzi, J. Chem. Soc. (1958) 719.
- 47. R. Belcher and A. Nutten, "Quantitative Inorganic Analysis", AMG McDonald, Butterworth and Co., Ltd., London, 1970, p. 131.
- 48. H. F. Klein and H. H. Karsch, Chem. Ber. 105, 2628 (1972).
- 49. R. A. Charles and M. A. Pawlchowski, <u>J. Phys. Chem.</u> 62, 440 (1958).
- 50. R. A. Schunn, <u>Inorg. Syn.</u> 15, 5 (1974).
- 51. N. Hagihara, et al., Chem. Letters (1974) 1363.
- 52. (a) T. J. Katz, <u>Advan. Organomet. Chem.</u> 16, Chapter 7 (1977).
 - (b) T. J. Katz, et al., J. Am. Chem. Soc. ,, 2519 (1976).
 - (c) R. H. Grubbs, et al., J. Am. Chem. Soc. 28, 3478 (1976).
- 53. M. L. H. Green, et al., J. C. S. Chem. Comm. 604 (1978).

- 54. W. B. Hughes, <u>J. Am. Chem. Soc.</u> 92, 532 (1970).
- 55. J. Chatt, et al., J. Chem. Soc. (1976) 738.
- 56. M. L. H. Green, et al., J. C. S. Chem. Comm. 619 (1976).
- 57. M. L. H. Green, et al., J. Chem. Soc. Dalton, 1132 (1977).
- 58. D. B. Brown, et al., <u>J. Organomet. Chem.</u> 159, 431 (1978).
- 59. C. F. M. Tipper, et al., J. Organomet. Chem. 81, 423 (1974).
- 60. S. J. Ashcroft and C. T. Mortimer, J. Organometal. Chem. 24, 501 (1970).
- 61. M. L. H. Green and M. Ephritikhime, J. C. S. Chem. Comm. 926 (1976).
- 62. N. Hagihara, et al., Chem. Lett. 1363 (1974).
- 63. C. R. Hoppin, Ph.D. Dissertation, Michigan State University, 1978.
- 64. G. W. Parshall and R. R. Schrock, Chem. Rev. 76, 258 (1976).
- 65. R. R. Schrock, J. Am. Chem. Soc. 97, 6577 (1975).
- 66. P. G. Gassman and T. M. Johnson, J. Am. Chem. Soc. 99, 622 (1977).
- 67. H. Pichler and Erdoel Kohle, Endgas. Petro. Brennst.-Chem. 26, 625 (1973).
- 68. H. Pichler and H. Schulz, Chem. Ing. Tech. 42, 1162 (1970).
- 69. H. Storch, et al., The Fischer-Tropsch and Related Syntheses, Wiley, New York 1951.
- 70. Len Seglin, Ed. Methanation of Synthesis Gas, Advances in Chemistry Series 146, American Chemical Society, Washington, D.C. 1975.
- 71. F. Fischer: Herstellung Flüssiger Kraftstoffe aus Kohle Borntrager, Berlin, 1924.
- 72. E. L. Muetterties, <u>Science</u> 196, 839 (1977).

- 73. J. E. Bercaw, et al., J. Am. Chem. Soc. 28, 6733 (1976).
- 74. H. M. Feder and J. W. Rathke, <u>J. Am. Chem. Soc.</u> 100, 3623 (1978).
- 75. E. L. Muetterties, et al., J. Am. Chem. Soc. 28, 1296 (1976).
- 76. E. L. Muetterties and G. C. Demitras, <u>J. Am. Chem. Soc.</u> 99, 2796 (1977).
- 77. There is now precedent for the formation of formyl complexes. J. P. Collman, J. Am. Chem. Soc. 25, 4089 (1973) reports the preparation of [Fe(CO)4(CHO)] whereas C. P. Casey, J. Am. Chem. Soc. 28, 5395 (1976) reports a general method for the preparation of metal formyl complexes.
- 78. R. Fontaine, Ph.D. Dissertation, Cornell University, 1973.
- 79. V. M. Vlasenko, et al. Kinet. Katal. 6, 244 (1965).
- 80. G. Henrice-Olive and S. Olive, Angew. Chem. Int. Ed. Engl. 15, 136 (1976).
- 81. E. O. Fischer and A. Maasbol, <u>Angew. Chem.</u> 76, 645 (1964).
- 82. Vitride is Sodium bis(2-methoxyethoxy)aluminum hydride (NaAlH₂(OCH₂CH₂OCH₃)₂).
- 83. E. O. Fischer, et al., J. Orgmet. Chem. 56, C37 (1973).
- 84. E. O. Fischer, et al., Chem. Ber. 110, 2574 (1977).
- 85. E. O. Fischer, Advances in Organometallic Chemistry, Vol. 14, p. 1, 1976.

